ISAS - INTERNATIONAL SCHOOL
FOR ADVANCED STUDIES

Rotavirus NSP5-NSP2 interaction: biological consequences

Thesis submitted for the Degree of

Doctor Philosophiae

Candidate
Elsa Fabbretti

Supervisor
Dr. Oscar Burrone

Academic Year 2000/2001

SISSA - SCUOLA
INTERNAZIONALE
SUPERIORE
I STUDI AVANZATI
TRIESTE
Via Beirut 2-4

TRIESTE

Isas-International School for Advanced Studies

Rotavirus NSP5-NSP2 interaction: biological consequences

Thesis submitted for the Degree of

Doctor Philosophiae

Candidate
Elsa Fabbretti

Supervisor
Dr. Oscar Burrone

Academic Year 2000/2001

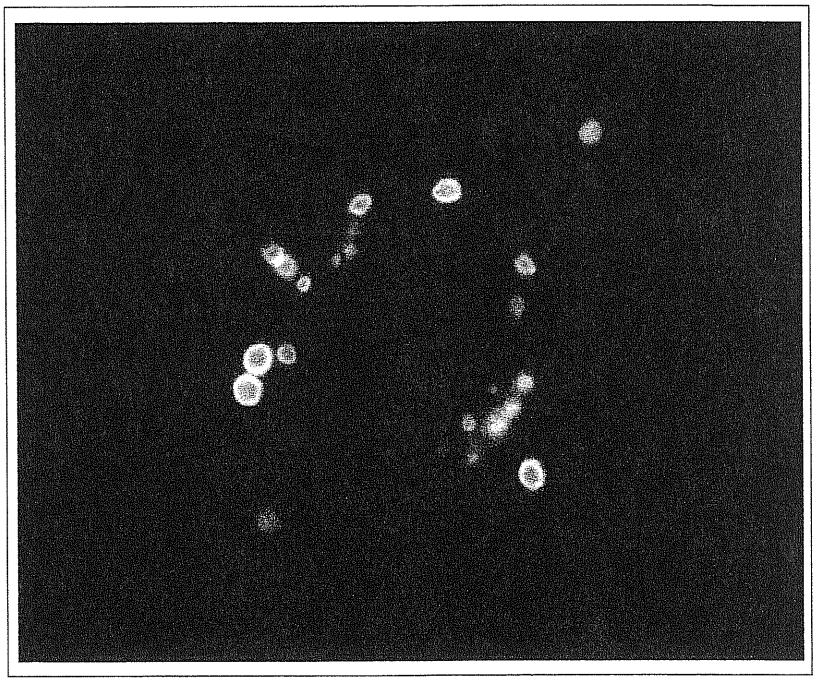

Viroplasm like structures obtained by the co-expression of rotavirus proteins NSP5 and NSP2

Acknowledgement

What can I say in this page? That I thank everybody knows me, who has supported me in all my human and humoral or hormonal days... Everybody knows everything about Lorenzo and Bianca, everybody knows everything about my mother and father "artisticity", and everybody knows all of my extra-laboratory attitudes, that influence me so much, and that occupy so much my mind...
Yes, these 3-4-5 years were long. Full of working satisfactions, illusions and depressions, but full also of thousand other things... I think that it was a good time, perhaps too long in terms of time:productivity, or not dense in terms of work as maybe my boss would like, or maybe discontinuous, I could say... but I am sure that it was a good time, equilibrated. Work and family and social in the right proportions, to be considered a complete positive period of my life...
5 years are long: now I feel incredibly emotional linked to the majority of my colleagues, my chief Oscar Burrone, the other students, the assistant personal of the ICGEB... I have a lot of nice memories about the time spent with all of them. I have also seen many friend leaving, following their carrier. As it happens maybe for them, the moment of the departure is never ready, the time is always post-pound... ok, I also promise to organise a farewell party, to arrive only laughing (or drunk) at the moments of the greetings...

After these melodrama, first of all I would like thank my boss Oscar Burrone. He has always put attention in my work and was really supporting me with propositive ideas. I remember the numbers of suggestions and the interesting and constructive discussions. I have learned a lot from his precision in the interpretation of the results and from his positive and enthusiastic way to approach the research. I want thank him also to have let me the freedom to try and verify my approaches giving me the necessary support and trust.

Than I would like to thank the Rota-girls: Fulvia Vascotto, Catherine Eichwald, Cecilia Miozzo, Ivka Afrikanova and Susana Giambiagi. Many of them are now working in other parts of the world, but the interesting improvements on the rotavirus-related projects that I have participied with them in these last years, were possible also thank them.

I would like to thank in particular my friend Fulvia Vascotto for her force and emotional and physical support. She has an incredible energy that profound everything is around. I want thank her because she has helped me really a lot in a number of situations, with her magnific cooperation, enthusiasm and spirit of group.

I would like to thank my friend Federica Benvenuti, of which I feel so much the distance now. Federica was my "open mental space" in the working day. I remember the brakes during the working days, speacking of incredible topics: chat, dreams, sex, "intellectualicicity" and politics.... Yes, I will go to visit her in Paris, as soon I can...

I would like to thank all the rest of the lab: Sabrina, Rossio, Michela, Monica, Paola and Marco, Jorge, Hulin, Luca, Roberto, Facundo, Martin, Dimitar. They have let me to speak and to laugh really a lot. Thanks!

I would like to thank the SISSA school to have provided me the fellowship and the opportunity to follow the PhD student program. I would thank all the other PhD students that, as me, have carried the heaviness of the PhD courses and the examinations at the end of the years... At this porpoise, I want thank the secretariat unit that has supported all the PhD courses.
I would like to thank all the ICGEB researchers for their support and patience, when I asked protocols or reagents... In particular I would like to remember Christian Khune, Paola Massimi, Sotir, Mudit Tyagi, MariaElena Lopez, Rodolfo Garcia, Gabriella Pittis and the colleagues of the SISSA lab. Moreover, I would like to thank Piero Giulianini of the University of Trieste for the electron microscopy figures.
I understand now the big organisation and the incredible help of the ICGEB efficient utilities and facilities, in particular I would like to thank Ann Crumm and Grazia Spina for the order assistance, Giancarlo Lunazzi and Mauro Sturnega for the animal care, and all the technical office super-men!
Ciao !!

Table of contents

Chapter 1
Introduction

Chapter 2
Material and Methods

Chapter 3
Results

Index of figure

Introduction

Methods

Results

List of abbreviations

3D = three-dimentional
Å = Angstrom
Amp = ampicellin
Arg = arginine
ATP = adenosine triphosphate
BAB = basic acidic basic
BSA = bovine serum albumin
Ci = Curie
C-terminal = carboxy-terminal
C60 = rotavirus strain
CMV = cytomegalovirus
cpe = cytopathic effect
CryoEM = cryoelectron microscopy
kDa = kilo Dalton
dil = dilution
DLP = double layered particles
DMEM = Dulbecco modified Eagle Medium
DMSO = dimethilsulfoxide
DOC = deoxycolate
ds = double shell (= double layer particles)
DSP = dithiobis (succinimidylpropionate
dsRNA = double stranded RNA
DTT = di-thio-eritol
E.coli = Escherichia coli
EGFP = eukriotic green fluorescence protein
EM = electron microscopy
ENS = enteric nervous system
ER = endoplasmic reticulum
FACS = fast analytical cell system
FCS= fetal calf serum
FITC = fluorescein
G418 = gentamycin
GlcNAc = N-Acetyl glucosamine
GST = Glutathion-S-transferase
h = hours
HRP = horse raddish peroxidase
Kan = kanamycin
IP3 = inositol 1,4,5-trisphosphate
IPTG =
λ-Ppase = lambda protein phosphatase
LB = Luria Bertani Broth
Lys = lysine
MA104 = Epithelial rat kidney cells
mAmp = milli Ampere
Met = methionine
min = minute
MMP = metalloproteases
moi = molteplicity of infection
N-terminal = amino-terminal
NSP1-NSP6 = non structural protein
NP40 = detergent
nt = nucleotides
o/n = over-night
°C = celsius degrees
OD = optical density
ORF = open reading frame
OSU = rotavirus strain
PAGE = polyacrylamide gel electrophoresis
PBS = phosphate buffer saline
P-BSA = PBS+BSA
PEST = protease domain
PFA = paraformaldehyde
pfu = plque forming unit
pi = post infection
^{32}Pi = inorganic phosphate
PMSF = protease inhibitor
RI = relication intermediate
RNAse = Ribonuclease
RITC = rhodamine
rpm = rotation per minute
RT = room temperature
^{35}S = solfour
SA11 = rotavirus strain
SDS = sodium dodecil sulfate
SF = serum free
ss = single shell immature viral particles
ssRNA = single stranded RNA
SV40 = simian virus 40
SVP = subviral particles
Thr = threonine
TNT = coupled transcription and translation
Ts = temperature sensitive
U = unit
UTR = untranslated region
UV = ultraviolet
V = Volt
VLP = virus like particles (from baculovirus)
VLS = viroplam-like structure
VP1-VP7 = viral structural proteins
vTF7.3 = vaccinia virus strain
w/o = without

Chapter 1

Introduction

General features of Rotavirus

Reoviridae are 65-85 nm diameter large viruses with a icosahedral non enveloped capsid, composed by a complex structure of 3 concentric protein layers (also called "shells") plus an enzymatic core containing a double stranded RNA genome of 10 to 12 fragments. The rotavirus genus is 75 nm diameter large and its genome is composed by 11 dsRNA segments coding for 6 structural proteins (VP), found in mature virus particles and 5 non structural proteins (NSP), found in infected cells. Simian rotavirus strain SA11 was the first completely sequenced rotavirus genome, becoming the virus prototype. The coding assignments and properties of the proteins encoded in each of the 11 genome segments were established by *in vitro* translation of rotavirus mRNA or denatured dsRNA and by analyses of reassortant viruses (54) as summarised in figure 1.1.

The rotavirus three protein layers have been studied by structural cryoelectron microscopy and image processing (159; 173). As summarised in the figure 1.1, the outer layer of the virion is consisting of VP7 and by 60 spikes of VP4 dimers. VP7 is the major outer capsid glycoprotein that represents the smooth external surface of the virus. VP4 is the rotavirus hemagglutinin and undergoes proteolytic cleavage previous to infection, generating VP8* and VP5* cleavage products (46, 51). The intermediate layer is constituted by VP6 required for active virus transcription (115; 15; 37). The inner layer is composed by the RNA binding protein VP2, with virus scaffold role (100; 101). The RNA dependent RNA polymerase VP1 and the guanyl-

transferase VP3 are located in the inner enzymatic core, along with the genomic dsRNA.

Although the non structural proteins (NSP1, NSP2, NSP3, NSP4, NSP5) have been detected in various stages of the rotavirus replication cycle, their specific functions are not yet completely established. All of them serve as helper proteins supporting virus replication, packaging and maturation or play some role in ssRNA stabilisation (49).

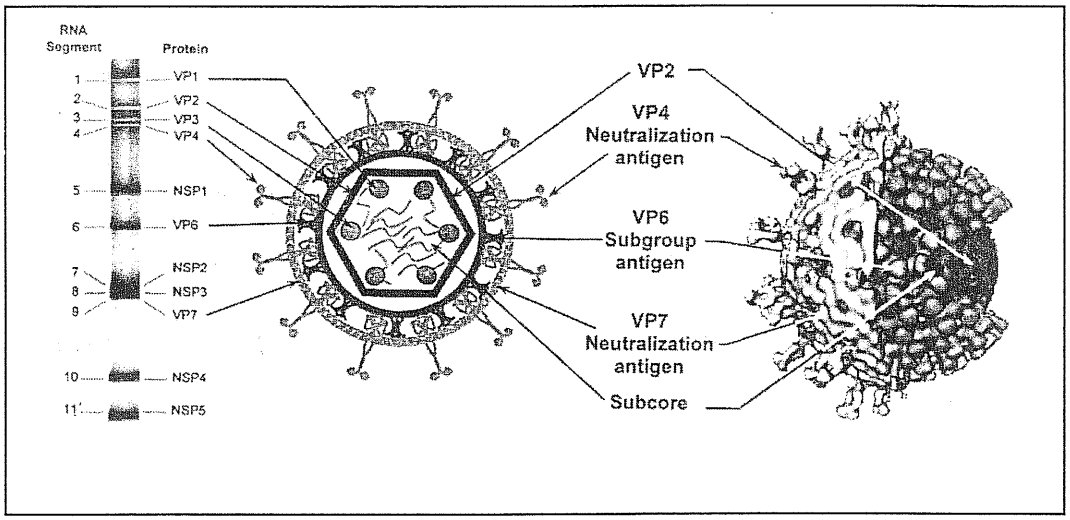

Figure 1.1. Gene coding assignements and three-dimesional structures of rotavirus particles. Left: a polyacrilamide gel shows the 11 segments of dsRNA of the SA11 rotavirus genome and the proteins encoded by each of these genes. Center: schematic representation of the rotavirus particle. The proteins in the different layers are indicated. Right: three-dimesional structures of a complete rotavirus particle, that shows in a portion the middle and the inner layers (49).

Rotavirus replication cycle

Rotavirus infection induces profound alterations in the morphology and biochemistry of the host cell. Rotavirus entry, activation of transcription, morphogenesis, cell lysis and particle release as well as the distant action of viral proteins are Ca^{2+}-dependent processes (170). Viral protein synthesis is sufficient to increase the intracellular calcium concentration and there are evidences that the expression of the single rotavirus protein NSP4, directly influence the Ca^{2+} homeostasis (189; 190). Ca^{2+} plays also a role in the replication cycle and pathogenesis of other viruses such as poliovirus, Cocksackie virus, cytomegalovirus, vaccinia and measles virus and HIV (170).

It has been reported that differences in Ca^{2+} concentration after rotavirus infection provokes also severe structural alterations of the cytoskeleton network, even if not always dependent by Ca^{2+} concentration. Viral infection in cultured cells is associated with microtubule network disassembly (vimentin and tubulin disorganisation), F-actin disassembly and alteration in intermediate filament (IF) keratins 8 and 18 phosphoglycoproteins (20; 130; 196; 49). *In vivo*, rotavirus infection reduces sucrase-isomaltase expression in human intestinal epithelial cells by perturbing protein targeting and organization of microvillar cytoskeleton (86).

The rotavirus infective cycle is totally cytoplasmatic and is schematised in figure 1.2.

Entry of rotavirus into cells in culture was studied by electron microscopy and starts with cell membrane attachment and virus cell penetration. The rotavirus attachment to the cellular membrane is mediated by the two outer layer proteins VP4 and VP7 (108; 59), and it is known that extracellular matrix proteins are required for virus attachment. Some, but not all animal rotavirus variants required the presence of sialic acid on cell membranes for efficient binding and infectivity (34; 126).

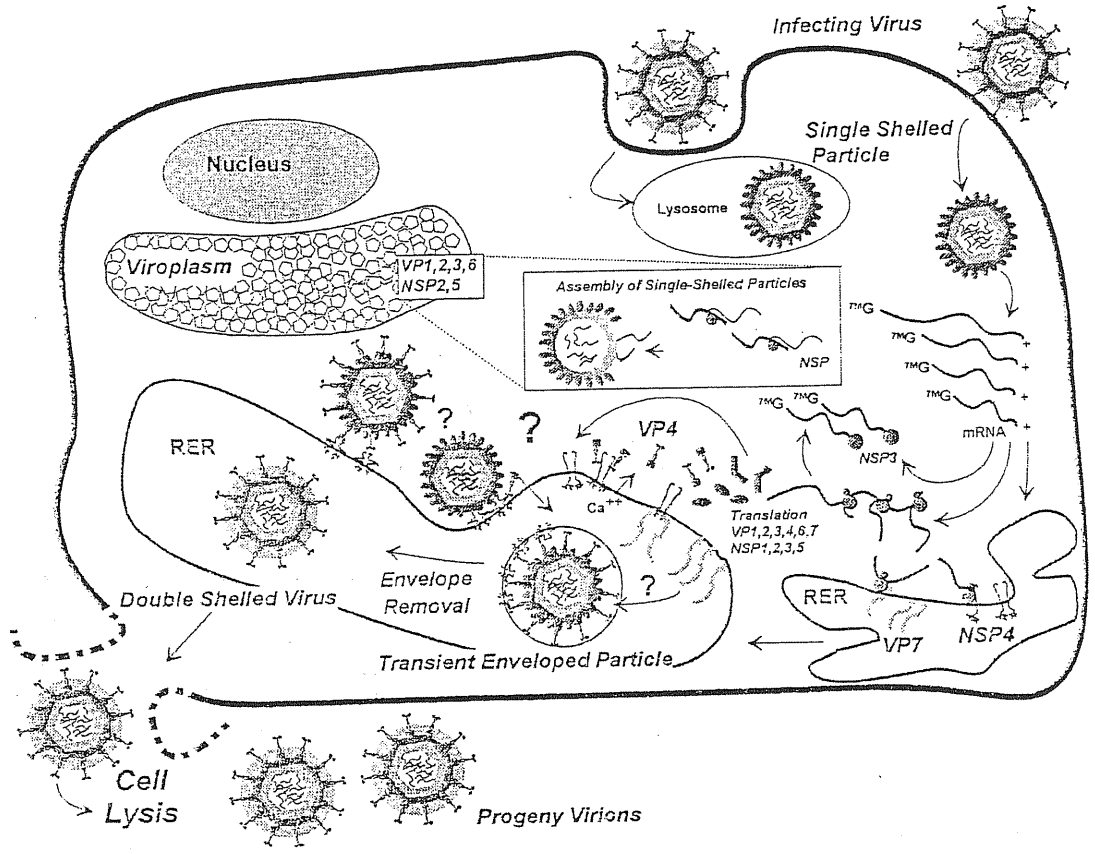

Figure 1.2. Major features of the rotavirus replication cycle (49).

Cell treatment with neuraminidases, which removes sialic acid, or incubation of the viruses with sialoglycoproteins (like glycophorin A), indeed dramatically reduces animal virus binding, with the consequent reduction of viral infectivity of some virus variants (108; 125).

Interestingly, two rotavirus cellular receptors were recently identified in integrins alpha2beta1 and alpha4beta1; VP4 and VP7 outer layer viral proteins in fact contain in their aminoacidic sequences tripeptides (DGE, GPR, LDV) that act as viral ligand for these integrins.

Moreover, incubation of the cells with these peptides or monoclonal antibodies directed to alpha2beta1 and alpha4beta1 integrins, block rotavirus infection (39). Recent studies show that the level of integrin alpha2beta1 on cell surface, directly correlates with rotavirus growth (105), and that non permissive K562 cells become permissive after expression of integrins alpha2beta1 or alpha4beta1 (76).

Rotavirus-induced membrane permeability and productive virus infection depends on the proteolytic cleavage of VP4 into VP8* and VP5* that takes place inside the small intestine by the action of pancreatic proteases. The importance of VP4 cleavage was studied in culture, and demonstrated that rotavirus replication does not occur after infection with uncleaved VP4 viruses (non-trypsin treated). Two different virus internalisation pathways have been described depending upon the proteolytic state of VP4: direct membrane and phagocytosis-lysosome penetration (181). However, only when VP4 is proteolitically cleaved, the virus enters directly into the cells and results in efficient replication (109).

Once the virus is internalised, a low cytoplasmic Ca^{2+} concentration induces the desegregation of the outer protein layer of the viral capsid in a process called "uncoating" (110). As a consequence, the double layered particles become transcriptionally active (37). Immediately, a high yield of single strand RNA with + polarity (+ssRNA) is synthesised (2). The newly made ssRNA transcripts carry out two functions: they are translated into the rotaviral proteins, and serve as templates for the production of – strands during dsRNA genome replication (175). With the exception of VP7 and NSP4, which are translated in association with the rough ER, all the other rotavirus proteins are translated by free ribosomes (49).

The place of rotavirus genome replication and virus assembly is viroplasms, highly electrondense protein-RNA aggregates that are detected in the cytoplasm from the early stage of infection (23, 6, 146, 182). Core proteins and several non structural proteins, such as NSP2 and NSP5, accumulate in these structures and may have some role in viral replication (146; 197). Other observations demonstrate an extensive co-localization of NSP4, VP7 and VP4

in a ring-like or semicircular structure in close association with viroplasm (72). The regulation of the packaging by which the correct set of 11 genome segments is encapsidated into each virion, remains a mystery. However, it is likely that some of the viral non-structural proteins may be involved in this process.

Nascent immature capsid particles (ICP) are budding from viroplasms and, through binding with the viral intracellular receptor NSP4, are targeted to ER where the final assembly of the outer layer proteins VP4 and VP7 occurs. During this unique morphogenetic process, the viral particles under final maturation are transiently enveloped. In the case of inefficient virus maturation, membrane enveloped double layered virus particles are accumulated in the cytoplasm (179). NSP4 contains a membrane destabilisation domain involved in the removal of the transitory membrane envelope from mature viral particles (188). Moreover, NSP4 is responsible for modulating the intracellular calcium concentration that induces cell death, and is important in further releasing of mature virions from infected cell.

Rotavirus infection determines the shut-off of the cellular protein synthesis (49), however, recently four different cellular proteins were found specifically upregulated after virus infection. Two of them were identified as the ER-associated proteins BiP and endoplasmin, members of a family of glucose-regulated chaperone proteins (203). Interestingly, the transcription of these genes is regulated directly by rotavirus ER-associated protein NSP4, in viral infected cells as well as in cells transiently expressing NSP4 alone (203). The mechanism by which these genes are upregulated is not known: however, NSP4 does not seem to be associated with either of BiP and endoplasmin. The important role of the correct viral protein glycosylation in the mechanism of viral envelope removing, was also confirmed by treatment of infected cells with tunicamycin, that did not abolish cell lysis but inhibited the liberation of particles (129). In particular, the specific block of NSP4 glycosylation results in the maintaining of enveloped viral particles.

During double-shelled (ds) particle assembly, subviral particles [possibly single-shelled (ss) particles] acquire the outer capsid proteins during their transport across the endoplasmic reticulum membrane by an exocytosis-like process, probably by a fusion-like mechanism. Fine reticular material is observed around the junction area between virus particles and the ER membrane on the cytoplasmic side of projecting ss particles, suggesting this is the site of assembly of ds particles. On the other hand, the budding process simply serves as a vehicle to transport ss particles from the cytoplasm to the ER lumen (180).

Rotavirus ethiology

Rotaviruses are the leading cause of severe, life-threatening viral gastroenteritis in infants and animals worldwide (88) and they assume a special significance in poor countries, where they constitute a major cause of mortality among the young (figure 1.3).

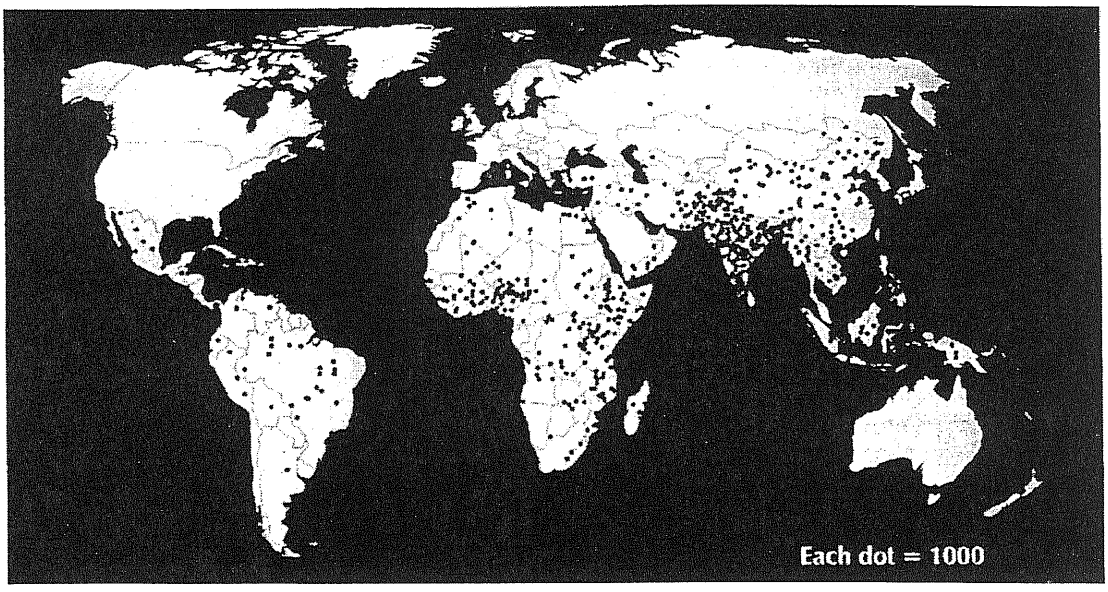

Figure 1.3. Distribution of rotavirus infection in the world (111).

In a recent epidemiology study, it was estimated that during a single year there were 1 billion cases of diarrhea in infants and young children in Asia, Africa and Latin America resulting in 3.3 million of deaths (66; 14).

The outcome of the infection is age related. Although rotavirus may infect individuals and animals of all ages, symptomatic infection (diarrhea) generally occurs in the young (6 months up to 2 years children, and up to 14 days mice).

Despite the prevalence of rotavirus infection and extensive studies in animal models, rotavirus pathogenesis and the mechanism underlying the intestinal fluid loss in rotavirus diarrhea are not completely known. There are evidences that transcription- and replication-defective rotaviruses cause diarrhea in animal models, suggesting that rotavirus attachment or entry into cells is sufficient for the induction of diarrhea (172). Rotaviruses have a limited tissue tropism, with infection restricted to cells of small intestine, and infects fully differentiated enterocytes via their apical surface. During infection the mucosal architecture undergoes remodelling, which results in the stunting of the villi and flattening and loss of enterocytes. The generation of diarrhea is a multifactorial process involving Ca^{2+}-dependent secretory processes of mediators, water and electrolytes, as well as the induction of cell death in the different cell types that compose the intestinal epithelium. It was moreover reported that rotavirus-induced diarrhea causes changes in the microcirculation of intestinal villi of neonatal mice in relation to the induction and persistence secretion (136; 176). Recently it was demonstrated that purified NSP4 causes diarrhea in young mice in an age-dependent, dose-dependent and specific manner. It is proposed that NSP4 acts as an enterotoxin, because it has toxin-like effect when transiently expressed in cells and is capable of inducing secretory diarrhea in neonatal mice; these effects are selectively blocked by anti-NSP4 antibodies (77; 47; 10). Moreover, NSP4 directly causes the inhibition of the Na^{+}-D-glucose symporter (SGLT1) (74). This effect, implying a concomitant inhibition of water reabsorption, is postulated to play a mechanicistic role in the pathogenesis of rotavirus diarrhea. Another interesting hypothesis is that rotavirus evokes intestinal

fluid and electrolyte secretion by systemic activation of the nervous system in the intestinal wall, that is the enteric nervous system (ENS). Four different drugs that inhibit ENS were tested and significantly attenuated the intestinal secretory response to rotavirus, strongly suggesting that ENS participates in the virus induced electrolyte and fluid secretion, as has been shown for bacterial enterotoxin (111). A possible interpretation of the ENS action, is that the increasing of Ca^{2+} concentration induced by NSP4, may trigger the release of amines or peptides from the endocrine cells of the gut to stimulate dendrites or free nerve endings located underneath the epithelial layer, thereby activating secretory nervous reflexes. Moreover, as a possible therapeutic approach, the intestinal secretion that activate ENS via the intestinal endocrine cells can be significantly inhibited by the calcium channels blockers, which markedly attenuate the release of amines and peptides from these cells (191).

In trying to explain how rotavirus loses its infectivity in adults, a model has been recently proposed in which the contemporaneous presence of two categories of cellular receptors is necessary for symptomatic diarrhea (10). One of the two is important for virus entry and gene expression, but not needed in disease, whereas the second may regulate NSP4-specific functions. According to this model, the concentration of NSP4 receptor may be substantially reduced in adult animals, thus resulting in no disease.

No vaccine is yet available, since the oral tetravalent rhesus reassortant vaccine proposed a few years ago (89) has been withdrawn from the market (USA only) because unsafe, causing death in a number of children treated (201). The early attempts to develop a vaccine focused on animal forms of rotavirus, recently are shifted to effort to create human-animal reassortants that have been far more successful (84).

Rotavirus genome

Rotavirus genome consists of 11 segments of base paired double stranded RNA with a size range of 0.6 to 3.3 kilobase pairs (51). Rotavirus dsRNA genes could be purified and resolved according to their length on 10% polyacrilamide gels, resolving rotavirus genome fragments into 11 bands (see figure 1.1, page 2), while possible viral single strand mRNA has lower mobility and remain near the origin (144). Deproteinased rotavirus dsRNA genome is not infectious, reflecting the need for the viral RNA polymerase for genome transcription and replication. The newly replicated dsRNA genome is formed within nascent subviral particles in viroplasms, and free dsRNA or free ssRNA with negative polarity was never found in infected cells.

The genome sequences of the different rotavirus strains show general features about the structure of each genome segments, and are A+T rich (58-67%) (figure 1.4). Peculiarities in rotavirus genome are also common to other members of Reoviridae family (reovirus, cytoplasmic polyhedrosis virus, orbivirus) and to others virus families with segmented genome (Ortomyxoviradae, Arenaviridae, Bunyaviridae) (60, 49).

Segment[a]	Base pairs	G + C (%)	Noncoding sequences[b] 5′	Noncoding sequences[b] 3′	First AUG is a favored sequence for initiation	Additional long ORF[c]	Amino acids[d]	References
1	3,302	34.6	18	17	Yes	No	1,088	211
2	2,690	32.9	16	28	Yes	No	881	211
3	2,591	28.9	49	35	Yes	No	835	170,211
4	2,362	34.7	9	22	Yes	No	776	222
5	1,581	33.9	32	73	Yes	No	491	211
6	1,356	38.6	23	139	Yes	No	397	95
7	1,104	33.5	25	131	No	Yes (2-i)	315 (312,306)	29
8	1,059	35.5	46	59	Yes	No	317	30
9	1,062	35.9	48	33	No	Yes (1-i)	326 (297)	9,31
10	751	40.2	41	182	Yes	Yes (2-i)	175	32
11	667	38.6	21	49	Yes	Yes (1-o)	198 (92)	210

Figure 1.4a. Nucleotide sequences of rotavirus genome segments.

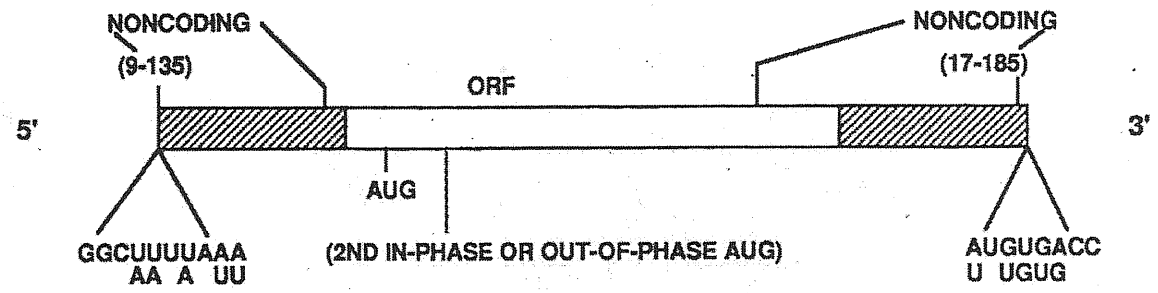

Figure 1.4b. Major features of rotavirus gene structure. (49).

Rotavirus dsRNA segments contain cap structures at the 5'end of the positive strand RNA (Imai, 1983), while lacking in the 3'-end polyadenilation signals (122). Each RNA segment starts with a 5'-guanylate followed by a set of conserved sequences that are part of the 5' non-coding sequences (called untranslated region, UTR). Usually, the 5' UTR is followed by a unique open reading frame (ORF), coding for a single protein product and ending with the stop codon. Although some of the genes possess additional in-phase or out-of-phase ORFs, current evidences indicate that they are monocystronic, except possibly for genes 9 and 11 (22; 119). Gene transcription starts under strong initiation codon based on Kozak's rules. The 3' set of non-coding sequences (3' UTR) contain a subset of conserved terminal 3' sequences, and end with a 3'-terminal cytidine (49). The strong conservation of 5' and 3' terminal UTRs in rotavirus genome segments suggests that they contain signals important for transcription, RNA transport, replication and assembly of the viral genome. Indeed cis-acting signals that promote minus-strand synthesis were found in rotavirus UTRs (50).

Rearrangements

An interesting aspect of segmented viruses in general, and of rotavirus in particular, is the ability of the virions to assemble a precise set of genome segments into newly made virions. Understanding how this occurs remains a major challenge because this knowledge might lead to the development of reverse genetics systems to allow dissections of the gene functions of these viruses as well as their use as vectors for delivery of other genes. In the absence of a reverse genetic system, genetic analysis has exploited the fact that the genome segments can undergo reassortment during mixed infections (49).

Analysis of the genomic electropherotypes is the popular technique for virus detection and is used for molecular epidemiology studies. However, because distinct RNA patterns can arise through different mechanisms, the genome profiles can not be used as the sole criterion for the classification of a virus strain. The electrophoretic migration rate of cognate RNA segments (segments encoding the same protein) in different virus strains often shows heterogeneity. In contrast, sequence data show that cognate genes from different strains usually contain the same number of nucleotides. Therefore, the heterogeneity in RNA segment mobility in cognate fragments is to be attributed to sequence differences, and secondary and tertiary structures that remain during the electrophoresis of these segments.

Whereas a total of 11 RNA segments are invariably packaged, there seem to be much less constraint on the length of individual RNA fragment assembled into mature virus particle. One mechanism which generates heterogeneity in RNA segment mobility in cognate RNA fragments is genome rearrangements that consists preliminary in concatamerisation and duplication with evident changes in gel mobility. Virus with rearrangements in segments 5, 6, 8, 10 and 11 have been characterised (67). Modifications in fragment 11 are very frequent, with unknown apparent reason (33; 64). It is

unknown whether the rearrangements in fragament 11 occur more frequently, or if these viruses have some selective advantage (better growth or stability), so that they are more easily detected (120). Viruses containing rearranged genome fragments are generally not defective structurally and functionally. Biophysical characterization of rearranged gene segment viruses has shown that up to 1800 additional nucleotides can be packaged into particles, without causing detectable changes in particle diameter or in sedimentation values. However the density of particles containing rearranged genomes may be increased proportionally to the additional base pairs added (123). These studies indicate that rotavirus have a considerable capacity of packaging additional RNA, although the upper limit is obscure. Interestingly, a series of temperature-sensitive mutants that map to rotavirus segments have been characterised (114; 160; 161; 30) and their different infective phenotypes were important to rotavirus gene assignment and proteins function as shown in figure 1.5.infective phenotypes were important to rotavirus gene assignment and proteins function as shown in figure 1.5.

Mutant group	Prototype mutant	% wild-type synthesis at 39°C			Host shut-off	Mapped to genome segment (protein)
		ssRNA	dsRNA	Protein		
A	tsA(778)	100	75	100	+	4 (VP4)
B	tsB(339)	5	5	25	+	3 (VP3)
C	tsC(606)	5	5	25	+	1 (VP1)
D	tsD(975)	100	100	150	+	NA
E	tsE(400)	<5	<5	20	+	8 (NSP2)
F	tsF(2124)	100	<5	20	−	2 (VP2)
G	tsG(2130)	100	<5	20	−	6 (VP6)
H	tsH(2384)	100	100	100	−	NA
I	tsI(2403)	100	100	100	−	NA
J	tsJ(2131)	100	75	100	+	NA

Data from Gombold and Ramig (114) and Ramig and Petrie (263).
NA, no assignment.

Figure 1.5. Summary of the characteristics of rotavirus temperature sensitive mutants.

Viral proteins

Genome segment	Protein product	Nascent polypeptide (M_r)	Mature protein modified	Location in virus particles	Number of molecules per virion[c]	Function
1	VP1	125,005 (125K)	—	Inner core	ND	RNA polymerase
2	VP2	102,431 (94K)	Cleaved	Inner core	120	RNA binding
3	VP3	98,120 (88K)	—	Inner core	ND	Guanylyltransferase
4	VP4 (VP5* + VP8*)	86,782 (88K)	Cleaved VP5* (529) VP8 (247)[e]	Outer capsid	120	Hemagglutinin, neutralization antigen, protease-enhanced infectivity, virulence, putative fusion region, cell attachment
5	NSP1 (NS53)	58,654 (53K)	—	Nonstructural		Slightly basic, zinc finger, RNA binding
6	VP6	44,816 (41K)	—	Inner capsid	780	Hydrophobic, trimer, subgroup antigen
7	NSP3 (NS34)	34,600 (34K)	—	Nonstructural		Slightly acidic, RNA binding
8	NSP2 (NS35)	36,700 (35K)	—	Nonstructural		Basic, RNA binding
9	VP7	37,368 (38K)	Cleaved signal sequence, high mannose clycosylation and trimming	Outer capsid	780	RER integral membrane glycoprotein neutralization antigen, bicistronic gene two hydrophobic NH_2-terminal regions
10	NSP4 (NS28)	20,290 (28K)	29K–28K, uncleaved signal sequence, high mannose glycosylation and trimming	Nonstructural		RER transmembrane glycoprotein, role in morphogenesis, three hydrophobic NH_2-terminal regions
11	NSP5 (NS26)	21,725 (26K)	28K, phosphorylated *O*-glycosylated	Nonstructural		Slightly basic, rich in serine and threonine, RNA binding

Figure 1.6. Summary of the characteristics of rotavirus structural (VP) and non-structural (NSP) proteins (49).

Structural proteins

VP1 is a component of the rotavirus inner enzymatic core and is part of the viral replicase and the transcriptase complex. Temperature-sensitive (ts) mutants that map to rotavirus segment encoding VP1 (gene 1) (tsC) indeed have a ss and ds RNA-negative phenotype (30; 66b). Moreover, the VP1 sequence shares the common motifs conserved in the sequences of all the polymerase showing RNA template specificity (151). The conclusive demonstration that VP1 is the rotavirus RNA-dependent RNA polymerase, has been obtained with radiolabelling of rotavirus VP1 with the photoreactable nucleotide analog ^{32}P-8-azido-ATP, that inhibits the transcription activity of the polymerase after UV light exposure (193). Interestingly, VP1 specifically binds to the 3'-end of viral mRNA in the absence of any other viral proteins, but this interaction is not sufficient to initiate minus-strand synthesis (139). VP1 expressed in baculovirus has replicase activity only after contemporaneous expression of VP2 (207), and recent evidences have demonstrated that VP1 indeed requires the core shell proteins to synthesise the double-stranded RNA genome (138). Moreover, it has been asserted that VP1 interacts with other structural (VP2 or VP3) (208) or non structural (NSP2) viral proteins (7; 4), in specific structural and functional manner.

VP2 constitutes the inner protein layer of the rotavirus structure and it has been demonstrated that its amino-terminus possesses unspecific single- and double-stranded RNA binding activity (18). Moreover, rotavirus ts mutants for rotavirus gene 2 (tsF), do not synthesise ss and dsRNA at the not permissive temperature and have improper viral capsid assembly (114).
It has been demonstrated that the amino-terminus of VP2 is essential for the final assembly of the polymerase enzyme VP1 and guanylyltransferase VP3 into the core of the virion (208). Baculovirus-expressed VP1 and VP2 have been shown to assemble into the simplest protein structures with replicase activity, called core-like particles (CLPs) (138). Biochemical and structural

studies obtained with electron cryomicroscopy and image reconstruction have thus suggested that VP2 appears to act as a scaffold for the proper assembly of the components of the viral core (100; 101).

VP3 is a component of the inner enzymatic core with sequence independent ssRNA-binding activity and, interestingly, with preferential affinity for uncapped over capped RNA (137). Baculovirus expressed VP3 protein was found to covalently bind γ-[32P]-GTP, suggesting its role as rotavirus guanylyltransferase (104; 150). In virus infected cells, VP3 guanylyltransferase activity is nonspecific and is able to cap RNAs initiating with indifferently G or A residue (137). After UV crosslinking, VP3 covalently binds S-adenosyl-l-methionine (SAM), the usual substrate required for methyltransferase activity (25). These studies indicates that VP3 may be a multifunctional capping enzyme, with both guanylyltransferase and methyltransferase activity.
The phenotype of rotavirus ts mutants (tsB) carrying a mutation in VP3 encoding gene (gene 3), was initially identified negative for viral transcription and replication (68). Analysis of viral particles made by tsB infected cells at the restrictive temperature, showed however that only empty single-shelled particles were assembled (194). This indicates that viral morphogenesis is haltered after the initial viral transcription and before RNA replication, suggesting that VP3 may also have an eventual early function in the replication but not in further viral particle assembly.

VP4 is an unglycosylated protein of the rotavirus outer layer that has been implicated in cell attachment, penetration, hemagglutination, neutralization, virulence, and host range. From three-dimensional structure it was discovered that the sixty surface spikes that project from the outer layer of mature virions are made up of dimer of VP4 (205; 158).
The involvement of VP4 in cell binding was suggested by analysis of VP4-containing virus like particles expressed in baculovirus (40). Both sialic acid-dependent and -independent virus-cell attachments are mediated by VP4

(107; 108). It was moreover found that VP4 is directly involved in the recognition of cellular integrin receptor. Aminoacidic sequence of VP4 (as VP7) contains in fact a specific tripeptide (DGE) that is ligand for alpha2beta1 integrin (39).

Peculiarity of VP4 protein, is its trypsin-dependent cleavage into two polypeptides, VP8* and VP5*, that are respectively the N- and the C-terminal portion of VP4 and that remain associated to the virus outer layer (109). The cleavage site is highly conserved (arginine 247) and the two cleavage products remain linked through an intrachain disulfide bond (140). Biologically, VP4 cleavage results in enhancement of viral infectivity, enhancing the virus penetration into cells, but not cell attachment (59; 36). VP5* has a direct role in viral cell entry and may have a membrane interactive domain. Recombinant expressed VP5* is able to permeabilize cell membranes in the absence of other rotavirus proteins as demonstrated by specific release of fluorocrome carboxyfluorescein after membrane permeabilisation (42). Moreover, site-directed mutagenesis of the VP5* hydrophobic domain (VP5*-HD, residues 385 to 404) has demonstrated the importance of this region of VP5* to induce membrane permeability (44).

Studies on cell attachment, have demonstrated that the two VP4 cleavage products, VP5* and VP8* have different functions depending on the rotavirus variants and their dependence on sialic acid-containing cell receptor (SA). Among the SA-dependent rhesus rotavirus (RRV), it was isolated a virus variants (nar3) that no longer depend on the presence of SA on the cell surface for efficient infection (126). This variant was important to demonstrate that VP5* domain of VP4 mediates nar3 SA-dependent cells attachment (206), while the wt RRV binds cell surface via VP8* (83). These results were also confirmed using recombinant GST-VP8* and GST-VP5* proteins produced in bacteria or neutralizing monoclonal antibodies directed to VP8* or VP5* (206). SA-binding domain has been mapped between aminoacids 93 and 208 of fragment VP8* (102), while mutations in positions 150 and 187 of VP4 mediate SA-independent cell interaction (107).

In infected cells VP4 is located in the space between the periphery of the viroplasm and the outside of the endoplasmic reticulum (130). However, more recent confocal microscopy analysis revealed that early after infection a fraction of VP4 is present at the plasma membrane and another fraction is cytoplasmic and colocalizes with beta-tubulin of the microtubule network (130). Recent studies performed with biotin labelling of infected cell surface monolayers allowed the identification of the existence of the non cleaved form of VP4 that is associated with the glycoprotein VP7 (130).
VP4 induces neutralising antibodies and protective immunity in animals and in children (131). Using a murine rotavirus model it has been demonstrated that intragastric administration of VP4-peptide protects subjects from challenge with virulent rotavirus (82), suggesting their potential use in rotavirus vaccine and therapy.

VP6 (SA11 strain segment 6) is the major structural component of the virions, highly conserved along the different rotavirus strains, is highly hydrophobic and immunogenic.
The structural relationship between VP6 (inner capsid polypeptide) and the viral core was studied using chemical cross-linking, suggesting the existence of a complex organization of VP6 with both the inner and the outer virus protein layer (78). VP6 interacts directly with the VP4 and core polypeptide VP2 and VP3 (171). VP6 protein expressed in baculovirus spontaneously forms trimers and has permitted to map the domains responsible for the trimerisation (residues 154-179 and 251-310) and for the interaction between the different viral structural proteins (residues 353-397) (3). VP6 N-terminus has an amphiphatic alpha-helix critical for virus assembly, and ts mutant analysis of mutants mapping in the VP6 gene (tsG), have an assembly negative phenotype, indicating that it possibly functions transporting VP6 to viroplasmic inclusions for double layer particles assembly (114). Removal of VP6 from double layered particles results in a loss of polymerase activity associated to viral transcription (15), suggesting that it may influence the correct structure of the transcriptase complex.

VP7 is a component of the virus outer layer encoded by gene 9 in SA11 virus strain. VP7 nucleotide sequence shows up to three in-frame initiation codons, even if the second is more represented in virus infected cells. Moreover, VP7 contains up to three glycosylation sites, of which only two are apparently used. VP7 protein is synthesised associated to the rough ER (200) and has an highly conserved signal peptide with a known cleavage site at glutamine 51 (178). VP7 aminoacid sequence lacks of characteristic sequence KDEL found to confer ER retention for some cellular proteins, but contains a conserved region of hydrophobic aminoacids (consensus peptide LPXTG) that acts as the signal sequence to direct VP7 ER targeting (49). Deletions in these sequences interestingly showed an abnormal VP7 processing through the Golgi apparatus by addition of several carbohydrate residues followed by erroneous VP7 secretion into the extracellular medium.
As VP4, VP7 is the virus protein responsible of integrin-mediated virus-cell binding and its aminoacidic sequence contains tripeptides sequences (GPR and LDV) that are ligands respectively for integrins alphaxbeta2 and alpha4beta1 (39). In VP7, these sequences are embedded in a disintegrin-like domain that also shows sequence similarity to fibronectin and the Tie receptor tyrosine kinase (39).
Protein folding of VP7 requires ATP and cellular, but not viral, factors for correct disulfide bond formation (127). Studying the relation of cellular proteins with viral proteins, it was found indeed that the ER-associated chaperone calnexin interacts with the ER-associated rotavirus proteins, VP7 and NSP4 (128), suggesting that calnexin promotes folding and assembly of these glycoproteins during viral infection.

Non structural proteins

Properties of most of the non-structural proteins are only beginning to be understood. However, it was observed that the non-structural proteins possess a basic charge, are able to bind RNA, are present in subviral particles with replicase activity and that ts mutants that map to their segments have RNA replication negative phenotype (30; 66b). These data suggest that the rotavirus non structural proteins function as part of the replication complex, as chaperones to transport RNAs or proteins to the sites of RNA replication, assembly and packaging.

Rotavirus NSP1 (also previously known as NS53) is encoded by gene 5 and is interesting for its extreme sequence diversity. Recently, the comparison of NSP1 protein sequences among the different species showed poor amino acid homologies (respectively 36-38% and 68%) reflecting their extreme divergence. In infected cells NSP1 is present in association with the cytoskeletal matrix, thus providing evidence that the subcellular localization signal in NSP1 resides in the amino terminal half of the protein (79). However, a large amount of NSP1 is diffused in the cytosol and studying NSP1 mutants it was identified the domain responsible for intracellular soluble localization of the protein (residues 84 and 176) (81).
NSP1 has RNA-binding activity specific for elements located at the 5' end of viral mRNAs. The RNA-binding domain of NSP1 resides within the first 81 aminoacids of the protein (141). As predicted also for other RNA-binding protein of rotavirus (as NSP2), RNA-folding predictions suggest that the 5′ end of the NSP1 mRNA interacts with itself, producing a stem-loop structure.
Peculiarity of NSP1 aminoacid sequence is the highly conserved cysteine-rich region forming zinc finger motif (nucleotides 156 to 248). The importance of this region is unknown (184). The carboxyl-terminal 233 aa of NSP1 are not required for rotavirus replication *in vitro* and deletion of the cystein rich region (up to 500 nucleotides) originates in non-defective

reassortant rotavirus mutants that normally replicate in cultured cells (79, 80). However, it is known that the cystein rich region is essential for NSP1 RNA-binding activity (134; 185).

The viral non-structural protein NSP3 is encoded by gene 7 has been implicated in the assembly of the 11 viral positive sense ssRNAs into the early replication intermediates during rotavirus morphogenesis (155). Immunofluorescence technique of virus infected cells reveals that NSP3 shows a diffuse cytoplasmic distribution, thus not localising in viroplasm (8). NSP3 is a rotavirus sequence-specific RNA binding protein that binds specifically the non polyadenylated 3'-end of rotavirus mRNAs (155), probably stabilising the viral ssRNA. Recombinant NSP3 protein expressed in baculovirus and UV cross-linking, have demonstrated that the minimal sequence recognized by NSP3 is GACC located from nucleotides 8 to 15 at the 3-terminal end of the viral RNA (153, 154). NSP3 is a protein slightly acidic organised in alpha-helices, with several heptad repeats of hydrophobic aminoacids present in its carboxyl half (118). NSP3 sequence analysis did not reveal significant homologies with other RNA binding proteins (163), thus NSP3 proteins of rotavirus may be the prototype of a new kind of sequence-specific RNA binding protein.

Recently it was reported that recombinant NSP3 is responsible of viral translation enhancement in transfected cells as well as in the rabbit reticulocyte translation system (195). These data were supported by the important discovery that the last C-terminal 107 aminoacids of NSP3 interacts with the eukaryotic translation initiation factor 4-GI subunit (eIF-4GI) (149). Studies on NSP3 mutants and yeast two-hybrid system, have indicated that the NSP3 RNA- and eIF4G-binding domains are separated by a dimerization domain (aminoacids 150 -206), that is required for strong RNA binding (148). It was hypothesised that NSP3 may form a link between the viral mRNA and the cellular translation machinery (195). Interestingly, the amount of cellular poly(A)-binding protein (PABP) present in eIF4F complexes decreases during rotavirus infection (149), suggesting that NSP3

is working as a functional analogue of PABP. These results also suggest that NSP3, by taking the place of PABP on eIF4GI, is responsible for the shut-off of cellular protein synthesis.

SA11 gene 10 codes for NSP4, a non-structural glycosylated protein that localises in the ER membrane. The amino-terminus of NSP4 contains 3 hydrophobic domains and 2 N-linked mannose glycosylation sites, that are tunicamycin sesitive (147). The amino-terminus of NSP4 has a non-cleavable signal sequence to ER retention, connected through a protease-resistant alpha-helical coiled-coil stem with the C-terminus protruding in the cytoplasm (187). The cytoplasmic C-terminal domain of NSP4 acts as viral receptor to bind immature double layered viral particles (immature capsid particles, ICP) and to mediate the budding of immature virions into the lumen of the ER (9), where takes place the final steps of viral morphogenesis. The structure model of NSP4 cytoplasmic region suggests that four NSP4 molecules tetramerise trough their four flexible C-terminal 28 aminoacids projecting from the ER (187). The ICP-binding site was map indeed in the last 20 aminoacids of each tetramer-forming peptide (133). This organization suggests a novel NSP4 structure for its icosahedral virus receptor function.

Purified NSP4 or a peptide corresponding to NSP4 residues 114 to 135, is sufficient to induce diarrhea in young mice in a age-dependent and dose-dependent manner, thus acting as a viral enterotoxin (10). This effect depends by trans-epithelial chloride secretion by calcium-dependent signalling pathway. NSP4 is infact the only viral protein noted to be responsible for the increase in cytosolic calcium concentration observed in rotavirus-infected cells (190). Studies on NSP4-induced $[Ca^{2+}]i$ mobilisation propose a transient stimulation of inositol 1,4,5-trisphosphate (IP3) production through receptor-mediated phospholipase C activation (43). Moreover, NSP4 peptide 114-135 that causes diarrhea in young rodents, is a specific inhibitor of the Na^+-D-glucose symporter (SGLT1), while peptide 464-483 inhibits Na^+-L-leucine symport during rotavirus infection *in vivo*

(74). Moreover, the glucose-regulated chaperone proteins BiP and Endoplasmin, were found directly upregulated by rotavirus NSP4 (203).
It has been hypothesized that NSP4 is involved in the removal of the transient envelope acquired during viral morphogenesis (50; 147). Interestingly, glycosylation of NSP4 is required for removal of the transient envelope from ER-budding mature viral particles; in fact treatment of infected cells with tunicamycin maintains enveloped viral particles (129; 147). Consistently, NSP4 possesses a direct membrane-destabilization activity (MDA, residues 48 - 91), that may cause ER membrane damage, playing a role in the removing of the transient viral envelope (19; 188). Last studies suggest that the membrane-destabilizing and the enterotoxic properties of NSP4 may be mediated by different regions of the polypeptide (19).

Rotavirus non-structural protein NSP5

In strain SA11, NSP5 (previously known as NS26) is the product of the longer open reading frame of genome segment 11 and encodes for a protein of 198 aminoacids (197). However, a second internal open reading frame (position 52) encodes for a shorter phosphoprotein of 92 aa (22 kDa), named NSP6 (119). No significance of the presence of NSP6 was found until now, but NSP6 was not always synthesised in the different rotavirus strains, as in fact absent in OSU strain. However, recently using the yeast two hybrid system it was described the existence of NSP5-NSP6 heterodimers in infected cells, that involve the last C-terminal 35 residues of NSP5 (192).
NSP5 aminoacid sequence is highly conserved among the different rotavirus species (106) and no mutants in NSP5 gene was ever found, suggesting that NSP5 may play a fundamental role in rotavirus cycle (64; 69; 70; 71). Some rotavirus strains carry a gene 11 head-to-tail duplication that however as the parental strain, results in identical NSP5 protein synthesis and virus replication (33; 93; 64). There are no sequence structure predictions for NSP5 and the sequence characteristics have still unknown significance. As shown

and the sequence characteristics have still unknown significance. As shown in figure 1.7, NSP5 primary sequence is characterised by an overall high content of Serine (21%) and Threonine (4.5%), that is even higher in the last N-terminal 131 aminoacids (30.5%). Moreover, there are interesting SDS repeats with unknown significance and a "basic-acid-basic domain" (BAB) of highly charged 49 aminoacid residues (60% charged residues), located between residues 131 and 179, similar to that found in other RNA binding proteins.

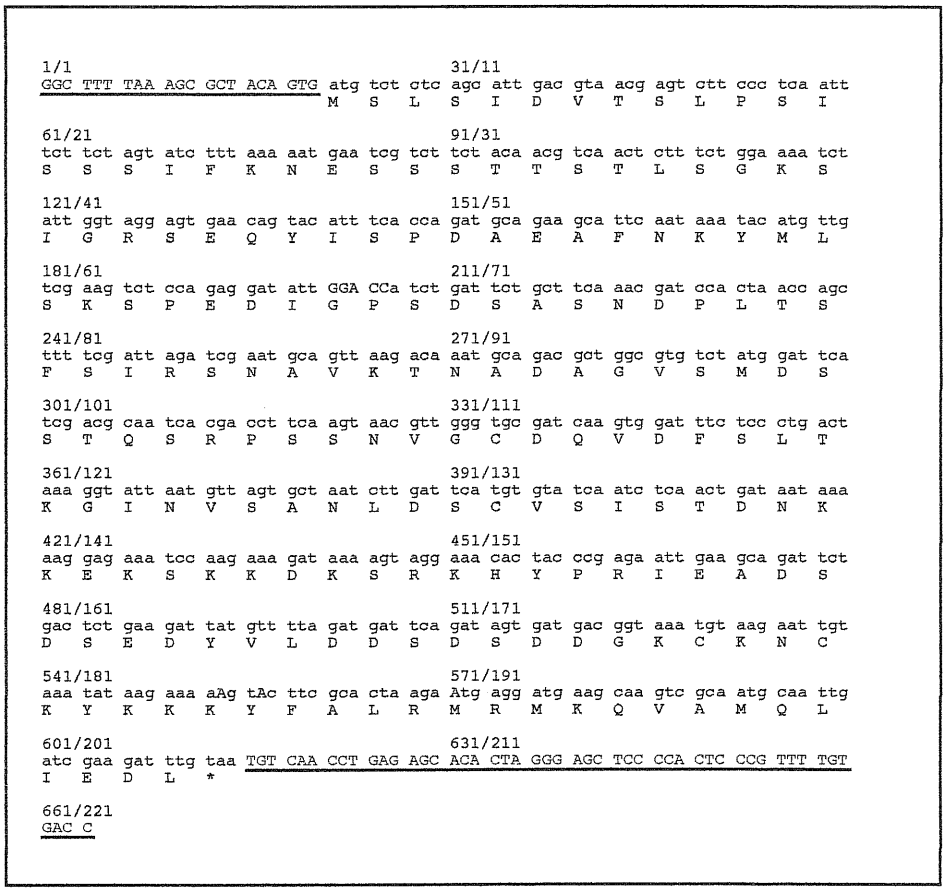

Figure 1.7. Nucleotide sequence of rotavirus SA11 gene 11, and aminoacid translation of NSP5. Underlined nucleotides represent the gene 11 5′ and 3′ untranslated region (UTRs).

In NSP5 protein sequence there are phosphorylation recognition sites for protein kinase C (SXR/KR/KXXS and K/RXS at residues 22, 30, 75, 100 and 136) and serine residues (at position 56, 154 and 165) potential substrates of casein kinase II (SXXD/E) (17). The last 18 C-terminal aminoacids of NSP5 are highly conserved (120; 119). It was found that the last 20 C-terminal aminoacids of NSP5 are the homomultimerization domain, which have a predicted alpha-helical structure (192).

NSP5 was originally described with an apparent molecular mass of 26 kDa in SDS-PAGE (45; 116) that further undergoes hyperphosphorylation and cytoplasmatic glycosylation changing its gel mobility (5; 69). The main modification of NSP5 is the hyperphosphorylation that produces NSP5 mature species from 28 to 32-34 kDa (figure 1.8) (5). NSP5 phosphorylation occurs on serine and threonine residues (5) and is sensitive to λ-phosphatase treatment (λ-Ppase), converting all the hyperphosphorylated species to an unique band of 26 kDa (figure 1.8b, lane 4).

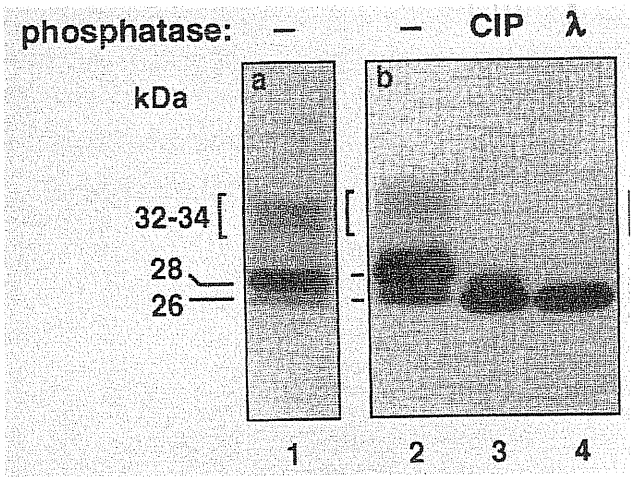

Figure 1.8. SDS-PAGE analysis of NSP5.
a. Immunoblot analysis of extracts of rotavirus infeceted cells and reacted with anti-NSP5 serum.
b. Immunoprecipitation of NSP5 from virus infected cells
c. labelled with ^{35}S-Met. Calf intestinal phosphatase (CIP) and λ-Ppase treatments are indicated (5).

Phosphorylated NSP5 isolated from infected cells, is sensitive also to protein phosphatasae 2A (PP2A) and calf intestinal phosphatase that dephosphorylate NSP5 28- 30- and 24 kDa species and induce accumulation of the 26 kDa form that however remain phophorylated (5; 17; 152). Treatment of NSP5-expressing cells with staurosporine, a board-range of protein serin/threonin kinase inhibitor (124; 183), has only a limited negative effect on the NSP5 phosphorylation and moreover, does not inhibit autophosphorylation of NSP5 *in vitro* (16). Inhibition of cellular phosphatases (PP1 and PP2A) with okadaic acid has demonstrated that NSP5 phosphorylation partially is increased in transfected cells as in rotavirus-infected cells, even if these last in lower extent (16). The mechanism that regulates NSP5 phosphorylation however, is not completely known. There are evidences that it may be an autophosphorylation activity. NSP5 obtained from infected cells, could be phosphorylated *in vitro* by incubation of immunoprecipitates with γ-[^{32}P]-ATP, producing mainly phosphorylated products of 28 and 32-34 kDa, suggesting that indeed NSP5 may have a kinase activity (5). It has been described that purified NSP5 isolated from bacterial expressing cells, is capable of autophosphorylation but with much lower activity than the protein isolated from rotavirus infected cells (17; 152). However, we have never observed that NSP5 recombinant protein purified from bacteria shows autophosphorylation activity, while it occurs in a large extent in presence of cellular protein extracts (Vascotto, Eichwald and Burrone, unpublished).
As it will described extensively in this thesis, NSP5 phosphorylation is dependent by the presence of viral proteins as NSP2 as well as cellular proteins, activating different sites responsible of the NSP5 hyperphosphorylation.

NSP5 is also modified by addition of N-acetylglucosamine (NAcGlc) on serine residues (O-glycosylation) in the cytoplasm of infected cells (69). NSP5 *in vivo* labelling with 1,6-[^{3}H]-glucosammine, shows that the NSP5

glycosylation occurs mainly on 26 and 28 kDa species, and that the glycosylated form of 28 kDa is converted to 26 kDa by λ-Ppase treatment (5). It was also suggested that the level of phosphorylation and/or O-glycosylation of the NSP5 might play a fine regulatory function during viral infection.

Early EM and specific immunofluorescence studies of viral infected cells, show that NSP5 is associated from the early stages of infection to cytoplasmic viroplasms, where the replication occurs (146). Moreover, as it is described in this thesis, NSP5 and NSP2 in absence of other rotavirus proteins, are sufficient to form cytoplasmic viroplasm-like structures (VLS), analogous to viroplasms found in infected cells (53).

Until now, no function has yet been assigned to NSP5, even if its presence in viroplasms and the absence of ts mutant for NSP5-encoding segment 11 ever found, highly suggest that it may have a role in virus replication.

Rotavirus non-structural protein NSP2

NSP2 is a conserved basic protein of 35 kDa encoded in SA11 strain by gene segment 8. NSP2 aminoacid sequence (see figure 3.1 page 57) is highly conserved in the different rotavirus strains (141) and residues 54 and 87 show region of high similarity with bacterial metallo-proteinases (30% identity, 70% similarity) (117).

NSP2, as also NSP5, accumulates in infected cells in viroplasms (146) and it was found also associated to purified immature particles ("sub-viral particles") with replicase activity (143; 89; 75). Cells infected with NSP2 temperature sensitive mutants (tsE), contain few viroplasms, lack replication intermediates with replicase activity and produce empty virus particles lacking RNA (68; 30), thus suggesting that may play an essential role in RNA packaging and may coordinate virion assembly. Moreover, at the non-permissive temperature, the tsE strains lose the ability to synthesize dsRNA and also have a significant reduction in the synthesis of the ssRNA (30).

UV crosslinking of virus infected cells has demonstrated that NSP2 possesses sequence unspecific RNA-binding capacity directed versus as viral ss- and as dsRNA (91), even though displayed little affinity for dsRNA (186).
Moreover, NSP2 was found bound to the partially replicated 11 dsRNA genome fragments of the virus (7), indicating that may be directly involved in the replication process. Chemical (DSP)-crosslinking of infected cells and specific immunoprecipitation indeed revealed that NSP2 interacts with the viral RNA polymerase VP1 (90; 4). Moreover, a complex with *in vitro* replicase activity was recovered from infected cells only after incubation with antibodies against NSP2 (7), suggesting that NSP2, but not other non structural proteins, is directly linked to the replicase complex. We have also demonstrated that the direct interaction with NSP5 and NSP2 regulates NSP5 phosphorylation state (4). It was hypothesised that NSP2 and NSP5 may have a role in viroplasm formation, since the two proteins are sufficient to form viroplasm-like structure *in vivo* (53).
Sedimentation analysis of NSP2 expressed in infected cells or in the reticulocyte-dependent translation system, showed that it assembles into multimers of approximately 10S (90). In a recent study in fact, it was shown that the C-terminally His-tagged NSP2 expressed in bacteria (rNSP2) did not exist as a monomer but rather was present as an 8S-10S homomultimers consisting of 6±2 subunits of rNSP2 (186). Interestingly, the authors assess that enzymatic analysis on rNSP2 revealed that it possessed an associated nucleoside triphosphatase (NTPase) activity *in vitro*, which in the presence of Mg^{2+} catalyzed the hydrolysis of each of the four NTPs to NDPs with equal efficiency (186).
Recently, the solution structure of rNSP2 was characterized revealing that indeed NSP2 exists as an octamer, which is functional and with more compact conformation in the binding of RNA and ADP, while undergoes partial dissociation into smaller oligomers in the presence of magnesium. The secondary structure of NSP2 showed a high fraction of beta-sheet. It was proposed that NSP2 functions as a molecular motor, catalysing the packaging of viral mRNA into core-like replication intermediates through

the energy derived from its NTPase activity. That NSP2 can exist in different conformations lends support this hypothesis.

Virus-like particles produced in insect cells

A peculiarity of some rotavirus structural proteins is their ability to self-assemble *in vitro*. Baculovirus-expressed VP6, for example, spontaneously forms into trimeric conformation and can further assembles with VP7 into empty particles constituted by two concentric protein layers (165, 167, 40). The baculovirus expression of different subsets of viral proteins, originates sometimes in stable self-assembled empty particles, called virus-like particles (VLP) on the bases of their virus-like structure. Interestingly, the presence of VP2 is essential for the stabilisation of VP6-VP7 baculovirus formed virus-like particles (208; 97). Baculovirus expressed virus-like particles were formed as example by VP2/6, VP2/4/6, VP2/6/7 and VP2/4/6/7) (40). These results suggest the intrinsic properties of self assembly and the high affinity interactions among these proteins even in absence of rotavirus non structural proteins or nucleic acid. Baculovirus expression of viral proteins autoassembled into triple and double layered viral particles, and has provided an original system to study virus structure, assembly, and replication (159, 172, 205).

Non replicating self-assembled VLP are morphologically and antigenically similar to the native virus particles (112). For their antigenic characteristics and their recombinant origin, VLPs have features, which are advantageous for their use as candidate subunit vaccine (135; 38; 167). In fact, VLPs are immunogenic when administered parentally to rabbits (35). In addition, VLP could be useful as carriers of foreigner epitopes from heterologues pathogens or of drugs that need to be delivered to the gastrointestinal truck (48).

Structure of rotavirus capsid and genome organisation

Three-dimensional structural analyses, using cryoelectron microscopy and computer image reconstruction procedures, have been carried out on different members of Reoviridae family, as bluetongue virus (BTV) of the orbivirus genus and several strains of reovirus genus (49; 156). The overall organisation is similar among these viruses. However, the distinctive features of rotavirus genus are the presence of 120 protruding spikes and of 132 channels per virions (156).

The aqueous channels are spanning both the layers and link the outer surface with the inner core (about 140Å deep). 3 types of channels can be distinguished based on their position and size (12 type I, 60 type II and 60 type III) (159). The base of the type I channels is closed in the centre by the VP2 pavement (101, 157). Interestingly the VP6 intermediate layer, defines itself the type I channels that are the only with a circular opening of around 40Å diameter, while all the other channels constrict before widening in the interior. The function of type I channels is not known but there are models in which it was suggested that they are involved in allowing import of metabolites required for RNA transcription and export of the nascent ssRNA (100).

The 120Å long surface spikes are composed by dimers of VP4 that extend from the surface of the outer shell and have bilobed structure (158). These spikes are located at an edge of type II channels (173). The described VP4-VP7 and VP4-VP6 interactions imply that VP4 structurally may participate in maintaining the precise geometric register between the inner and the outer layers (156).

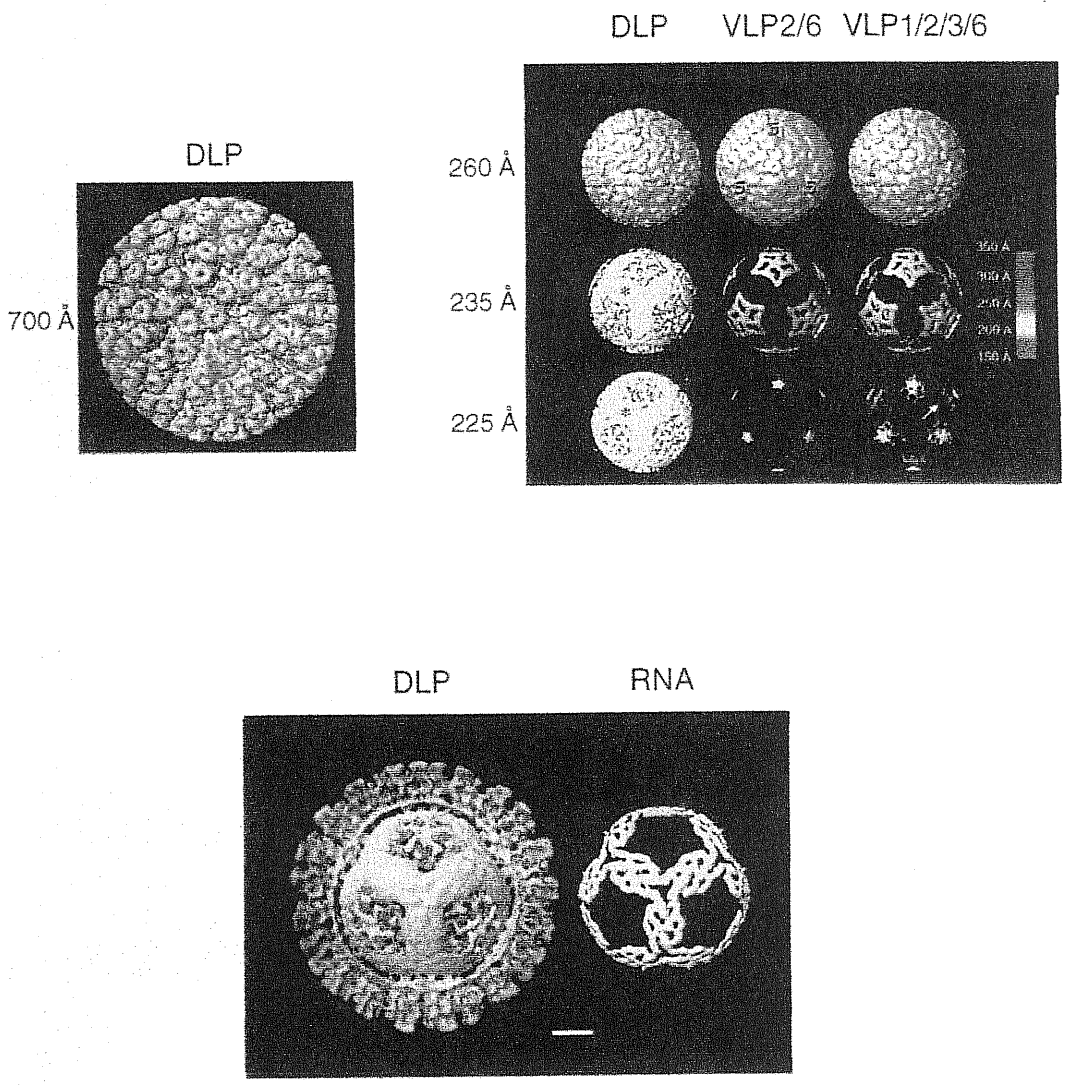

Figure 1.9.
A. Surface representation of the 3-dimenswional structure of the DLP at a reolution of 19Å viewed along the icosahedral 3-fold axis. VP6 is stained in blue. The 5-fold positions on one of the icosahedral facets are shown. An original feature is the hole at the centre of each VP6 trimer.
B. Structural organisation of RNA inside rotavirus. Left, cutaway from the 19Å structure of the rotavirus DLP, showing internal organisation. VP2 is represented in green and VP6 in blue. VP1-VP3 complex at the 5-fold axes is shown in red. Portions of VP2 at the 5-fold axis are shown in green. Right, the icosahedral shell of the ordered RNA (yellow), showed separately for clarity. Each strand is about 20 Å in diameter. The strands are separated from each other by 25-30 Å. Scale bar, 100Å.
These figures are modified from Prasad et al. 1996 (157).

Recently, electron microscope of VLP obtained from baculovirus expression system and image processing techniques have given important informations on rotavirus ultrastructure, providing conclusive evidences of a T=13 icosahedral surface lattice for the two virus outer layers. Cryoelectron microscopy of rotavirus inner core has demonstrated the presence of a flower-shaped structure that may represent a portion of the enzyme complex, constituted by VP1 and VP3. Mass calculation and biochemical analysis indicate that there are 12 molecules of VP1-VP3 per virion (157). Moreover it becomes evident that VP2 is icosahedrally assembled and induces icosahedral ordering on closely interacting portions of the RNA. The inner surface of VP2 not only provides a structural support for the RNA, but also helps to position the transcription complex properly. The outer surface of VP2 provides a structural platform for assembly of VP6 trimers, preventing mis-aggregation of genome or other high hydrophobic proteins (157).

Baculovirus-expressed VLPs were also important because they permitted to obtain the first three-dimensional organisation of the Reoviridae genome (157). Different types of recombinant VLPs were compared by cryoelectron microscopy with transcriptionally active native double layered particles (DLP) purified from viral infected cells. Interestingly, VLP-DLP comparative structural analysis helps also for the localisation of the virus transcription complex. Viral dsRNA forms a dodecahedral structure in which the RNA double helices appear as a tube of 20Å diameter, interacting closely with the inner capsid layer (VP2) and packed around the enzyme complex (figure 1.9). However, icosahedral ordering of dsRNA does not seems to be maintained in the deep core, and it has been estimated that in Reoviridae, only 1/5 of the genomic RNA is ordered. This extensive ordering genome may be critical for the endogenous transcriptase activity, perhaps facilitating a RNA movement through the enzyme complex, driving the continuous exit of newly synthesised mRNA. Although it is not possible to determine the position of the different dsRNA segments, it is possible to hypothesised that

a substantial portion of each of the genome fragments could interact with a VP1-VP3 complex. The understanding in the transcription process will improve by observing changes in conformation of RNA and proteins in conditions of native active transcribing DLP and in DLP transcriptionally incompetent (lacking the VP6 protein layer).

Rotavirus transcription

Genome transcription is a critical stage in the viral life cycle, as the process by which the viral genetic information is presented to the host cell protein synthesis machinery for the production of viral proteins needed for genome replication and virion assembly. Despite numerous architectural and organizational differences among the families of dsRNA viruses, numerous studies suggest that the basic mechanism of mRNA production may be similar in most, if not all, viruses having dsRNA genomes, and of them rotavirus was chosen as the transcription model system (99). The viral transcriptase is latent in triple layer particles and is activated by the uncoating process after virus cell entry or experimentally by chelating agents that destabilise the outer layer. Viruses with dsRNA genomes contain all the necessary enzymatic machinery to synthesize complete mRNA transcripts within the core, without virion disassembly. The synthesis of viral transcripts is mediated by the endogenous capsid-bound RNA-dependent RNA polymerase VP1 that directs the copy of the parental minus single strand template to yield progeny positive strand mRNA (transcription) and regenerates the dsRNA genome (2; 122). Interestingly, recently were characterised the nucleotidic sequences in the viral mRNA UTR regions have function of translation enhancer (32). The infected eukaryotic host cells provide all the enzymatic activities needed to generate the 5'-cap required by the eukaryotic translation machinery. Rotavirus mRNA capping is directed by the multifunctional activity of the viral core protein VP3, that recently was found possess guanylyltransferase and methyltransferase activities (25). It has been suggested that In reovirus genus, the transcription is not an active process, and it does not required the modification of the enzymatic complex, but only releases the templates from structural constrains, allowing them to move past the transcriptase catalytic site. In rotavirus however, ATP inhibitors could block viral transcription, suggesting that this process is dependent by ATP hydrolysis.

One of the more striking observations about genome transcription in rotavirus is that occurs efficiently only when the transcriptionally competent particles (double layered particles) are fully intact (15). This observation suggests that all of the components of the transcribing particles, including the viral genome, the transcription enzymes, and the viral capsid, function together to produce and release mRNA transcripts and that each component has a specific and critical role to play in promoting the efficiency of this process. Interesting observations confirm that the particles do indeed remain structurally intact during transcription. The structural integrity of the transcribing particles may be required to hold the components of the transcription machinery in their proper arrangements throughout repeated initiation-elongation cycles as well as to enable the efficient release of mRNA transcripts. To understand how the conformation of the capsid could affect the efficiency of transcription in the viral core, a series of comparative structural and biochemical studies was carried out. The integrity of the transcribing particles could be affected using monoclonal antibodies specific for distinct VP6 antigenic sites that in fact have the capacity to block their transcriptase activity (92; 65). Some of the antibodies tested, can introduce conformational changes in the capsid, similar to those seen into transcriptionally incompetent abnormal particle found in infected cells. As a consequence, mRNA synthesis is prematurely arrested after limited elongation with the resulting oligonucleotide transcripts remaining trapped inside the particles.

The precise pathway of mRNA through the VP2 layer is still not known. However, recently cryoelectron microscopy observations of viral particles that are actively transcribing and releasing mRNA, have suggested the precise route that nascent viral mRNA molecules follows in their way of exit from viral particle. On the base of these observations, it is thus hypothesised that the viral nascent mRNA is exported through the VP2-VP6 made type I channels (100; 101). Antibodies directed against specific sites VP6 thus can produce conformational and structural changes in the mRNA-release

channels or perhaps can reduce the effective diameter of their opening (99). These results indicate how through the integrity of the capsid is critical for the continuous translocation and efficient transcript elongation of nascent mRNA.

Rotavirus replication

During replication dsRNA molecules are incorporated into virions and remain associated to viral particles. Although not examined directly, it is assumed that rotavirus replication takes place in a conservative manner, thus both parental dsRNA strands remain within uncoated particles. Positive single strand viral RNA transcripts serve as templates for the synthesis of progeny minus strands RNA to yield dsRNA (2; 89; 145). Replication intermediates (RI) can be separated from infected cells through sedimentation on CsCl or sucrose gradients and consist in particles at the different stage of genome replication. Characterisation of RI indicates that they consist of the inner most viral structural proteins (VP1, VP2, VP3, VP6) and of co-purified small amount of some of the NSPs (NSP3, NSP1, NSP2 and NSP5) (143).

Rotavirus RI, purified at the initial stage of virus replication, are associated to the nuclease-sensitive positive ssRNA template and were called sub-viral particles (SVP). Interestingly, these particles could support *in vitro*, in a cell free system, the synthesis of their own dsRNA genome, mRNAs and proteins (144; 145; 142; 75; 41). SVP *in vitro* genome synthesis represents the elongation of nascent minus strands RNA on a positive strand RNA rotavirus template co-purified together with SVP, resulting in fully packaged newly made dsRNA protected to nuclease digestion (143; 145). From these experiments it was hypothesised that the replication of rotavirus genome consists in the moving of the RNA templates from outside to inside the replicative active particles as dsRNA synthesis occurs. Moreover,

biochemical analysis of RI reveals that they undergo continuous decrease in overall size as dsRNA is synthesised, thus replication and packaging confer a change in density and diameter to the viral particles (142; 89; 75).
Surprisingly, purified SVP works as an *in vitro* replication system supporting the initiation and synthesis of rotavirus (-) strands on (+) strand template RNA (27) and it has been extensively used to examine several parameters related to rotavirus RNA replication. Native rotavirus mRNAs or exogenously added *in vitro* transcripts, with bona fide 3' and 5' termini, derived from rotavirus cDNAs, works as templates and efficiently interacts with SVP components. After RNA replication, dsRNA is fully packaged into SVP becoming nuclease resistant (27; 145). De novo synthesis of full-size input ssRNA by previously nuclease treated SVP, indicates that SVP indeed support both the initiation and the complete elongation of the exogenous RNA. Recently it was described that the initiation of the minus strand RNA by the rotavirus RNA polymerase in a cell-free system, involves a novel mechanism of initiation. It consists in the formation of a ternary complex consisting of the viral RNA-dependent RNA polymerase VP1, viral (+) strand RNA, and possibly a 5'-phosphorylated dinucleotide, that is, pGpG or ppGpG (24).

The synthesis of input reporter RNA to generate dsRNA is supported not only by SVP obtained from infected cells, but also by recombinant core-like particles, purified from baculovirus that structurally have the characteristics of empty rotavirus double-layered particles. Equally replicative active *in vitro* are also structurally destroyed mature rotavirus called "open cores" that have loosed the outer and the intermediate proteins layers and the viral dsRNA genome. These results suggest that the replication itself is an intrinsic spontaneous process and does not require viral non structural proteins. Preliminary data indicate that VP1 in the absence of other viral proteins lacks replicase activity, even if alone is sufficient to bind viral ssRNA (139). Analysis of different baculovirus expressed VLPs has demonstrated in fact that VP2 is required for the replicative activity and VP1/2 is the minimal

replicase particle. Moreover, the role of VP2 in the replicase activity is most likely structural and VP3 is not required for replicase activity of VLPs (208). *In vitro* replication reactions, using reporter template, were performed to map cis-acting elements that regulate replication. Templates with internal deletions indicated that no essential replication signals were present within the open reading frame of the different rotavirus RNA genes and that key elements were present in the 5' and 3' non coding UTRs. Terminal truncations of the reporter RNA showed that the minimum requirement for replication (minimal promoter) of (-) strand synthesis was contained in the 3'-terminal 7 nucleotides (nt 1056-1062) (5'-UGUGACC-3') and the conserved the 3'-terminal -CC residues of all rotavirus genes are required for efficient replication (198; 199). Analysis of additional chimeric templates demonstrated that sequences capable of enhancing replication from the minimal promoter were located immediately upstream of the 3'end minimal promoter and at the extreme 5' terminus of the template (198).

In addition to RNA polymerase activity, open cores have been shown to contain a nonspecific guanylyltransferase activity that caps viral and nonviral RNAs *in vitro* (137). However, the majority (approximately 70%) of caps made by open cores contain an extra GMP moiety with unknown significance and the tetraphosphate linkage, GppppG, rather than the triphosphate linkage, GpppG, found on mRNAs made by rotavirus double-layered particles. Enzymatic analysis indicated these GppppG caps result from the lack of a functional RNA 5'-triphosphatase in open cores, that removes the gamma-phosphate from the RNA prior to capping (25).

Chapter 2

Methods

Cells and stable transfectants

MA104 cells are monkey epithelial kidney cells and are the permissive cell line for rotavirus infection.

MA104 cells were routinely cultured in Dulbecco modified Eagle Medium (DMEM) supplemented with 10% fetal calf serum (FCS), 2 mM L-glutamine and 50 µg/ml gentamycin (Gibco Laboratories).

For virus infection or DNA transfection, cell culture was maintained in absence of serum and antibiotics (serum free medium, SF).

Viruses and infection

Rotavirus simian 11 rotavirus (SA11 strain) was propagated and grown in MA104 cells as described (52). Briefly, the inoculum was activated in presence of 0.25 mg/ml of Tripsin for 30 min at 37°C and let to absorb on the cell monolayer for 1 h. Cells were thus washed and cultured in SF medium with 0.25 mg/ml Tripsin until complete cytopathic effect (c.p.e.). For current virus propagation, cells were infected with virus at a multiplicity of infection (m.o.i.) of 5-10. Using this virus title the infection was completed usually after 15 h. The infective medium was frozen and thaw 3 times and than centrifugated at the maximum speed to eliminate cellular debris. The inoculum was aliquoted and stored at -80 °C.

To assay NSP2 or NSP5 viral proteins, the cells were lysed 3-4 h post-infection.

Anti-NSP5 and anti-NSP2 antibodies

Guinea pig anti-NSP5 polyclonal antiserum was obtained by Susana Gianbiagi (5).

Mouse anti-NSP2 serum was obtained with the DNA-immunisation technique (164; 61). Balb/c mice, 6-7 weeks old, were injected intradermally in the tail base with plasmid DNA used as immunogen. In each boost, it was injected a total amount of 100 µg of DNA in 100 µl of NaCl 0.8%. The DNA immunisation mixture account 50 µg of pcDNA-NSP2-ss plus 50 µg of pCDNA3-GM-CSF encoding for the human Granulocyte monocyte colony stimulation factor, used as immunisation enhancer (187b). The boosts were repeated three times every 7 days. Thus the animal were bleeded 3 weeks later (after 42 days from the first boost). From each blood extraction was recovered 200 µl of serum.

Anti-NSP2 serum was checked by immunofluorescence, immunoprecipitation and western immonoblot analysis of extracts of infected cells (see figure 3.2, page 61).

Hyperimmune sera were aliquoted and stored at -20°C in presence of 0.02% Sodium Azide (NaN_3).

Transient transfections of MA104 cells

Cell transfections were performed in presence of Vaccinia virus infection. Vaccinia strain vTF7.3, recombinant for the T7 RNA polymerase gene (57; 58), is used to obtain an efficient transient expression of genes under the control of the T7 promoter. Since vaccinia virus cycle is cytoplasmatic, exogenous gene transcription and translation are coupled in the cytoplasm of the transfected cells.

Before transfection, cells were infected with Vaccinia virus (kindly prepared by Maria Elena Lopez) at multiplicity of 20 PFU/cell. One hour later, the cells were incubated with a mixture of 5 µl of Transfectam reagent (Promega) and 5 µg of

plasmid DNA (Qiagen purified). The Transfectam-DNA complex was maintained onto the cells for 15 h in the incubator in SF medium. Cells were then washed two times with PBS and analysed either by immunoprecipitation, western immunoblots or immunofluorescence usually at 16 h post-transfection.
For co-transfection experiments, they were transfected 3 µg of pCDNA3-NSP5 (or mutants) and 2 µg of pCDNA3-NSP2 (or pCDNA3 empty vector). The ratio of the amount of NSP5 and NSP2 plasmids used in co-transfection experiments was 1:0.6 and optimised to detect VLS by immunofluorescence.
In all cases in which NSP2 was co-transfected with either wt NSP5 or mutants, the expression of NSP2 was assessed by western immunoblot or double immunofluorescence.

To detect EGFP or NSP5-EGFP fusion proteins, 2 µg of pN1-EGFP or pNSP5-EGFP plasmids were transfected into MA104 cells with classic liposome-mediated protocols, in absence of vaccinia virus infection. EGFP gene expression was dirved by CMV promoter. To detect GFP green fluorescence living cells were analysed 36h after transfection. To obtain the localisation of the recombinant NSP5-EGFP in specific rotavirus viroplasms, cells were infected with rotavirus 30 h after NSP5-EGFP transfection. Viroplasms were analysed 10 h later.

Cellular extracts

Lysates (corresponding to $0.5x10^5$ cells), were prepared in 100 µl of TNN lysis buffer (100 mM Tris-HCl pH8; 250 mM NaCl; 0.5% NP40; 1mM PMSF) at 4°C. Extracts were spun at 10000 g for 10 min and supernatants were stored at -80°C. Usually, 1/10 of extracts was loaded on SDS-PAGE for western immunoblot and 1/3 of eventually labelled extracts was used for immunoprecipitation.

Immunofluorescence microscopy and immunohistocheimistry

For indirect immunofluorescence microscopy, cells were washed twice with PBS supplemented with Ca^{++}/Mg^{++} (1mM each), fixed and permeabilized with ice-cold acetone for 2 min at -20°C. The coverslips were let to dry, re-hydrated in PBS and blocked with 0.25% of gelatin (Sigma) in PBS for 30 min at RT. Slides were incubated with the guinea pig anti-NSP5 or a mouse anti-NSP2 antisera at a dilution of 1:50 in PBS-3% BSA for 1 h in a moist chamber at RT. After three 5-min washing in PBS, a secondary reaction was performed with FITC-conjugated goat anti-guinea pig (Sigma) for 40 min. Samples were thus washed and mounted with KPL mounting medium (Gaithersburg, MD) and analysed either with the Argon-Helium double laser confocal microscopy (Zeiss) or with conventional UV-lamp microscopy (Nikon).

For double immunofluorescence experiments, two distinct rounds of primary antibodies incubation were performed, followed by a single secondary immunoreaction with a mixture of RITC-conjugated goat anti-guinea pig (Sigma) and FITC-conjugated goat anti-mouse (Dako) antibodies (both used at a dilution of 1:50 in PBS-3% BSA).

To detect EGFP or NSP5-EGFP, cells were observed alternatively living or fixed in 3% paraformaldeyde (PFA) for 20 min at RT. Fixed cells were mounted on glasses and analysed.

For immunohystocheimistry, the glasses were fixed with 2% PFA plus 0.2% gluteraldehyde in 0.1M Na-cocodilate buffer pH7.4 and incubated with specific mouse anti-NSP5 or mouse anti-NSP2 antisera. As secondary antibody was used an HRP-conjugated anti-mouse antibody (Dako). The immunodetection was obtained with diaminobenzidine (Sigma) and analysed with the conventional microscopy under transmitted light.

Electron microscopy

The electron microscopy experiments were obtained with the help and the supervision of Piero Giulianini of the University of Trieste.

Morphological electronical analysis of viroplasms or VLS

Cell monolayers were fixed for 30 min with 2% PFA and 2.5% glutaraldehyde in 0.1M cacodylate buffer (pH 7.5), at RT and post-fixed in 1% osmium tetroxide in the same buffer. They were dehydrated in a graded series of ethanol (70%, 96%, 100%) and embedded, via propylene oxide, in Araldite 502/Embed 812 (Electron Microscopy Sciences).

Immunogold labelling of viroplasms

Cells were fixed as before, washed four times with ice-cold PBS and permeabilized with 0.1% Triton X-100 in PBS for 5 minutes, at RT. Free aldehyde groups were then blocked with 0.02% glycine in PBS for 10 minutes. Cells were then incubated for 20 min with PBS-0.5% BSA (PBSA) containing 20% of normal goat serum. Incubation with the primary antibodies was then performed for 1 h at RT. Cells were washed six times (5 min each) with PBSA, at RT, and incubated for 1 hr at RT with the secondary antibodies (goat anti-mouse and rabbit anti-goat IgG 1nm gold conjugates (British Biocell International), diluted 1:100 in PBSA. After several rounds of PBSA/PBS washings, cells were treated with 1% glutaraldehyde in PBS for 15 minutes, washed again and treated with 0.5% osmium tetroxide in PBS for 15 minutes, at RT. After 3 washes with deionized water (milliQ water), gold-labelled cells were silver enhanced with HQ SilverTM Enhancement Kit (Nanoprobes) for 3 min, at RT and in the dark. Cells were rinsed 3 times with water and dehydrated with ethanol (70, 96 and 100%). Once dehydrated, cells were scraped off the plates, pelleted at 7,000 rpm for 10 min and embedded.For pre-embedding EM of infected or transfected cells, monolayers were fixed directly on petri dish with EM grade 2% PFA and 0.2% gluteraldehyde in 0.1M

Na-cocodilate buffer pH7.4. After permeabilisation with Triton 0.1% and specific immunostaining, cells were post-fixed in 1% gluteraldehyde and in 05% osmium tetraoxide.

Sections were cut using an ultramicrotome (Pabisch Top Ultra 150) and placed on 300 mesh uncoated nickel grids. The latter were stained with 2% aqueous uranyl acetate and 0.5% lead citrate (10 minutes each). Sections were observed under a Philips EM 208 transmission electron microscope, at 80 kV acceleration voltage. All measurements and statistical analyses were performed with an Image-Pro Plus ver 4.1 software (Media Cybernetics), on digitized images.

E.coli protein expression and *in vitro* binding assay

GST-NSP5 fusion protein was expressed in pGEX-NSP5 transformed E.coli cells and purified using the RediPack GST purification modules (Pharmacia). pGEX-NSP5 expressing bacteria were inoculated and induced with 3 mM IPTG for 3-4 h at 37°C (56). The GST-NSP5 fusion protein was purified on Glutathion-Agarose beads (Pharmacia) for 1 h at 4°C. After boiling of the resin, GST-NSP5 protein was loaded directly on SDS-PAGE and analysed by Comassie staining.

The *in vitro* binding assay was performed by incubation of 1 µg of GST-NSP5 protein (Commassie determined) still attached to the Glutathion-Sepharose resin with 1/5 of unpurified *in vitro* synthetised ^{35}S-Met-labelled NSP2. The binding reaction was performed at 37°C for 1 h in a PBS-1% BSA buffer under continuous agitation. The beads were thus washed several times with RIPA buffer (50mM Tris-HCl pH8; 150mM NaCl; 1% NP40; 0.5% DOC, 0.1% SDS), boiled and the supernatant loaded onto 12% SDS-PAGE. The protein binding was thus analysed after autoradiography.

Western immunoblot analysisFor western immunoblots, lysates were resolved on a SDS-PAGE, transferred onto a PVDF membrane (Millipore), previously activated in methanol (2 min at RT). Transfer occurred in a Tris-Glycine buffer (Tris-HCl 12.12 g/l and Glycine 57.04 g/l) supplemented with 20% methanol. The membrane saturation, antibodies incubation and membrane washes were performed in TBS buffer (Tris-HCl 50mM pH7.5, NaCl 150mM) containing 5% milk at RT.

The transferred proteins were reacted to guinea pig anti-NSP5 serum (dil. 1:1000) or to mouse anti-NSP2 serum (dil. 1:300) polyclonal primary antibodies for 1 h at RT. As secondary antibodies were used commercial anti-guinea pig or anti-mouse HRP-conjugated antibodies (DAKO immunoglobulins) (dil. 1:1000). Commercial mouse anti-EGFP antiserum (dil. 1:1000) (Clontech) was used to verify the quality of EGFP or NSP5-EGFP expression.

The immunoreaction was analysed developing the membranes with the ECL-chemioluminescence system (Amersham).

Immunoprecipitations

1/3 of ^{35}S or ^{32}P labelled cellular extracts were diluted up to 100 µl with TNN buffer and incubated from 2 h to o/n at 4°C in presence of 1 µl of specific antisera (anti-NSP5 or anti-NSP2 antibody) and with 40 µl of 50% Protein-A Sepharose CL-4B beads (Pharmacia). Beads were than washed three times with RIPA buffer. The immunoprecipitates were eluted from the sepharose by boiling in 2x Laemmli's sample loading buffer and the supernatants were loaded onto SDS-PAGE. In reducing electrophoresis conditions, the samples were eluted in the Laemmli loading buffer containing 4% of β-mercaptoethanol. Radioactive ^{35}S-Met gel electrophoresis were incubated with Fluorografy-Amplifyer (Amersham) for 30 min at RT to enhance the intensity of the radioactive signal.

Immunoprecipitated proteins were detected by autoradiography (-80°C o/n on Kodak film).

Reticolocyte dependent transcription and translation

In vitro protein translation, were performed using the Reticolocyte dependent transcription and translation coupled system (TNT) (Promega). 2 µg of circular template DNA plasmid encoding for the protein of interest under the transcriptional control of the T7 RNA polymerase promoter, were added to the TNT reaction mix in presence of 15 U of T7 RNA polymerase (Promega) and 10 µCi of ^{35}S-Met. The reaction was incubated at 30°C for 1 h. 1/10 of the *in vitro* transcribed polypeptides were immunoprecipitated with specific antibodies and analysed on SDS-PAGE gel.

Phosphatase treatment

Lambda protein phosphatase (λ-Ppase) (New England Biolabs) treatment was performed by resuspending the immunoprecipitated Sepharose beads in a total volume of 40 µl of a reaction buffer (50mM Tris-HCl pH7.8; 5mM DTT, 2mM $MnCl_2$, 100 µg/ml BSA) in presence of 80 U/µl λ-Ppase. The reaction was incubated at 30°C for 1h. The reaction was boiled in 2x Laemmly sample buffer and the supernatant loaded on SDS-PAGE.

In vitro "degradation assay"

^{35}S-Met-labelled protein polypeptides (wt NSP5 or Δd81-130) were incubated with NSP2 obtained from transient cell transfection or from *in vitro* translation of pCDNA3-NSP2 plasmid. *In vitro* synthetised polypeptides were prepared using 1 µg of template DNA and 1/10 of the translation reaction was used in the

assay. The reaction was performed in TNN buffer at either 37°C or 4°C, immunoprecipitated with anti-NSP5 antibody and analysed on 15% SDS-PAGE. pCDNA3-VP4 plasmid and anti-VP4 antibody, used to perform internal negative experimental controls, were provided by Cecilia Miozzo.

^{35}S-Met *in vivo* labelling

For *in vivo* labelling of Rotavirus proteins with ^{35}S-Met, rotavirus infected cells were starved with 2 ml of Met-free DMEM SF medium for 30 min. The labelling was performed with 2.5 µCi of ^{35}S-Met for 1 h. Total cellular extracts were prepared in TNN buffer and 1/3 of the cell lysate was used for immunoprecipitation.

Radiolabeling with ^{32}P inorganic ortophosphate

For ^{32}Pi labeling, cells were transfected with the interested plasmids and 12 h later were fed with 2 ml of phosphate-free DMEM SF medium for 30 min. Afterwards cells were incubated for 1 h with 1 mCi of ^{32}Pi ortophosphate for 30 min and thus lysed and analysed by immunoprecipitation.

Chemical DSP-crosslinking

Living ^{35}S-Met labelled cell monolayers were washed twice with washing buffer (PBS-$Ca^{++}Mg^{++}$) and incubated with 600 µM (final concentration) of DSP (dithiobis succinimidylpropionate) chemical crosslinker (Pierce) in 1.5 ml washing buffer at 4°C for 10 min. After this time, the crosslinker was removed with 3 steps washings and the excess of DSP was quenched with two 5 min steps of washings in 1.5 ml of washing buffer (50mM Tris pH 7.5, 150mM NaCl). Cellular extracts were thus prepared in TNN plus 20 mM iodoacetamide

(Sigma) used as antioxidant. After the immunoprecipitation, the crosslinked species were analysed in reducing conditions in 12% SDS-PAGE.

UV treatment of living cells

For UV treatment of cell monolayers, PBS washed cells were overlayed with 1 ml of TBS buffer and exposed to a UV-Stratalinker^{TM}1800 for 5 min (total dose: 486000 mJ) on ice. The distance between the cell monolayer and the UV lamp was kept to 10 cm. Cell extracts were prepared in RIPA buffer cointaining 20 mM iodoacetamide and thus subjected to immunoprecipitation.
To evaluate the presence of crosslinked RNA, before immunoprecipitation, UV crosslinked extracts were incubated with RNAseH (Sigma) at 37 °C for 1 h.

In vitro phosphorylation assays

To perform the *in vitro* phosphorylation of ^{35}S-Met labelled DSP crosslinked virus infected cells or ^{35}S-Met labelled precursors, the immunoprecipitates were incubated with 10 mM of cold ATP for 30 min at 37 °C a kinase buffer containing 50 mM Tris-HCl pH 8.0, 1.5 mM spermidine, 5 mM $MgCl_2$, 1 mM DTT and 5% glycerol.
To test the phosphorylation of NSP5 different deletion mutants obtained from specific transient transfected cells, cell extracts were immunoprecipitated with anti-NSP5 antibody. Afterwards, the immunoprecipitates were labelled with 0.1 μCi of γ-^{32}P-ATP in the kinase buffer. The reaction was performed at 37°C for 1 h.
In both the cases, at the end of the kinase reaction the immunoprecipitated beads were washed in RIPA buffer and loaded in 12% SDS-PAGE.

Plasmid constructs

NSP5 containing plasmids

NSP5 original cDNA fragment, completed of its proper 5' and 3' ends untranslated regions (UTR), was cloned by Susana Gianbiagi from rotavirus total RNA in pBluescript (pBlue-NSP5) and further subcloned in a pUC-derivated plasmid containing the T7 promoter recognition region, to generate pT7+1/OSU11. KpnI-HindIII NSP5 full lenght fragment, was thus subcloned under the control of the CMV and T7 promoter region in pCDNA3 (pCDNA3-NSP5).

To obtain GST-NSP5 fusion protein, BamHI-NSP5 restriction fragment was subcloned from pBlue-NSP5 to p-GEX-2T (pGEX-NSP5).

To obtain NSP5-EGFP fusion protein, the coding region of NSP5 was amplified from pCDNA3-NSP5 with the oligonucleotides EcoRI-ATG-NSP5 (5'-AAgaattcATGTCTCTCAGCATTGAC-3') and NSP5-PstI-up (5'-GATCCTTActgcagCAAATCTTCGATCAATTGCA-3') to obtain an NSP5 PCR fragment, that was restricted with EcoRI-PstI to lack of the 3'-end stop codon. To frame at the amino terminus NSP5 sequence with EGFP (eukariotic mutagenised version) obtaining pNSP5-EGFP plasmid, the fragment was thus cloned in the respective polylinker sites of the original pN1-EGFP vector (Clontech).

NSP5 deletion mutants plasmids

All the oligonucleotides used for the NSP5 deletion mutants constructions are summarised in figure 2.1.

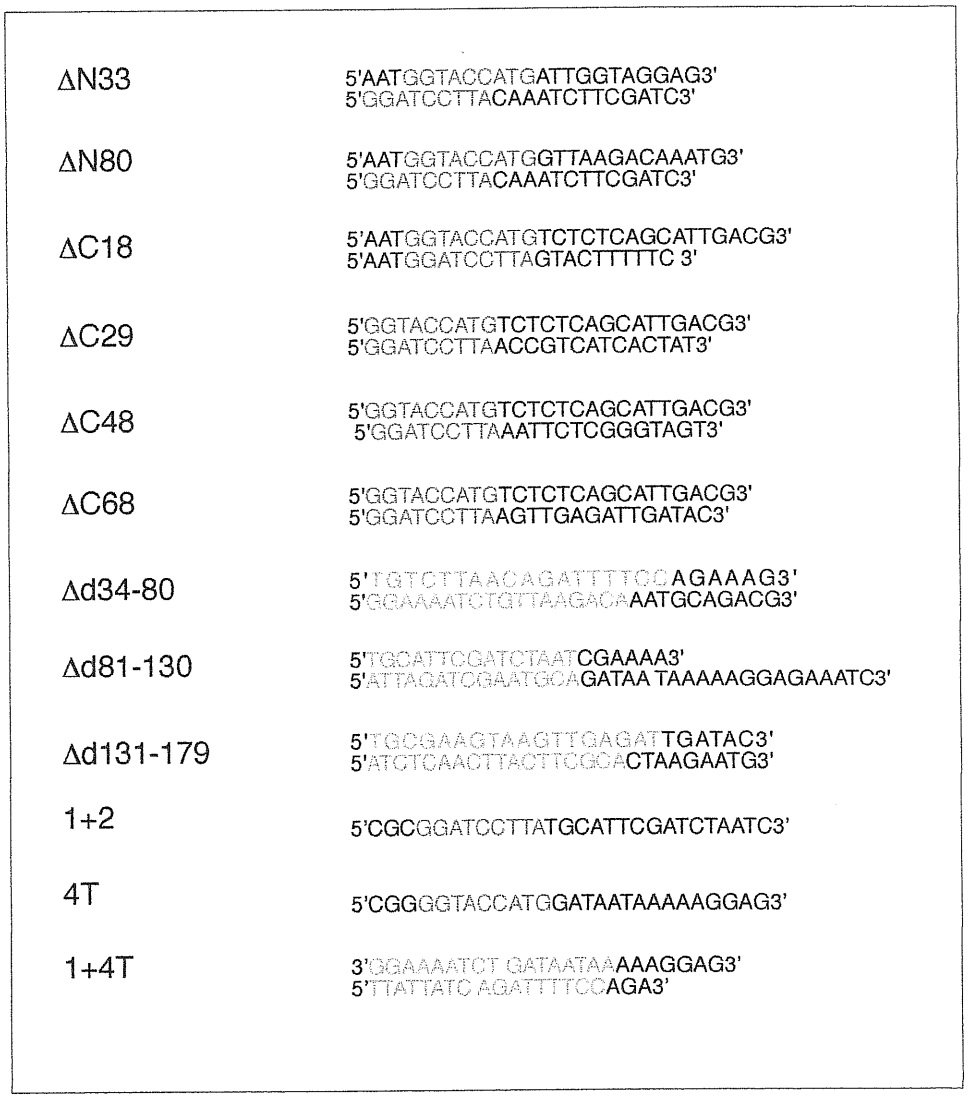

Figure 2.1. Oligonucleotides sequences.
Start codon (ATG) and stop codon (TAA) are labelled in red.
KpnI-BamHI restriction enzymes are labelled in blue.
Overlapping sequences are labelled in yellow.
Oligonucleotides ovelrlapping sequences are in green.

All the deletion mutants were obtained by PCR truncation of the original NSP5 cDNA (pCDNA3-NSP5) using specific primers on either the 5' or the 3' end either internal, generating a variable length of KpnI-BamHI fragments. After PUC intermediate cloning, they were fully sequenced with external (Forward and Reverse pUC based oligonucleotides) and proper internal primers. Thus they were subcloned using KpnI-BamHI restriction sites in pcDNA3 vector (Invitrogen) under the control of T7 RNA polymerase promoter, to generate pCDNA3- different NSP5 mutants constructs.

pCDNA3-ΔN18, pCDNA3-ΔN33, pCDNA3-ΔN80, pCDNA3-ΔC29, pCDNA3-ΔC48, pCDNA3-ΔC68 were obtained by PCR and were prepared by Ivka Afrikanova as described (4). In particular, for ΔN33 The 34-Isoleucine was mutated to Methionine (using 5'-N33 primer); and for ΔC68 a stop codon was introduced immediately downstream of Thr130 (using 3'-C68).

To obtain the pCDNA3-Δd34-80, pCDNA3-Δd81-130, pCDNA3-Δd131-179, NSP5 internal deletion mutants, three different PCR amplifications were performed on pCDNA3-NSP5 template, as explained in figure 2.2. A first round of PCR involved two separate amplifications of the regions that span the domain to delete, using the NSP5 peripheral primers and specific internal oligonucleotides (figure 2.2). The specific internal oligonucleotides have an overlapping region that permits the aneeling of the two PCR purified fragments. The internal deletion fragment was thus extended and reamplified using the peripheral NSP5 primers (containing KpnI or BamHI restriction sites).
The same strategy was also used to obtain pCDNA3-1+4, but as PCR template was used pCDNA3-131-180 NSP5 internal deletion mutant.
To obtain pCDNA3-2+4T, pCDNA3-1+2T and pCDNA3-4 unique PCR amplifications were performed using as templates respectively pCDNA3-Δd81-130, pCDNA3-ΔC29 and pCDNA3-NSP5 using external either specific primers

as summarised in figure 2.1. All KpnI/BamHI deletion fragments were cloned in pcDNA3 (Invitrogen) and checked by complete sequencing of both strands.

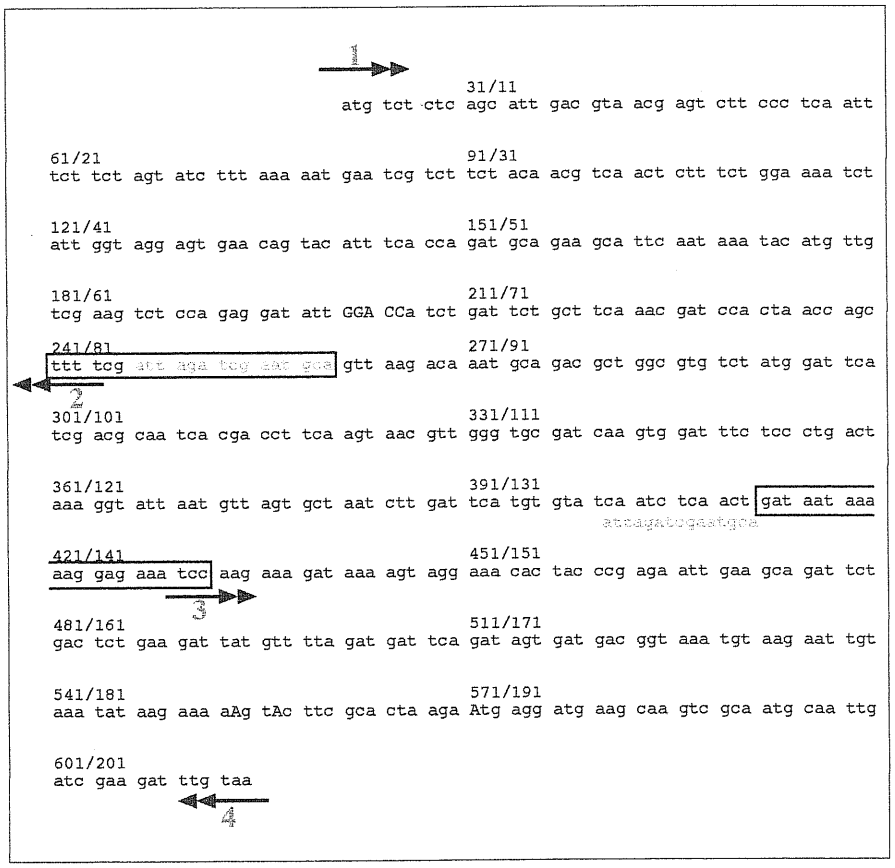

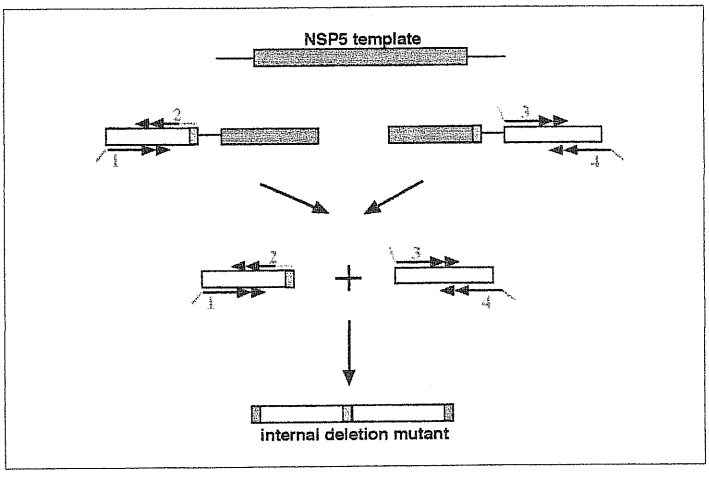

Figure 2.2. Sheme of the construction to obtain the NSP5 internal deletion mutants.

NSP2 containing plasmidsThe complete NSP2 coding region was amplified by Cecilia Miozzo from total SA11 rotavirus genomic RNA by RT-PCR specific oligonucleotides (5′-ATGGATCCGGCTTTTAAAGCGTCTCA-3′ and 5'-ACTTCAGAGGTCACATAAGCGCTTTCT-3′). The resulting 1060 nt-long band (BamHI-XbaI) corresponded to the complete NSP2 ORF and is flanked by the entire 5′ and 3′ untranslated region (UTR), was cloned in p-BluescriptKS (pBlu-NSP2) and fully sequenced with external and internal primers.
To eukariotic transient expression, NSP2 full length fragment (BamHI-XbaI) was subcloned into pCDNA3 under the T7 promoter, to generate pCDNA3-NSP2.

To obtain pCDNA3-NSP2-ss, used for the DNA immunisation technique, NSP2 was framed with a leader secretion peptide to permit the extracellular secretion into the immunised animals. To obtain that, NSP2-ORF was at first subcloned in a modified version of pUT-SEC plasmid (103) that has a shortest ApaLI-SpeI-KpnI poly-linker (pUT-SEC-linker). To frame NSP2 with the secretion peptide, NheI-SacI NSP2 fragment was subcloned from pBlu-NSP2 to pUT-SEC-linker open by SacI-SpeI restriction enzymes, obtaining pUT-SEC-NSP2. Finally, HindIII-XbaI fragment was subcloned into pCDNA3 (pCDNA3-NSP2-ss).
The pUT-SEC vector was designed to provide the recombinant proteins with a leader peptide required for secretion of proteins in the extracellular medium. PUT-SEC is a Tetracycline-selectable vector, based on pUC-19 (Neb-Biolabs), that it contains a HindIII/ApaLI fragment constituted by 163 bp genomic sequence encoding the mouse heavy-chain immunoglobuline secretion signal. A 82 bp-long intron is present, efficiently spliced into eukariotic nuclei, generating a mature transcript that is translated into a 18 aa-long peptide.

Chapter 3

Results

Introduction

In the past few years, the characterization of the rotavirus structural and non structural proteins had a big improvement. In particular in our laboratory, it was extensively characterised the phosphorylation of NSP5 bot *in vivo* and *in vitro*. When NSP5 is specifically immunoprecipitated from infected cells, different gel mobility forms, from 26 to 34 kDa are detected (see figure 1.8, page 26) (5). All these species are sensitive to treatment with λ-phosphatase (λ-Ppase) demonstrating the phosphorylated origin of the same NSP5 protein (26 kDa). Thus λ-Ppase was often used to confirm the origin of the hyper-phosphorylated mobility forms of NSP5. Interestingly, in mild washing conditions, anti-NSP5 antibody co-immunoprecipitated an extra band of 35 kDa unsensitive to λ-Ppase (4). We hypothesised that the 35 kDa protein involved was NSP2, another rotavirus non structural protein that, as NSP5, localises in the cytoplasmic viroplasms (146; 197), where viral replication and packaging occur.
The aim of my work was to study the NSP5 interaction with NSP2 and its functional and biochemical consequences.

Cloning of Rotavirus NSP2 and specific anti-NSP2 antibodies

To test the possibility of a direct or indirect NSP5-NSP2 interaction in virus infected cells, we decide to clone NSP2 gene from total genomic RNA of rotavirus SA11 strain and to produce specific anti-NSP2 antibody. In panel A of figure 3.1 is represented the sequence of Rotavirus OSU NSP2 gene (OSU fragment 8) and its relative aminoacidic translation. NSP2 aminoacids sequence between residues 54 and 87, corresponds to the region with high homology to metalloproteinases and comprehends a Proline rich region (position 53-55) (117).

To produce anti-NSP2 antibodies we decided to use the DNA immunisation technique, that offer the advantage of immunising mice directly with the DNA plasmid encoding the antigen to obtain specific sera of high quality, in a few weeks.

The mechanism by which the DNA itself can be used for *in vivo* expression to stimulate the immune system of the animals is not completely clear. However, recent studies have demonstrated the involvement of the epidermal dendritic cells in antigen presentation and in selective activation of the immune system. The current hypothesis is that epidermic cells are able to efficient internalisation of the plasmid, followed by expression and secretion of the encoded immunogen. The antigen is thus captured by B cells and epidermal dendritic cells and presented to the immune system (13).

As described in detail in the methods section (page 54), the immunogen ORF-NSP2 was cloned under CMV promoter (pCDNA3-NSP2-ss) and framed at the amino-terminus with a leader peptide that is required for protein secretion. The final pCDNA3-NSP2-ss construction is shown in the panel B of figure 3.1. The leader peptide sequence chosen was a 163 bp genomic sequence encoding a mouse heavy-chain immunoglobulin secretion signal (103), that is translated into a 18 aminoacid long peptide after a nuclear splicing of 82 nt (see figure 3.1B).

A

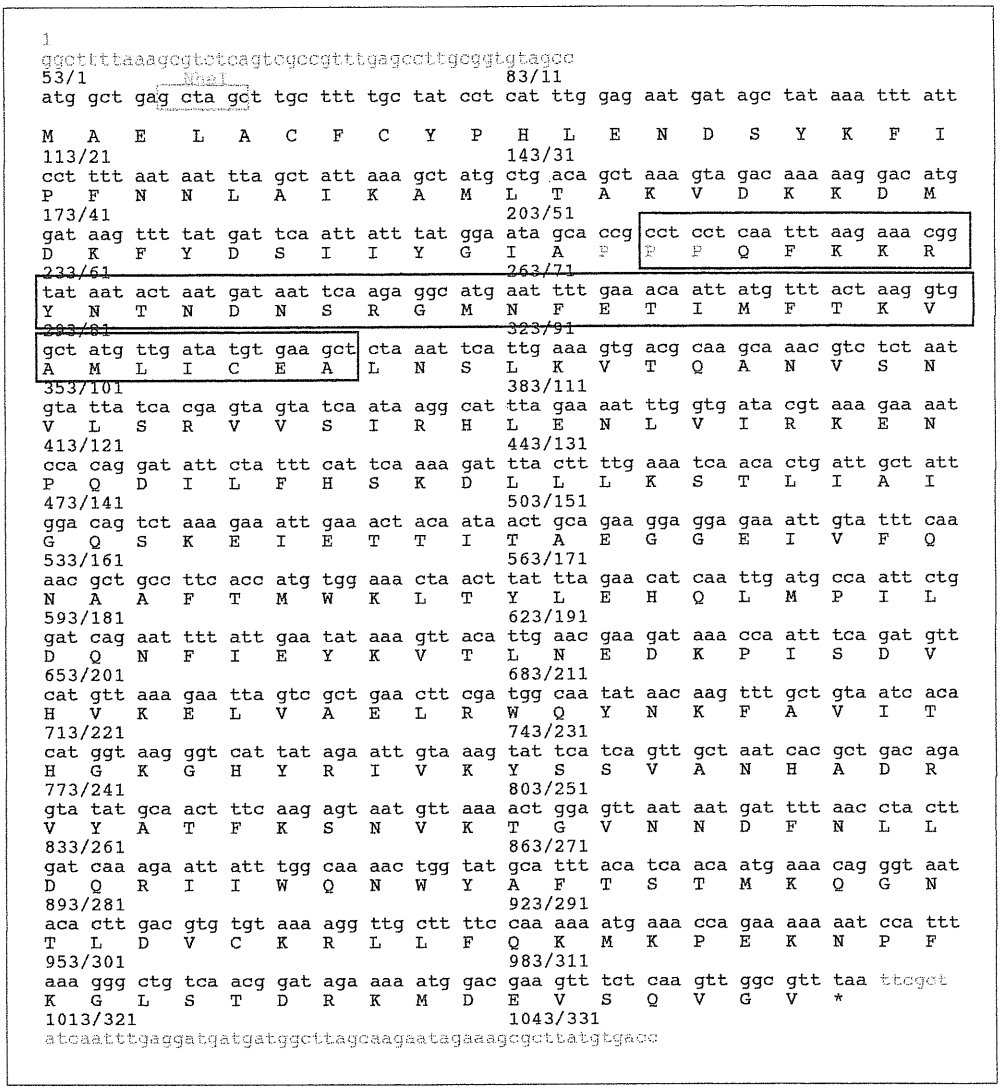

B

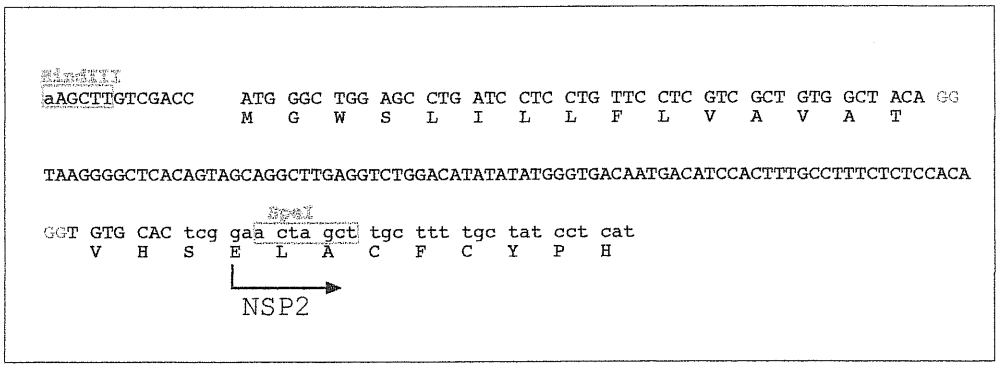

Figure 3.1. NSP2 sequence and secretion peptide.
A. Nucleotide sequence and aminoacid translation of Rotavirus OSU NSP2. Blue: characteristic 5' and 3' untranslated region (UTR). Underlined: sequence with high homology to metalloproteases (aa 54-87). Pink: proline rich region (aa 53-55).
B. Schematic representation of the resulting cloning of NSP2 downstream the IgG-derived secretion leader peptide. NSP2 gene cloning SpeI restriction site (position 61) is indicated. In the fusion construct, the first two aminoacids of NSP2 are missing.

Plasmid DNA was intradermally injected and anti-NSP2 serum was recovered after 3 weeks from the first DNA injection.

The quality of the antibody was very good as shown in figure 3.2. From each mouse bleeding, around 200 microliters of immune serum was obtained.

The activity of the sera obtained from immunised animals was tested for specific Rotavirus OSU NSP2 protein recognition by western immunoblot of MA104 non infected and infected cells (figure 3.2A, respectively lanes 1 and 2). NSP5 immunodetection performed on the same extracts (lane 4), indicates the relative migration of NSP5 in infected cell. Anti-NSP2 antibody immunoprecipitation of *in vitro* synthesised NSP2 polypeptide (TNT) was also performed (figure 3.2B, lane 2), as well as specific immunofluorescence of pCDNA3-NSP2 transfected MA104 cells (figure 3.2C). Anti-NSP2 immunofluorescence of untransfected cells did not show any specific signal (left panel of figure 3.2C).

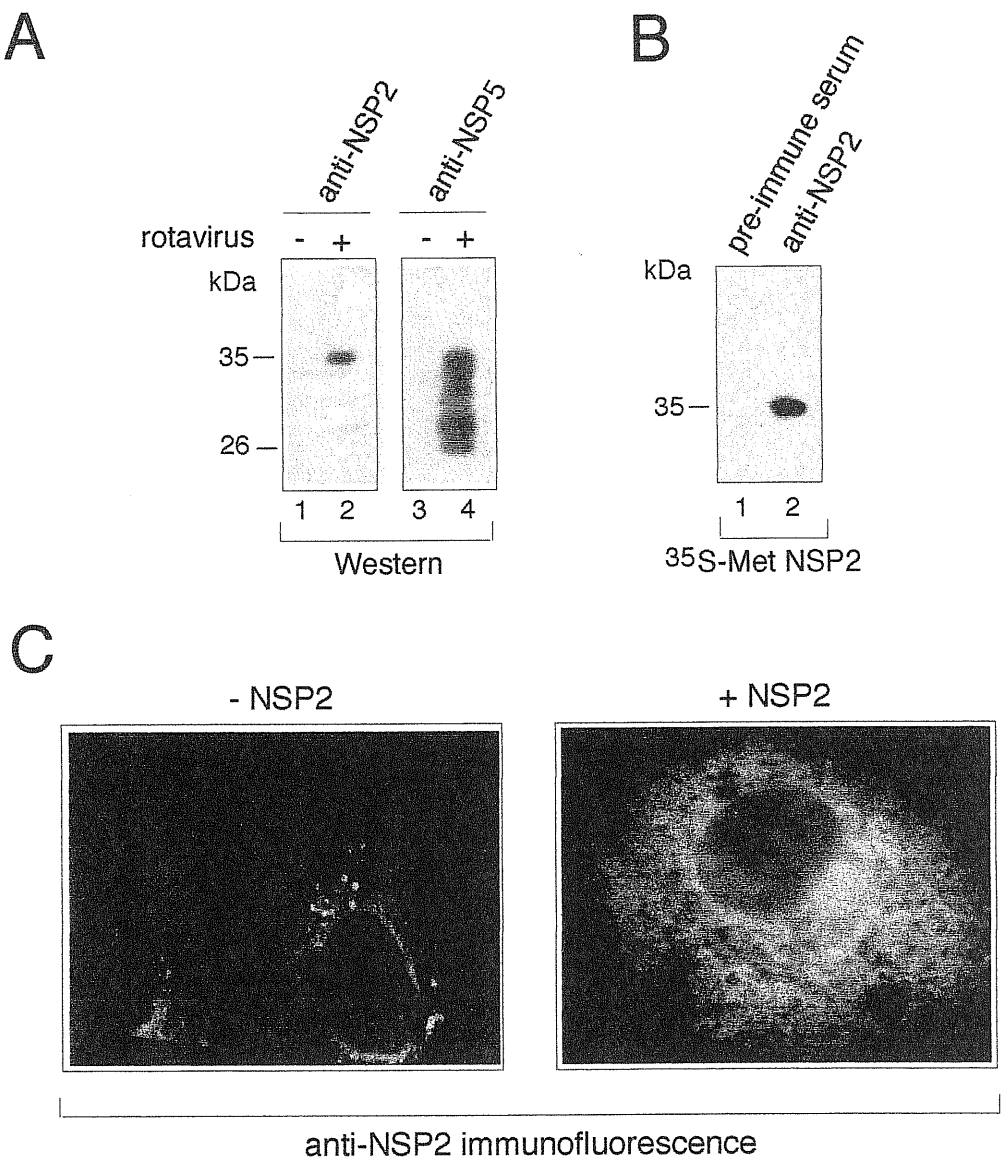

Figure 3.2. Characterisation of mouse anti-NSP2 antiserum obtained with DNA immunisation.
A. Western immunoblot of MA104 uninfected (lane 1) and rotavirus infected (lane 2) cell extracts reacted with anti-NSP2 antibody. As control, rotavirus NSP5 protein detected with anti-NSP5 antibody in infected cell extracts (lane 4).
B. Anti-NSP2 immunoprecipitation of in vitro synthesised NSP2 polypeptide (TNT) (lanes 1 and 2). Preimmune mouse serum was also tested (lane 1).
C. Anti-NSP2 indirect immunofluorescence of untransfected (left) and NSP2 transfected (right) MA104 cells stained with anti-NSP2 antibody and anti-mouse FITC-conjugated secondary antibody. No unspecific background is present in untransfected cells.

NSP5 chemical crosslinking

As previously mentioned, mild washing conditions of anti-NSP5 immunoprecipitates from virus infected cells, coprecipitated an additional band of 35 kDa. To better investigate NSP5 interaction with other viral or cellular proteins we decided to perform chemical crosslinking of rotavirus infected cells, followed by immunoprecipitation.

DSP is a water insoluble (membrane permeable) thiol cleavable homobifunctional crosslinker, with a 12 Å spacer arm. ^{35}S-Met-labeled rotavirus infected cells were incubated with DSP, lysed, immunoprecipitated with anti-NSP5 and characterised by SDS-PAGE, to determine the conjugated proteins. The results of these experiments are shown in figure 3.3A.

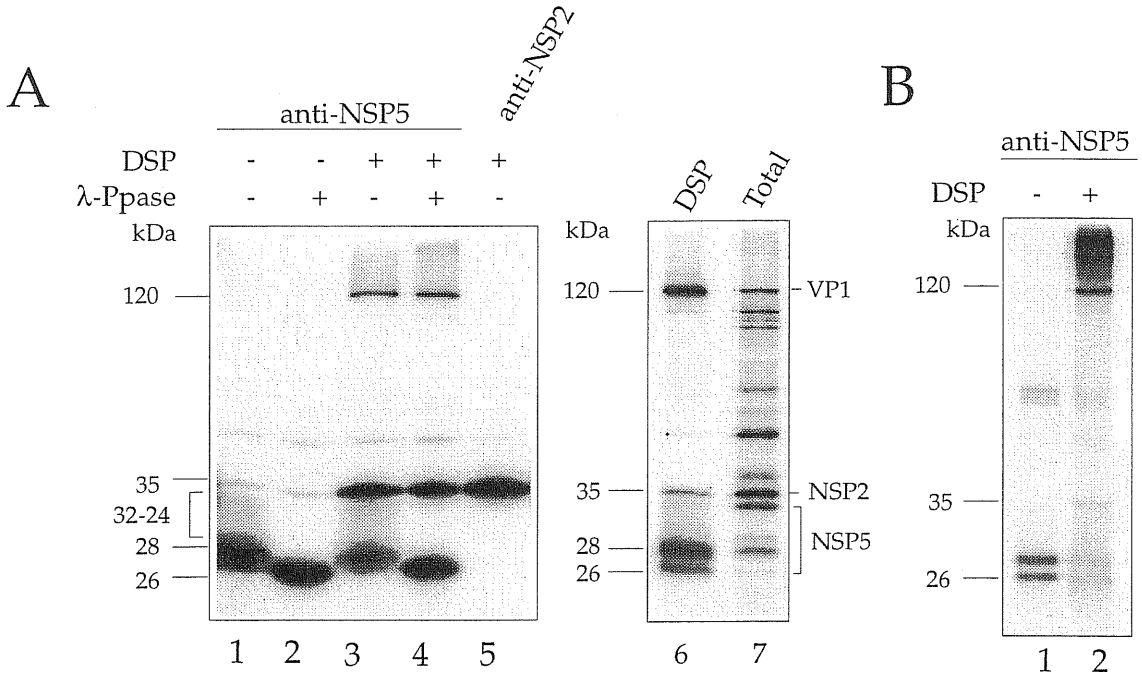

Figure 3.3. Analysis of DSP-crosslinked extracts.
^{35}S-labelled MA104 SA11 rotavirus infected cells were DSP crosslinked and subjected to immunoprecipitation.
A. Extracts were analysed in reducing SDS-PAGE conditions. Immunoprecipitates from non-crosslinked or DSP crosslinked extracts were eventually treated with l-Ppase before SDS-PAGE analysis (lanes 2 and 4). Total virus-infected cell extract is analysed in a parallel lane (lane 6). As control, anti-NSP2 immunoprecipitation of virus-infected cell extracts is also shown (lane 5).
B. Anti-NSP5 immunoprecipitates from non crosslinked or crosslinked extracts from virus infected cells analysed by SDS-PAGE in non reducing conditions (lanes 1 and 2).

As a consequence of the crosslinking, two new proteins of molecular masses, respectively of 120 and 35 kDa, were immunoprecipitated together with the different phosphorylated isoforms of NSP5 (lane 3). Total ^{35}S-Met-labeled extracts of rotavirus infected cells analysed on SDS-PAGE (lane 7), showed that the new NSP5 associated proteins migrated identically to the viral proteins VP1 (120 kDa) and NSP2 (35 kDa) (lanes 6 and 7). λ-Ppase treatment of the immunoprecipitates characterised the hyper-phosphorylated species (lane 4) producing the 26 kDa form corresponding to dephosphorylated NSP5, while the two other components of 35 and 120 kDa remained unchanged.

This result confirmed that all the bands smaller than 35 kDa corresponded to the different phosphorylated isoforms of NSP5. The specificity of the 35 kDa band was also confirmed by co-migration with NSP2 following specific immunoprecipitation from ^{35}S-labelled virus infected cells (lane 5).

Surprisingly, our anti-NSP2 antibody was not able to co-precipitate NSP5 from crosslinked extracts (not shown). However, DSP crosslinking experiments and specific anti-NSP2 immunoprecipitation performed on rotavirus infected cells, co-immunoprecipitated NSP2 and VP1 but not NSP5 (90). This suggests that most of the NSP2 interacting with NSP5, is hidden and not available for recognition by the antibody.

As expected, when analysed in non-reducing SDS-PAGE, NSP5 immunoprecipitates from DSP treated cells consist of a complex of high molecular mass, with most of the material remaining in the top of the gel, and some free NSP2 and NSP5 (figure 3.3B, lane 2).

UV crosslinking

By *in vivo* UV-crosslinking, NSP2 had been shown to have ss and ds RNA binding capacity suggesting a putative role in viral RNA stabilisation (91). To analyse if RNA molecules are present in the NSP5-NSP2 complex, we decided to perform UV crosslinking of ^{35}S–Met labeled virus infected cells. Figure 3.4 shows the result of the immunoprecipitations of untreated or UV treated extracts (lanes 1 and 3). Anti-NSP5 co-immunoprecipitated NSP2 (lane 3), thus confirming the NSP5-NSP2 interaction as observed by the chemical crosslinking (figure 3.3, lane 3). Interestingly, in this case no VP1 was co-immunoprecipitated. λ-Ppase treatment was also performed on the UV crosslinked immunoprecipitates (lane 2).

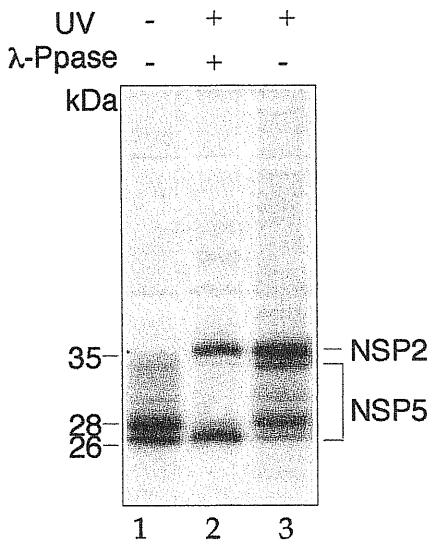

Figure 3.4. UV crosslinking.
SDS-PAGE analysis of anti-NSP5 immunoprecipitation from ^{35}S-labelled rotavirus infected cells that were irradiated (lane 3) or not with UV light (lane 1). l-Ppase treatment of UV immunoprecipitates demonstrated the hyper-phosphorylated species (lane 2).

As expected, NSP5 and NSP2 recovered from UV treated extracts, showed the same migration in reducing and non reducing conditions (not shown), demonstrating the non covalent nature of the interaction. However, the UV crosslinking is a technique used to covalently link nucleic acids to proteins (RNA/DNA binding proteins), and not protein to protein (21). For this reason, we consider the possibility that after UV crosslinking an RNA molecule could form a link between the two proteins. To evaluate this hypothesis, we incubated the UV treated cellular extracts with RNAseA before immunoprecipitation, without affecting the capacity of antibody against NSP5 to co-immunoprecipitate NSP2 (not shown). No differences in gel mobility of NSP2 or NSP5 were detected.

From these experiments, we conclude that, in this case, the NSP5-NSP2 co-precipitation could be the consequence of NSP2 conformational modifications induced by UV treatment. It could be that NSP2 crosslinked to a viral RNA molecule increases its affinity for NSP5, so that a non-covalent interaction would be sufficiently stable to resist immunoprecipitate washings.

NSP5-NSP2 *in vitro* binding assay

To evaluate the NSP2-NSP5 binding in vitro, we performed a pull-down experiment using a GST-NSP5 fusion protein purified from bacteria and the *in vitro* synthesised ^{35}S-Met-labeled NSP2.

The experiment was performed incubating NSP2 polypeptide at 37°C for 1 h using GST-NSP5 protein still bound to the GST-Sepharose resin. The amount of GST-NSP5 used is shown in a Coomassie stained gel shown in figure 3.5A. The NSP5-NSP2 binding, shown in the lane 1 of figure 3.5B, confirm that the two proteins have high intrinsic binding affinity. The binding is dramatically reduced when the reaction is performed at 4°C (lane 2). As internal negative controls, GST-NSP5 fusion protein was incubated at 37°C with mock reticulocyte extracts (lane 4) and with another *in vitro* synthesised rotavirus

protein VP4 (87 kDa) (lane 5). The amount of the input NSP2 and VP4 used in the reactions are also shown (lanes 6 and 7, respectively).

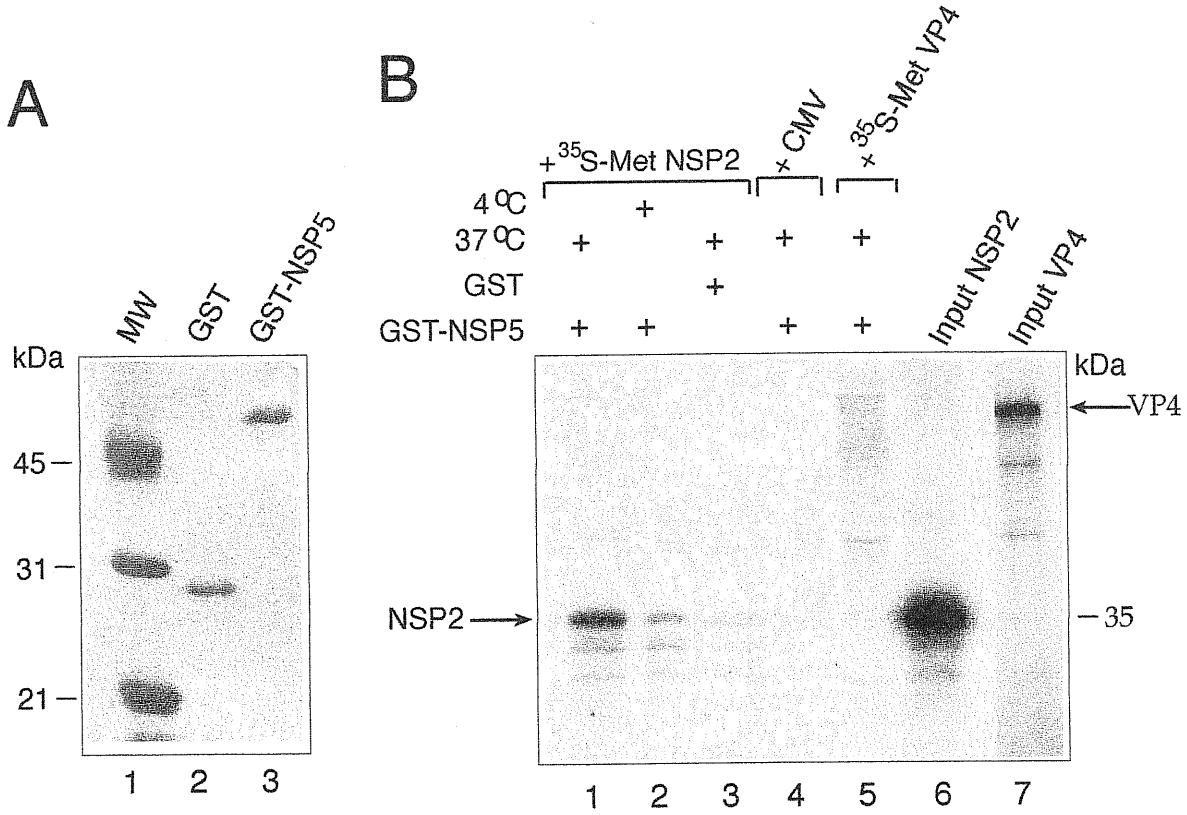

Figure 3.5. NSP2-NSP5 *in vitro* binding assay.
A. Coomassie staining of the GST-NSP5 fusion protein obtained from bacteria expression (lane 3).
B. SDS-PAGE analysis of pull down ^{35}S-Met-labelled NSP2 polypeptide. NSP2 and GST-NSP5 binding occurs better at 37°C (lane 1) than at 4°C (lane 2). No GST-dependent unspecific binding was detected (lane 3). In vitro synthesised ^{35}S-labelled VP4 polypeptide (lane 5), as well as mock translation reaction (lane 4), do not bound GST-NSP5 protein. The amount of input NSP2 and VP4 used, are shown in lane 6 and 7 respectively.

Biochemical and morphological consequences of NSP2-NSP5 interaction:

Phosphorylation of NSP5

NSP5 phosphorylation appears as a complex process, that involves the cooperation of different cellular and viral proteins. Indeed, only cell extracts from virus infected cells have a role in the phosphorylation of the *in vitro* synthesised NSP5 polypeptide, producing a shift from 26 kDa to 28 kDa after incubation with ATP (see figure 1.8, in the introduction) (5).

On the other hand, the crosslinking experiments indicated that in infected cells one of the NSP5 closer proteins is NSP2. We thus decided to investigate if its presence could regulate NSP5 phosphorylation.

^{35}S-Met-labelled non crosslinked and DSP crosslinked infected cell extracts were immunoprecipitated and the immunoprecipitates subjected to an *in vitro* kinase assay by incubation with [γ $^{-32}$P]-ATP. Figure 3.6A shows two autoradiographs of the same gel, where the right panel represents the ^{32}P-labelling only. Interestingly, a substantial increase in the 32-34 kDa hyperphosphorylated forms of NSP5 was obtained (lane 3), compared with the non-crosslinked immunoprecipitate (lane 1).

The total amount of NSP5 present in the immunoprecipitates subjected to the assay was the same for the non crosslinked and the crosslinked extracts, as evidenced by λ-Ppase treatment (left panel, lanes 2 and 4), that removed the phosphate residues.

This result suggested that the association of NSP5 with NSP2 have an enhancer effect on the phosphorylation of NSP5. An interesting hypothesis was that the binding of NSP2 to NSP5 regulates the accessibility of the NSP5 phosphorylation sites.

A

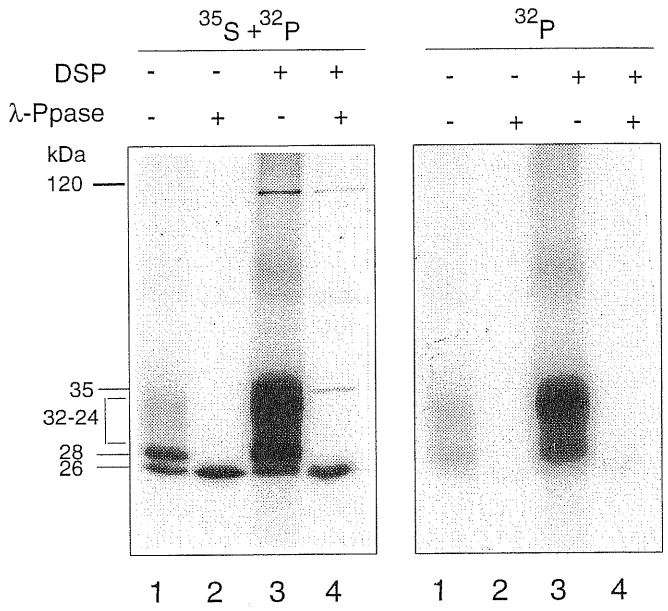

Figure 3.6A. NSP2 regulates NSP5 hyperphosphorylation *in vitro*.
A. Immunoprecipitates of ^{35}S-labelled rotavirus NSP5 from DSP non-crosslinked and crosslinked infected cell extracts, were subjected to *in vitro* phosphorylation in presence of [γ-^{32}P]-ATP and analysed in reducing conditions by SDS-PAGE. Left and right panels are two expositions of the same gel, corresponding to [^{35}S]+[^{32}P] and only [^{32}P], respectively. λ-Ppase treatment of the immunoprecipitates is indicated (lanes 2 and 4).

B

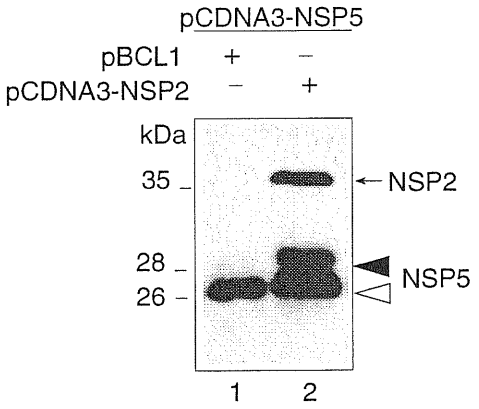

Figure 3.6 B.
Combined anti-NSP2/anti-NSP5 western immunoblot of MA104 cells extracts transfected with pCDNA3-NSP5 (lane 1) or co-transfected with pCDNA3-NSP5 and pCDNA3-NSP2 (lane 2). Control plasmid pBCL1 was used as the control (lane 1). Open and closed arrowheads indicate the NSP5 26 kDa precursor and the phosphorylated forms, respectively.

Although NSP2 appears to regulate NSP5 hyperphosphorylation, the involvement of other viral proteins, such as VP1, present in the crosslinked extracts could not be ruled out. To investigate this aspect, we co-transfected MA104 cells with plasmids containing the complete ORF of NSP5 and NSP2 (pCDNA3-NSP5 and pCDNA3-NSP2) in the absence of other rotavirus proteins. The extracts were analysed by western immunoblot as shown in figure 3.6B. When NSP5 is co-expressed together with NSP2, it was indeed hyperphosphorylated producing species of mobility of 32-34 kDa (lane 2). λ-Ppase treatment performed on total cell extracts confirmed the presence of phosphate residues in NSP5 (not shown) (4).

At this stage, there was no data to support this functional role for rotavirus non-structural protein NSP2. Now we have proved, in two different assays, *in vivo* and *in vitro*, that NSP5 hyperphosphorylation in highly dependent on the presence of NSP2. Moreover, these results indirectly confirmed the NSP2-NSP5 interaction *in vivo*.

Viroplasms in rotavirus infected cells

Early electron microscopy studies have demonstrated that both rotavirus non structural proteins NSP5 and NSP2 are found in viroplasms of infected cells at the early stages of infection (146).
Figure 3.7 shows an immunohystochemistry of rotavirus infected cells. NSP5 localisation in viroplasms was evidenced with an specific anti-NSP5 antibody and indirect immunoperoxidase reaction. Rotavirus viroplasms (arrows) appear as circular cytoplasmic structures with a strong NSP5 staining on the rim, suggesting a large accumulation of this protein on their surface.

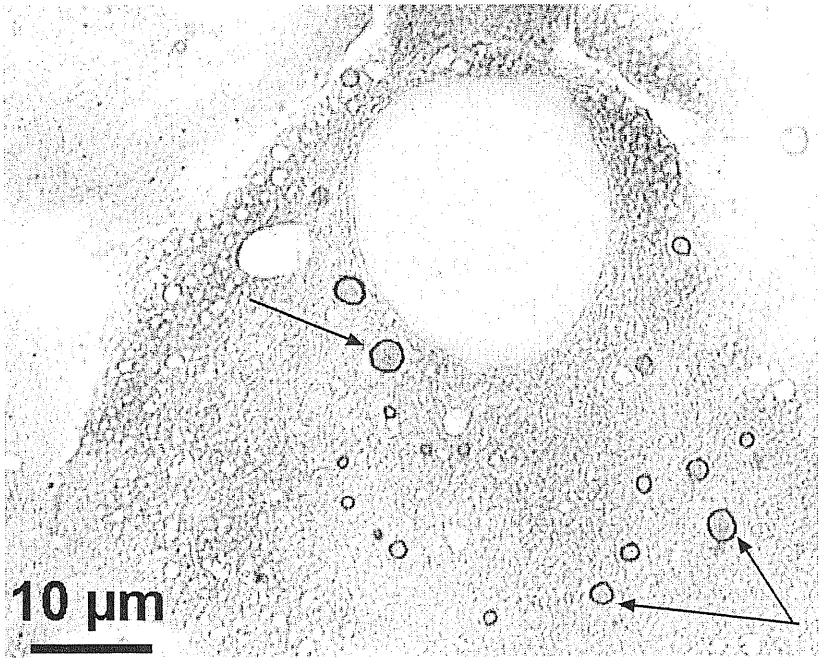

Figure 3.7. Immunohystochemistry of rotavirus infected cell.
Rotavirus viroplasms (arrows) are visualised with anti-NSP5 antibody and HRP immunostaining.

The significance of the presence of NSP5 and NSP2 in viroplasms is not known, although it has been hypothesised that both these proteins are involved in RNA stabilisation and in the support of virus packaging and replication. In part, the crosslinked of NSP5 with NSP2 and VP1 supports this view. In the same context, NSP5 does not crosslink with VP6, a highly abundant viroplasmic protein.

To further investigate the structure and, eventually, the relative spatial ultrastructural localisation of NSP5 and NSP2 in viroplasms, we decided to perform electron microscopy (EM) experiments.

Figure 3.8 shows an electronic transmission of rotavirus infected cells. The result is an image where the different subcellular compartments can be seen highly contrasted. Rotavirus viroplasms appear highly electrondense structures (vir) of a variable size from around 300 to 500 nm. Enveloped (e) and mature non enveloped (ne) virions in the lumen of the ER can be also clearly detected.

To identify the NSP5 ultralocalisation inside rotavirus viroplasms, we decided to performe immuno-electron microscopy experiments. Rotavirus infected cell monolayers were first reacted with a polyclonal mouse anti-NSP5 antibody and then embedded in the resin (pre-embedding technique). For the secondary immunoreaction, we chose 1 nm-diameter large gold-conjugated anti-mouse antibody, because are clearly distinguishable from the less defined biological structures. As shown in figure 3.9, anti-NSP5 gold immunolabelling identified specifically viroplasms (vir) and no unspecific reaction was found diffused in the cytoplasm or associated to immature viruses (arrows). Interestingly, fine cytoskeleton elements (sk) are also evident that seem to originate from viroplasms.

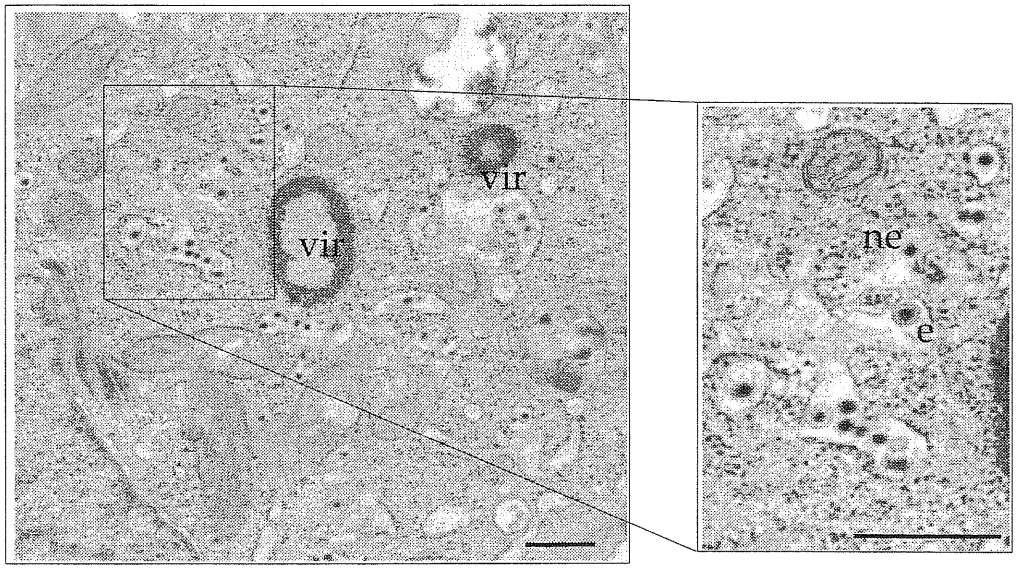

Figure 3.8. Transmission electron micrograph.
Electron microscopy of a rotavirus infected cell. Viroplasms are highly electrondense structures (vir). Immature enveloped (e) and non enveloped (ne) virions are emerging from the ER. Scale bar, 300 nm.

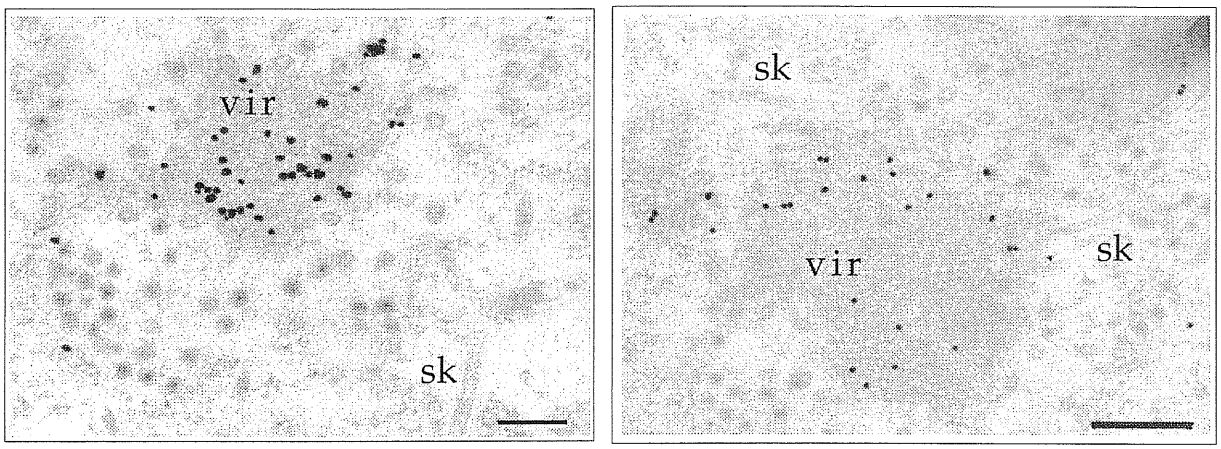

Figure 3.9. Immunogold NSP5 localisation.
Electron anti-NSP5 immunolocalization of rotavirus infected cells. 1 nm-diameter large gold-conjugated secondary anti-mouse antibody revealed that NSP5 protein is accumulated specifically in viroplasms (vir). Interestingly, virions under maturation (arrows), do not show gold labelling. Long cytoskeleton elements could be seen (sk). Scale bar, 300 nm.

Viroplasm-like particles

In the previous experiments, we had demonstrated that NSP5-NSP2 interaction had a biochemical consequence regarding the phosphorylation level of NSP5. However, since both proteins are found in virus infected cells in the viroplasm compartment, it suggests they could be involved in virion maturation. Thus, we decided to investigate their distribution in transfected cells, in the absence of any other rotavirus protein and rotavirus replication. To achieve this, we used the T7 DNA polymerase recombinant vaccinia virus (strain vTF7.3) (57; 58), that represents an efficient cytoplasmatic expression system for T7-dependent constructs. After vaccinia infection, we transfected MA104 cells with plasmids containing the complete ORF of NSP5 and NSP2 (pCDNA3-NSP5 and pCDNA3-NSP2). We assayed the expression of both expressed NSP5 and NSP2 proteins by immunofluorescence with specific antibodies. As shown in figure 3.10, NSP5 and NSP2 independent expression resulted in homogeneous distribution in the cytoplasm of the transfected cells (panels c and f). However, when both proteins were co-expressed, organisation of discrete structures with regular spherical shape became evident (panels g and h). For their similarity to rotavirus viroplasms (panels a and b), we called them viroplasm-like structures (VLS).

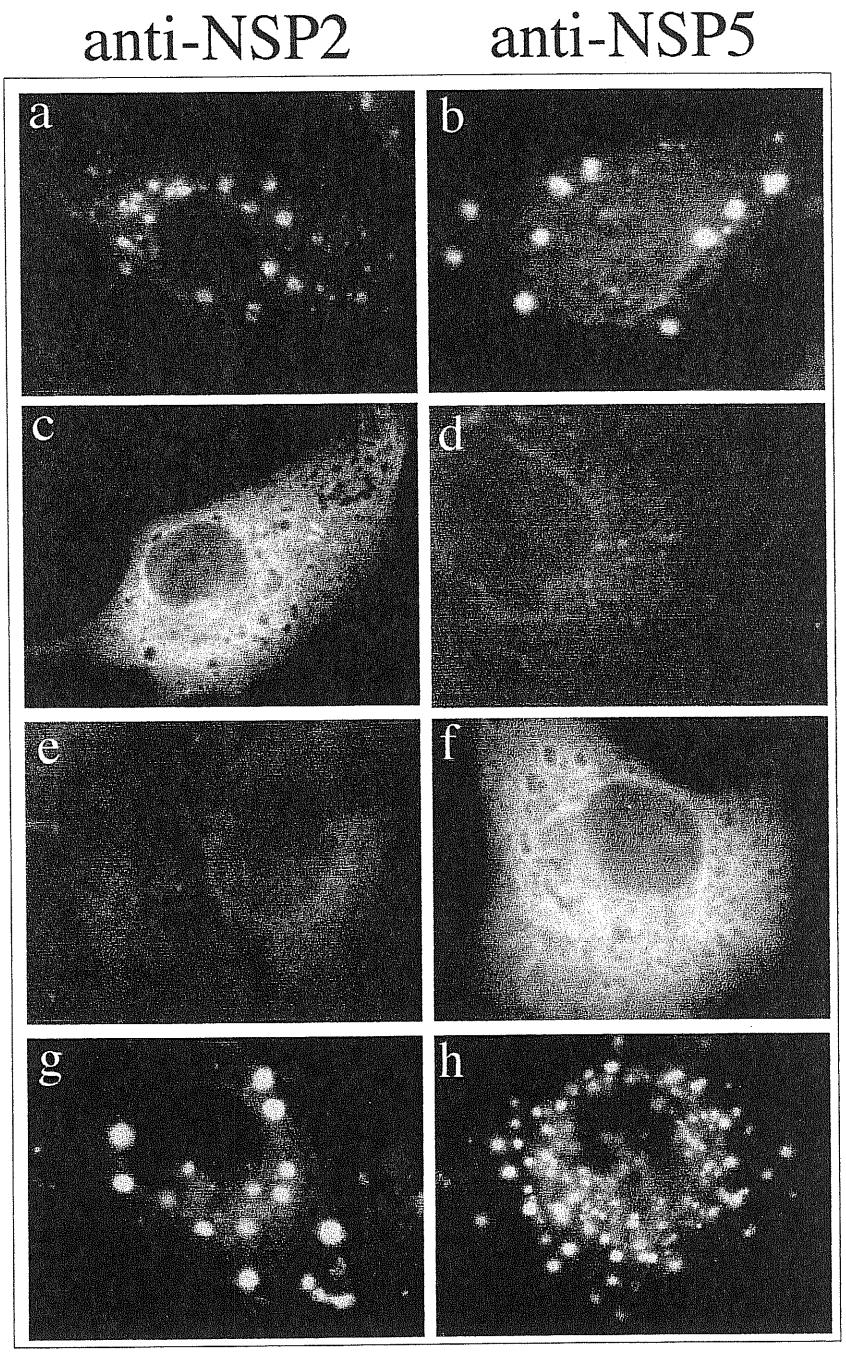

Figure 3.10. Cytoplasmatic localization of NSP2 and NSP5 in transfected cells. Anti-NSP2 (left) and anti-NSP5 (right) specific immunofluorescence microsocopy analysis. Viroplasms in SA11 rotavirus infected cells are evidenced (a, b). pCDNA3-NSP2 and pCDNA3-NSP5 single transfected cells showed an homogeneous protein cytoplasmatic distribution and no protein background (c, d and e, f). Viroplasm-like structures (VLS) are evidenced after pCDNA3-NSP2 and pCDNA3-NSP5 co-transfection (g, h).

NSP2 and NSP5 colocalise in viroplasms

The finding that *in vivo* NSP2 and NSP5 are sufficient to organise VLS in the absence of viral infection was an indirect confirmation of the NSP2-NSP5 interaction previously demonstrated biochemically. However, to demonstrate that NSP5 and NSP2 truly interact in VLS, we performed confocal (laser scanning) light microscopy analysis.
As demonstrated by the double staining immunofluorescence analysis presented in figure 3.11, rotavirus viroplasms as well as VLS can be visualised with both anti-NSP2 and anti-NSP5 antibodies, seen respectively in green and in red, showing a precise co-localisation of both NSP2 and NSP5.

VLS obtained by NSP5 and NSP2 co-expression are quite similar to rotavirus viroplasms, but a difference on protein "density" can be appreciated. While VLS appear as "empty" spheres, viroplasms are complex structures. The presence of the other viral proteins as well as the RNA in virus infected cells, could certainly account for the difference in morphology between viroplasms and VLS. However, this morphology in part could also depend on the conditions used for fixing the samples.

In addition, interesting informations resulted from analysis of images obtained by serial confocal sections. Figure 3.12B represents four different longitudinal planes (collected in 0.5 µm steps) of the same NSP5-NSP2 co-transfected cell. The result highly suggested that NSP5 immunostained VLS have a near spherical shape.

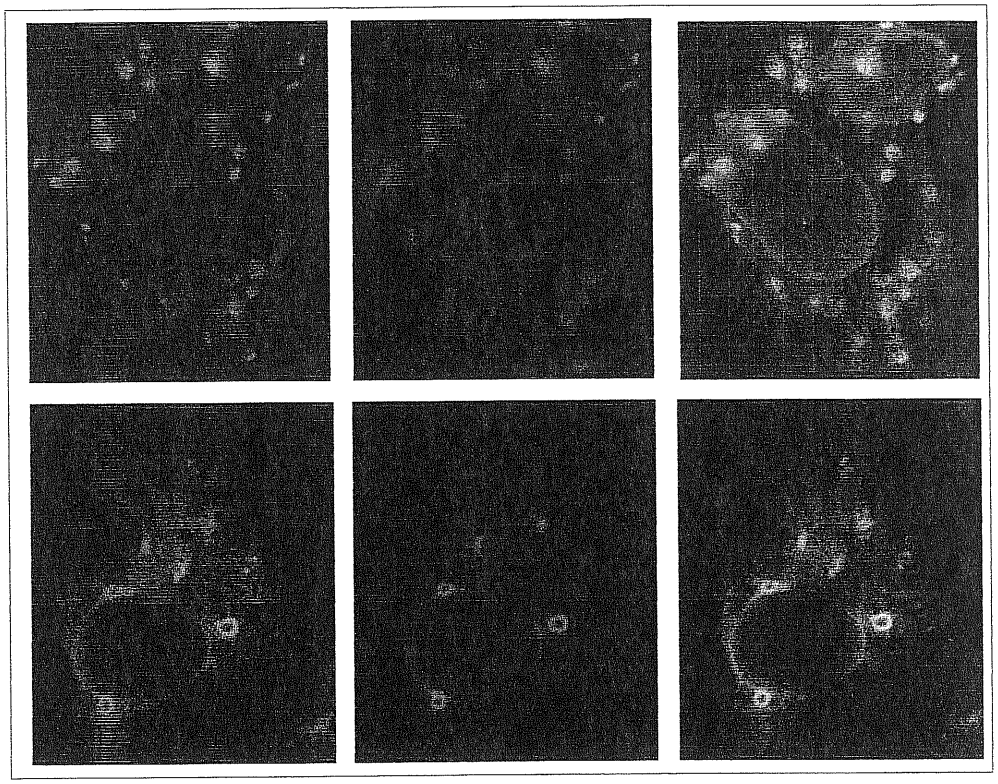

Figure 3.11. Double immunofluorescence of Viroplasm and VLS.
Rotavirus infected cells (A) and NSP5-NSP2 co-expressing cells (B) were subjected to double immunofluorescence to detect viroplasms and VLS. FITC and RITC contemporaneous immunostaining permitted to visualise respectively NSP2 (green) and NSP5 (red) localisation.

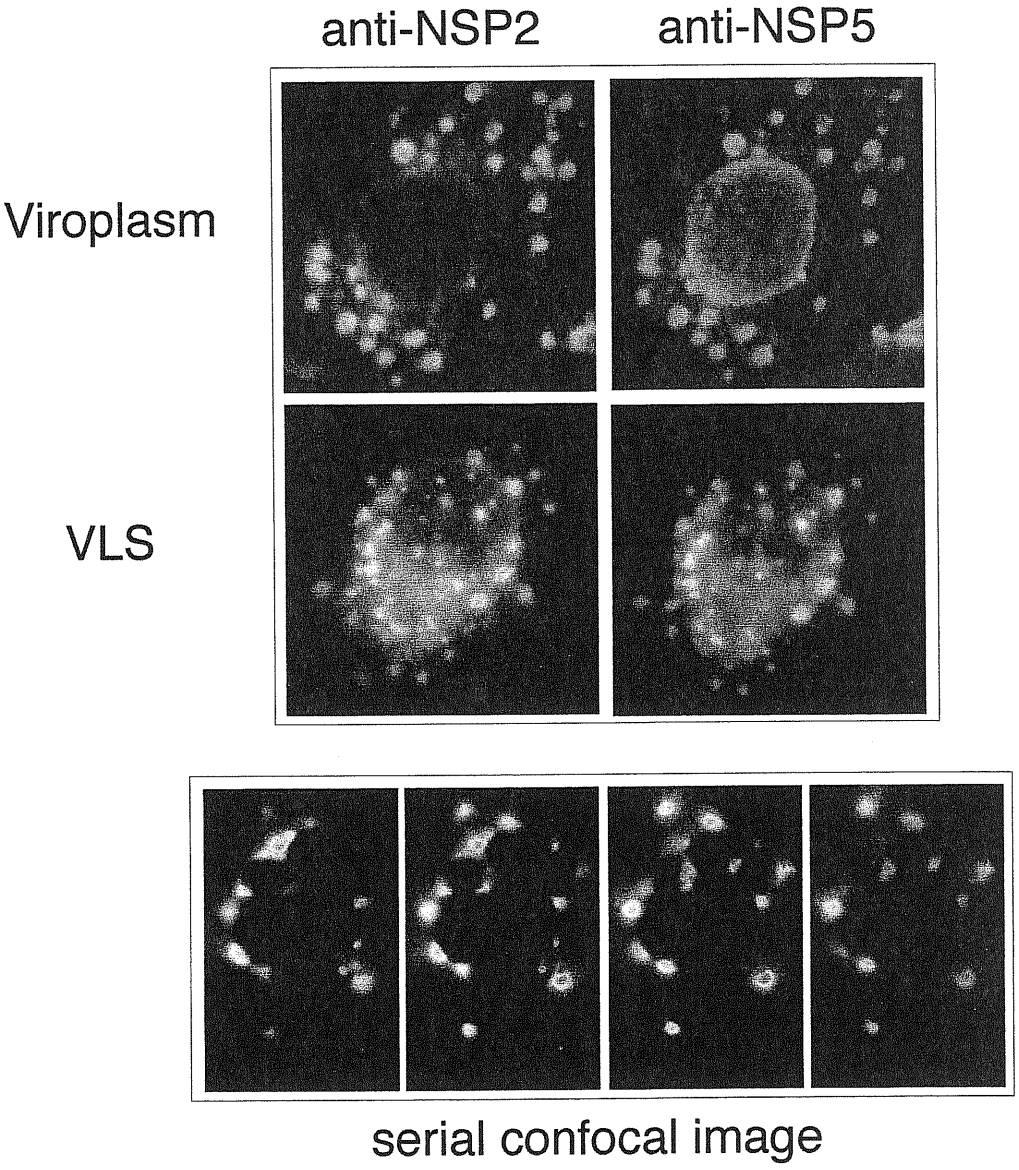

Figure 3.12. Confocal immunofluorescence microscopy.
A. MA104 cells, either infected with rotavirus SA11 or co-transfected with NSP2 and NSP5 as indicated, were reacted simultaneously with anti-NSP2 (green) and anti-NSP5 (red). The rightmost panel shows the superimposition of the two independently acquired images. B. Serial laser confocal images of a NSP2 and NSP5 co-transfected cell. Cells were immunoreacted with anti-NSP5 antibody to detect VLS. Parallel confocal sections were collected in 0.5 μm steps.

Under standard assay conditions, cells were fixed at 3 h post infection to visualise viroplasms and at 16 h post transfection to visualise VLS. Interestingly, in both the cases, at these times most of the total amount of NSP5 expressed is localised in viroplasms or in VLS with practically no NSP5 background diffused in the citosol (see figure 3.10 and 3.11). This suggest an efficient relocalisation of NSP5 in presence of NSP2, and moreover, it could presume an eventual NSP5 degradation mechanism of the protein not localised in VLS (see page 98). On the contrary, at longer times post-transfection (more than 20 h) NSP5 staining was almost absent and VLS were hardly detectable (not shown).

NSP5 mutants

To better characterise NSP5 in terms of VLS formation capacity and hyperphosphorylation, we decided to construct a series of NSP5 deletion mutants. NSP5 does not share any homology with other known proteins, so we had no hypothesis on its tertiary structure. We decided to divide it arbitrarily in 4 regions and a short C-terminus sequence of 18 aa long ("tail"). A schematic representation of wt NSP5 and all the N-, C- and internal deletion mutants obtained, is shown in figure 3.13.

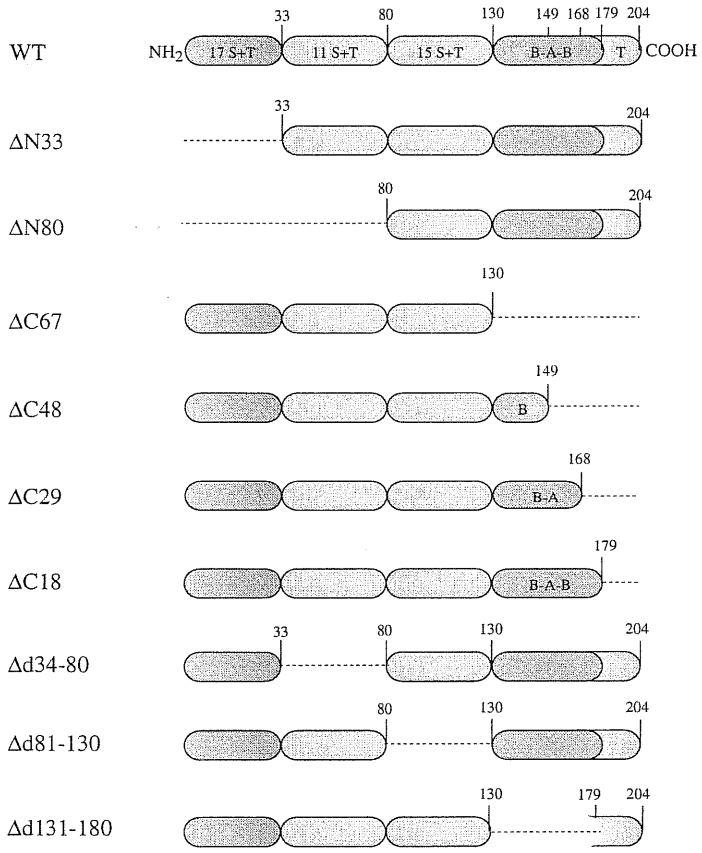

Figure 3.13. Schematic representation of internal NSP5 deletion mutants.
In each region of wt NSP5 is indicated the relative Ser+Thr content. B-A-B indicates the 49 aa long highly charged (61% of charged reidues) basic-acid-basic domain. The last 18 aa represent the "tail" (=T).

In wt NSP5, the number of Serine and Threonine residues per domain is indicated, as well as the basic-acid-basic region (BAB), characterised by highly charged aminoacids and the interesting S-D-S repetitions (for the NSP5 aminoacidic sequence, see in the introduction figure 1.7, page 25). The mutants were named according to the specific regions deleted.

All mutant constructs were fully sequenced and some of them (ΔN33, ΔC68, Δd34-80, Δd81-130 and Δd131-179) initially characterised by anti-NSP5 immunoprecipitation of the respective *in vitro* translated polypeptides (figure 3.14). Interestingly, their mobility in SDS-PAGE resulted strongly different from the one expected (see figure 3.14, right panel). In some cases (such as in ΔN33), a shorter band can be seen that corresponded to an internal translation initiation site.

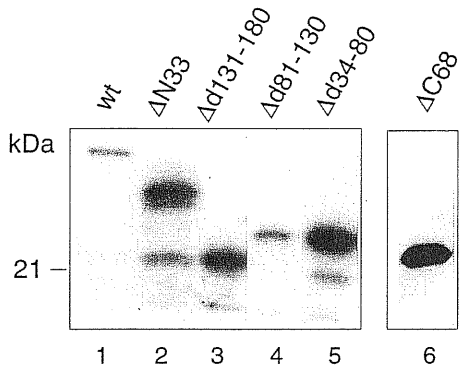

mutants	aa	expected MW (kDa)
wt NSP5	198	26
ΔN33	165	18.1
Δd131-180	149	16.4
Δd81-130	149	16.4
Δd34-80	152	16.7
ΔC68	130	14.3

Figure 3.14. Mobility of NSP5 deletion mutants.
Immunoprecipitation of different in vitro synthesised ^{35}S-Met-labelled NSP5 deletion mutants. The relative theoretical molecular weights are also summarised on the right.

The different NSP5 mutants were thus co-expressed together with NSP2 and tested for their capacity to assemble VLS. Figure 3.15 shows a series of different anti-NSP5 immunofluorescence assays of cells transfected either with the single NSP5 deletion mutants (left) or co-transfected together with NSP2 (right). Mutants lacking either N-terminal (ΔN33, ΔN80) or C-terminal (ΔC18, ΔC29, ΔC48, ΔC68) portions were completely inactive in forming VLS. In panels a and b of figure 3.15 are presented ΔN33 as an example of one of the NSP5 mutants unable to organise VLS. Cells transfected with ΔN33 alone (a) or co-transfected together with NSP2 (b), showed the same diffuse localisation of ΔN33 protein. Similar results were obtained with mutants ΔN80, ΔC18, ΔC29, ΔC48 and ΔC68 (not shown). Interestingly, the NSP5 internal deletion mutant which lacks the third domain (Δd81-130), was the only one able to produce VLS when co-expressed with NSP2 (d), even though smaller than the ones obtained with wt NSP5. Two other internal deletion mutants, Δd34-80 and Δd131-179, lacking respectively the second and the fourth B-A-B region, were not sufficient to form VLS in presence of NSP2 (respectively f and h). Δd131-179, however, showed a non homogeneous distribution with irregular spots and short spikes produced even in the absence of NSP2 (g). On the other hand, mutant Δd34-80, even though sensitive to the presence of NSP2, produced irregular structures rather than the spherical VLS (h). Taken together these data indicate that both N- and C-terminal region of NSP5 are required for VLS formation.

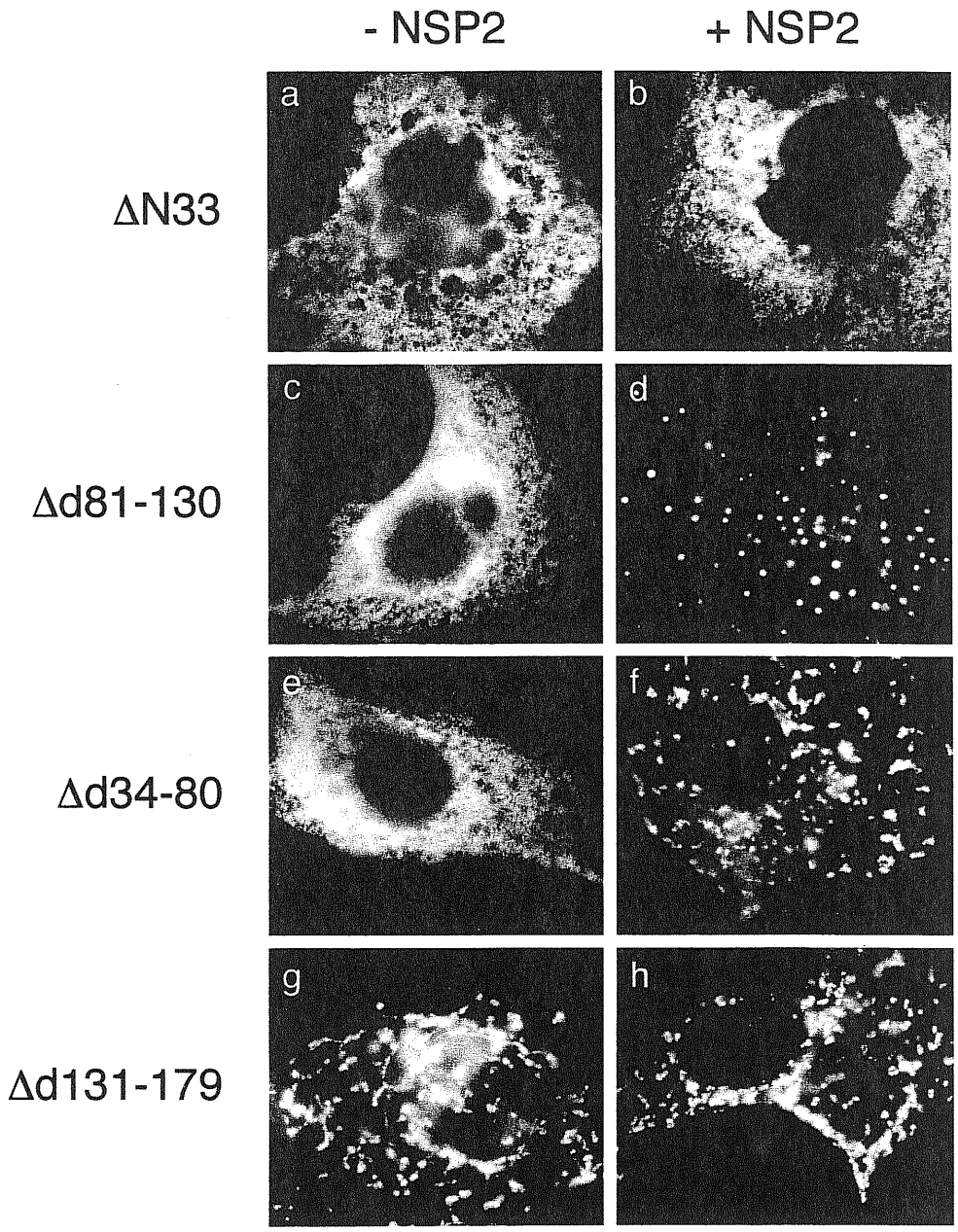

Figure 3.15. NSP5 mutants and VLS formation.
Anti-NSP2 (right) and anti-NSP5 (left) immunofluorescence of cells expressing NSP5 deletion mutants either alone (a, c, e, g) or in presence of NSP2 (b, d, f, h). As example of VLS negative phenotype, ΔN33 co-expression with NSP2 is shown (b). VLS were detected when Δd81-130 is co-expressed with NSP2 (d). Peculiar phenotype is observed with mutants Δd34-80 and Δd131-179 (f, h).

EGFP could be an NSP5 marker for its localisation in viroplasms

Until now, rotavirus reverse genetic has not been possible and recombiant virus for specific fragments was never obtained. The study of the viral proteins directly involved in viroplasms organisation during rotavirus infection thus is not possible. The importance of viroplasms in the virus replicative cycle has been suggested by early studies of temperature sensitive (ts) rotavirus mutants. In particular, mutants mapping in the NSP2 gene, are completely replication deficient with a viroplasm negative phenothype at the non permissive temperature (68). On the other hand, the sequence of NSP5 is conserved among the different rotavirus strains (106) and no NSP5 rotavirus mutants have been described (49), highly suggesting that NSP5 should play a key role in rotavirus replication. From these observations it has been concluded that viroplasms localisation of NSP5 might reflect a relevant aspect of the activity of this protein. However, rotavirus experimental models efficient to demonstrate the role of NSP5 are not available.

We decided to approach to this problem, investigating the effective role of NSP5 in viroplasms organisation expressing a recombinant form of NSP5 during rotavirus infection. Our question was whether the presence of a recombinant NSP5 during rotavirus infection could functionally interact with the other rotavirus proteins (such as NSP2 and wt NSP5) and thus be driven into true viroplasms, rather than VLS. To follow its intracellular destination and to discriminate from the original rotavirus NSP5, we fused NSP5 ORF at the N-terminus of the Green Fluorescent Protein (EGFP). We transiently transfected pEGFP-NSP5 plasmid DNA in MA104 cells and 48 h later approximately 70% of the cells showed green fluorescence. We then infected the NSP5-EGFP expressing cells with rotavirus and 4 h later we looked for NSP5-EGFP localisation in living cells.

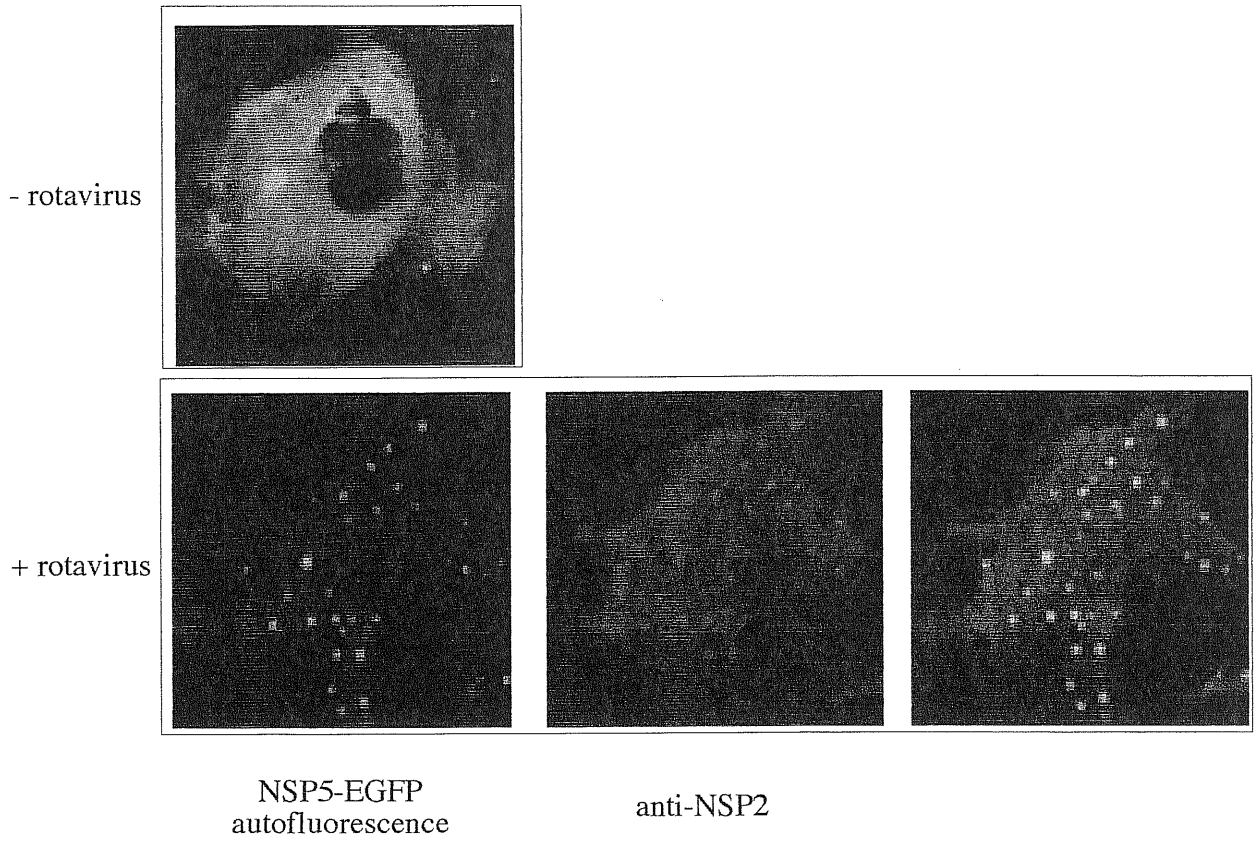

Figure 3.16. Viroplasm localisation of NSP5-EGFP fusion protein
A. Living NSP5-EGFP transfected cells shows homogenous green autofluorescence. B. Double fluorescence analysis performed on confocal microscope of rotavirus superinfected NSP5-EGFP expressing cells. Confocal co-localisation of recombinant NSP5-EGFP (green autofluorecence) and rotavirus NSP2 protein (red). Confocal image superimposition is also shown.

As shown in figure 3.16, in rotavirus infected cells GFP fluorescence was observed in viroplasms, demonstrating the correct localisation of the non viral fusion protein NSP5-EGFP, while in non-infected cells NSP5-EGFP had a normal homogeneous and diffuse cytoplasmatic distribution. Co-localisation of NSP5-EGFP and rotavirus NSP2 in viroplasms was confirmed by confocal specific immunofluorescence microscopy.
These last results permit to underline the intrinsic behaviour of NSP5 to localise in viroplasms. This approach opens the possibility to further investigate the behaviour of the different NSP5 mutants in the context of the capacity to localise in true viroplasms. In particular, it would be interesting to see if any of the NSP5 mutants could compromise viroplasm formation and rotavirus infection, thus working as dominant negative mutants.

In vivo expression and phosphorylation of NSP5 mutants

Since NSP5 phosphorylation and VLS formation are both related to the NSP5/NSP2 interaction, we decided to investigate the capacity of the different NSP5 mutants to be phosphorylated *in vivo*.
Hyperphosphorylation of wt NSP5 can be easily assessed because it largely affects its migration on SDS-PAGE and is λ–Ppase sensitive, even though, we know that NSP5 can also be phosphorylated without changes in mobility (5). NSP5 deletion mutants single transfections were tested by western immunoblot (figure 3.17A) and by ^{32}Pi *in vivo* labelling and inmmunoprecipitation (figure 3.17B).
As shown in figure 3.17, only ΔN33 and Δd81-130 mutants were characterised by spontaneous hyperphosphorylation detectable in western immunoblot (panel A, lanes 3 and 9) as well as in $^{32}P_i$ *in vivo* labelling (panel B, lanes 2 and 4).

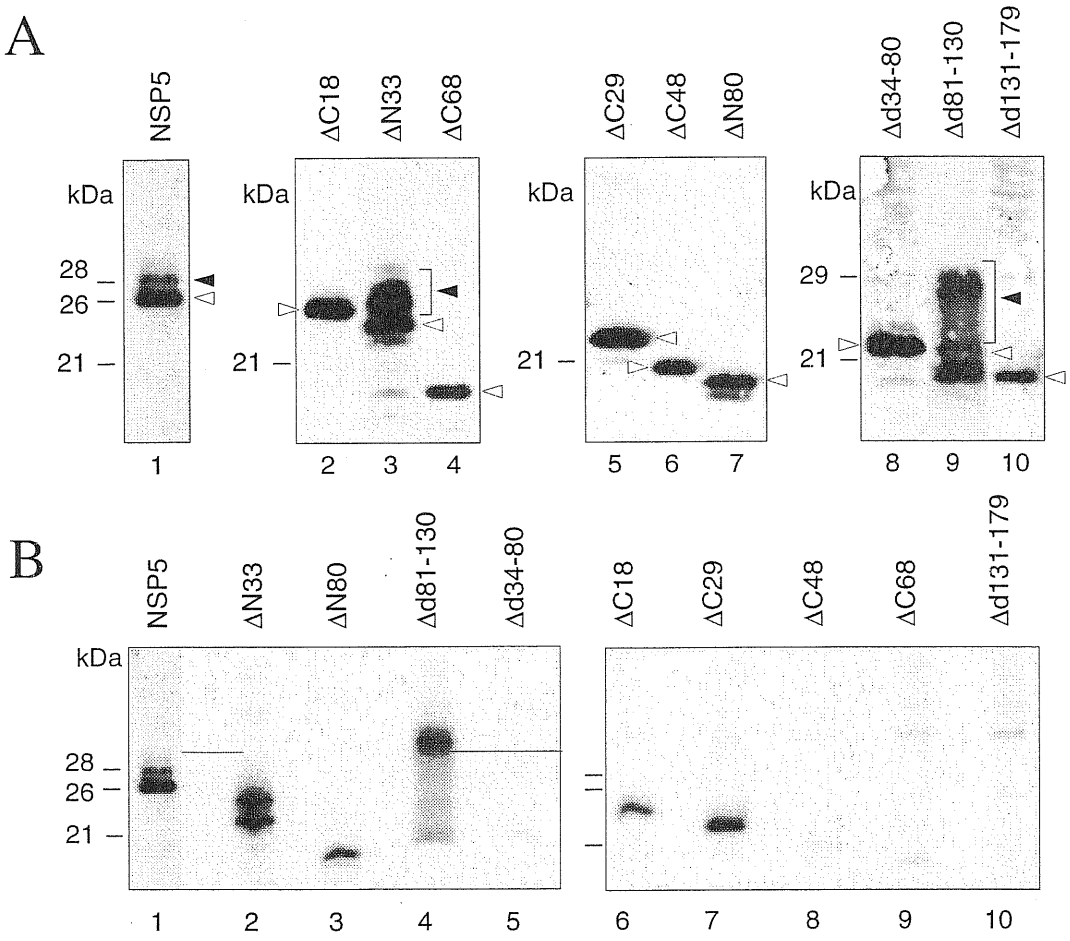

Figure 3.17. *In vivo* phosphorylation of NSP5 deletion mutants
A. Anti-NSP5 western immunoblot of extracts of each independently transfected NSP5 deletion construct. Filled arrowheads indicate l-Ppase sensitive hyperphosphorylated species with reduced gel mobility.
B. Immunoprecipitations of cells transfected with the indicated NSP5 deletion mutant constructs and labelled in vivo with $^{32}P_i$.
Relative molecular masses in kDa are shown to the left.

In particular, Δd81-130 hyperphosphorylation produced an enourmous mobility shift from around 21 to forms of up to 29-30 kDa (figure 3.17A lane 9). All the other N- and C-terminal deletion mutants (ΔC18, ΔC68, ΔC29, ΔC48 and ΔN80) did not show any mobility change in SDS-PAGE (figure 3.17A, lanes 2, 4, 5, 6 and 7), eventough ΔN80, ΔC18 and ΔC29 can be labelled *in vivo* with $^{32}P_i$ (figure 3.17B, lanes 3, 6 and 7). Interestingly, none of the two other internal deletion mutants Δd34-80 and Δd131-179 were phosphorylated (figure 3.17A, lanes 8 and 10; figure 3.17B, lanes 5 and 10). As expected, wt NSP5 phosphorylation was also observed (figure 3.17, lane 1).
The hyperphosphorylation of the deletion suggests that in wt NSP5 there are structural inhibitory constrains whose elimination allows the exposure of new phosphorylation sites. The different NSP5 domains might interact in a such way to mantain a general inhibitory effect, that is removed by NSP2 interaction, as suggested by the enhanced phosphorylation of NSP5 after crosslinking and in co-transfected cells (see figure 3.6A and B, page 66). Our hypothesis was that NSP2 have a key role in the activation of NSP5 during the virus infection.

In vitro phosphorylation of NSP5 mutants

Since NSP5 immunoprecipitates from virus infected cells were phosphorylated *in vitro* and moreover the *in vitro* synthesised 25 kDa NSP5 precursor was converted *in vitro* to 28 kDa phosphorylated form (5), we and other authors considered the possibility that NSP5 was the rotavirus kinase. Therefore we decided to set up an *in vitro* kinase assay to map the phosphorylated domains and eventually to characterise the domains required for NSP5 phosphorylation.
For that reason, the different NSP5 deletion mutants were transfected and the extracts immunoprecipitated and subsequently subjected to an *in vitro* kinase reaction in the presence of γ-^{32}P-ATP (figure 3.18A).

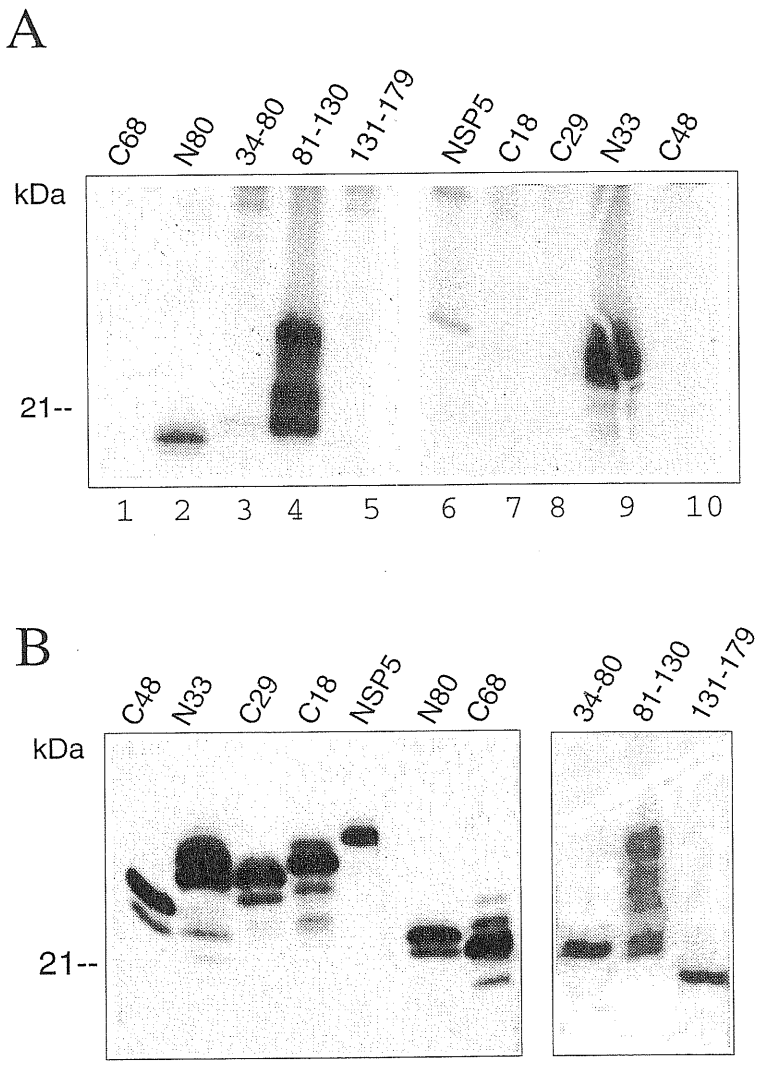

Figure 3.18. *In vitro* phosphorylation of NSP5 deletion mutants
A. SDS-PAGE analysis of *in vitro* [g-^{32}P]-ATP-labelled NSP5 deletion mutants immunoprecipitates. MA104 cells were transfected with the different mutant constructs, immuoprecipitated with specific anti-NSP5 antibody and thus subjected to the *in vitro* kinase assay.
B. Anti-NSP5 western immunoblot of the different extracts used for the kinase assay.

The immunoprecipitates were so labelled depending on their auto-phosphorylation ability. The results confirmed that the two mutants that *in vivo* underwent hyper-phosphorylation (Δd81-130 and ΔN33) (see figure 3.17B), were also able to auto-phosphorylation *in vitro* (figure 3.18A lanes 4 and 9). Interestingly, among all the other mutants that are phosphorylated *in vivo* ^{32}Pi-labelling (see figure 3.17B), ΔN80 was the only one which showed autophosphorylation ability (figure 3.18A, lane 2). This activity was however not present in ΔC18 and ΔC29. It is possible that different phosphorylation sites are regulated by different cellular kinases, or that the ΔC18 and ΔC29 phosphorylation sites were already completely saturated *in vivo*. The quality of the extracts used was checked in western immunoblot (figure 3.18B). However, we can not exclude that cellular contaminants working as kinase or phosphoprotein activator could also be present in our immunoprecipitates, and have some role in NSP5 mutants phosphorylation.

New NSP5 domain combination mutants and their characterisation

At this point it was clear that the division of NSP5 in different domains results in differently characterised phenotypes. To better investigate the role of the NSP5 domains in the phosphorylation, we decided to construct a second series of constructs derived from NSP5, summarised in figure 3.19. We named them according to the presence of the specific regions and of the C-terminal 18 aminoacids tail ("T"): 1+2, 2+3, 1+4T, 2+4T and 4T.

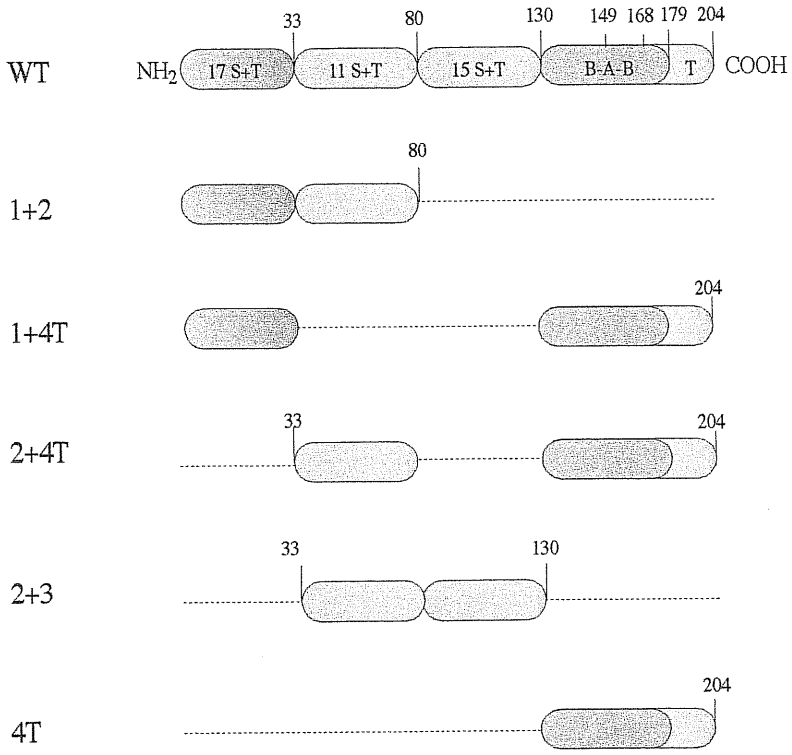

Figure 3.19. Schematic representation of different NSP5 domain combinations. Shortest NSP5 deletion mutants composed by different combinations of 2 NSP5 domains only. They are named them for their presence of specific domains and of the last C-terminal 18 aa (= tail, "T").

A preliminary series of experiments was performed to characterise the new NSP5 domain combinations by *in vitro* translation assays (TNT) (figure 3.20A) and by *in vivo* expression and western immunoblot (figure 3.20B). All of them *in vitro* or *in vivo* showed higher molecular weight than the one expected. Mutant 1+2 was efficiently translated *in vitro* and correctly immunoprecipitated by anti-NSP5 polyclonal antibody (part A, lane 1), but was not stable *in vivo* (part B, lanes 3 and 4).

The most interesting result derived from the analysis of the *in vivo* expression of mutant 2+4T, as shown in figure 3.21. Its *in vivo* expression was characterised by western immunoblot and by *in vivo* ^{32}Pi-labelling (parts A and B) demonstrating that 2+4T is hyper-phosphorylated *in vivo* and in vitro. Interestingly, MA104 cell expression of 2+4T showed that 2+4T, when co-expressed together with NSP2, is able to organise original peculiar structures that, even if less homogeneous, remember VLS (part C, right panel). Interestingly, mutant Δd81-130 that, in addition to domain 1, also contains domains 2+4T, the same phenotype that 2+4T in terms of hyperphosphorylation and VLS formation.

The colocalisation of NSP2 and NSP5 or mutants Δd81-130 and 2+4T in VLS, strongly suggested that the interaction is also required for VLS formation. The NSP5 region involved in the interaction with NSP2 is not easy to be hypothesised. The NSP5 domain study indicates that the minimum NSP5 domains required for localisation in VLS are the second and the fourth-tail, (2+4T), suggesting that the NSP5 portion that interacts with NSP2 should also map in these regions.

A

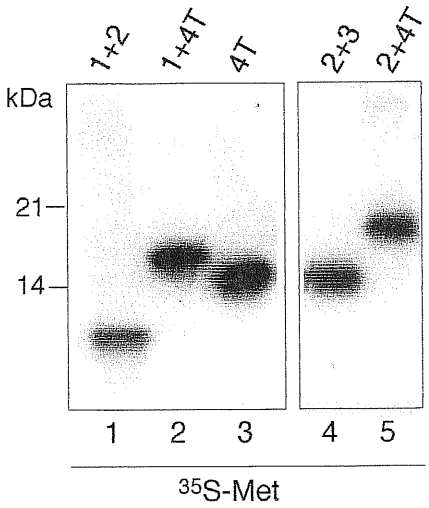

mutants	aa	expected MW (kDa)
1+2	80	8.8
1+4T	101	11.1
4T	68	7.5
2+3	97	10.7
2+4T	115	12.6

B

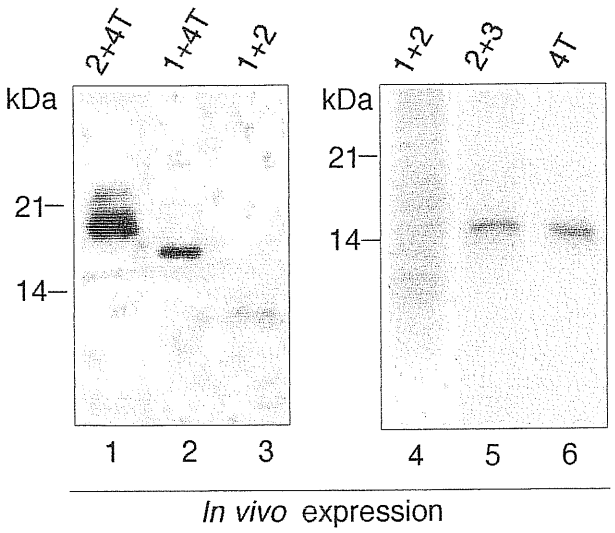

Figure 3.20. Gel mobility of NSP5 domain combinations.
A. SDS-PAGE analysis of different *in vitro* synthesised ^{35}S-Met-labelled NSP5 domain combinations. The relative theoretical molecular weights expected are also summarised.
B. Western immunoblot of cellular extracts of different NSP5 domain combinations transfected cells. The first 81 aa of NSP5 are not stable *in vivo*, as demonstrated by two independent transfections of mutant 1+2 (lanes 3 and 4).

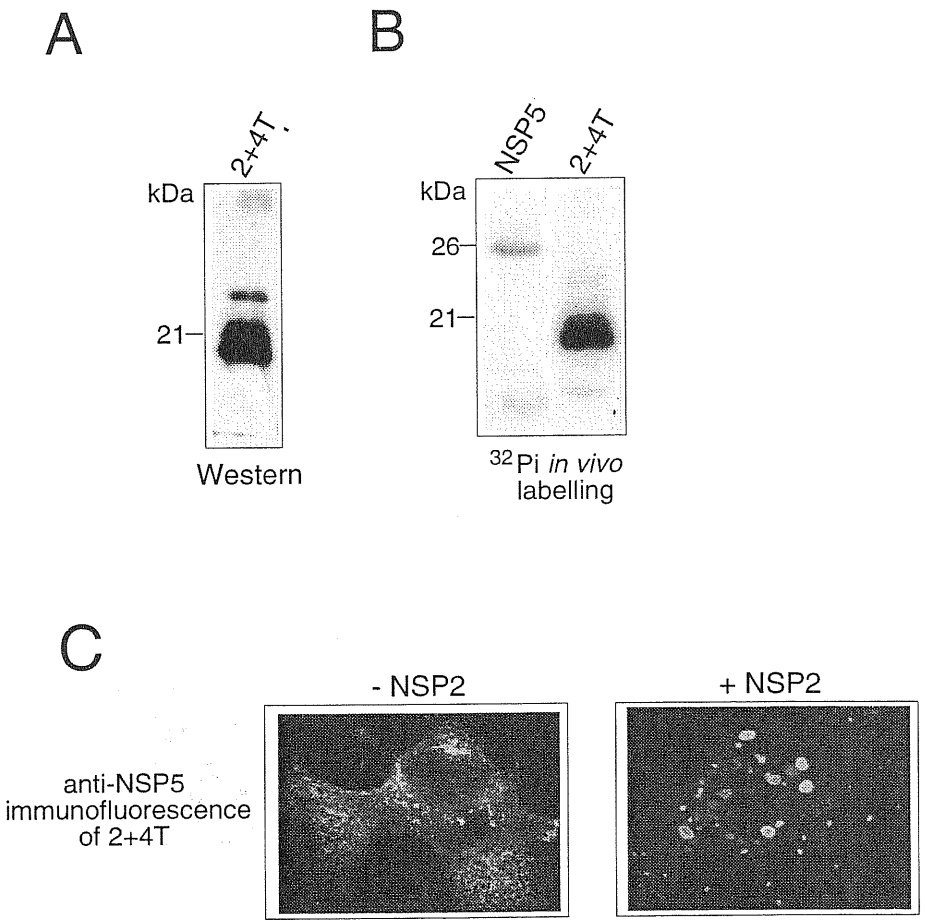

Figure 3.21. Characterisation of 2+4T *in vivo*.
A. Anti-NSP5 western immunoblot of 2+4T transfected cells.
B. *In vivo* ^{32}Pi -labelling of 2+4T transfected cells; as control, wt NSP5 protein was also *in vivo* ^{32}Pi-labelled (lane 1).
C. Immunofluorescence of 2+4T and 2+4T/NSP2 co-expressing cells.

In attempt to complement hyperphosphorylation negative mutants

From the previous studies, we hypothesised that the NSP5 enzymatic activity was concentrated on the C-terminal portion of the protein, since the absence of the last 68 aminoacids abolished any phopshorylation activity. It has also been reported that NSP5-NSP5 homodimerisation has a functional role in virus infection (192). Thus, it was possible that NSP5 would auto-phosphorylate by a trans-molecular phosphorylation event. Our efforts were thus oriented to the mapping of the substrate and the kinase regions of NSP5.

Since ΔN33 was hyperphosphorylated *in vivo*, we tested the possibility that this molecule could complement with ΔC68 (hyperphosphorylation negative mutant) (Figure 3.22).

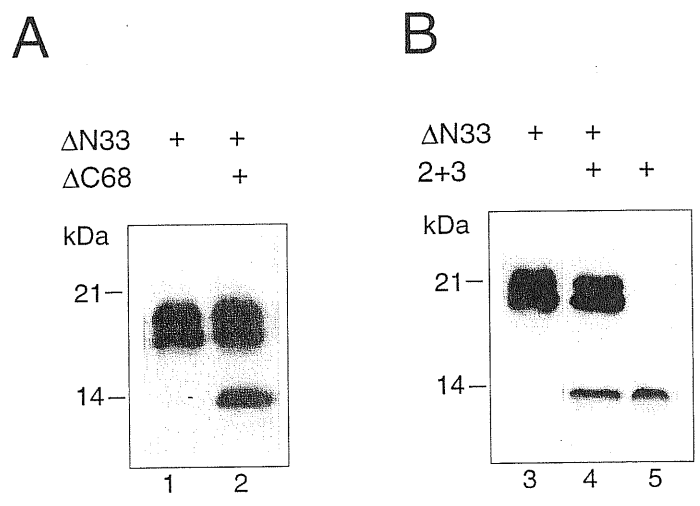

Figure 3.22. *In vivo* trans kinase activity of ΔN33.
Anti-NSP5 western immunoblot of cell extracts transfected with pCDNA3-ΔN33 and pCDNA3-ΔC68 (A) or pCDNA3-ΔN33 and pCDNA3-(2+3) (B).

Figure 3.22A shows a western immunoblot of total extract of ΔN33 and ΔC68 co-transfected cells. This approach was unsuccessful; in spite of the fact that the two species can be clearly separated on SDS-PAGE, it was never observed ΔC68 hyperphosphorylation. Using the same strategy, ΔN33 was tested as enzyme on mutant 2+3 (see figure 3.19). Also in this case, ΔN33 did not change the mobility of the mutant (figure 3.22B).

In vitro kinase assay

After the previous preliminary negative experiments, we started to characterise the substrate and kinase domains of NSP5 with a different approach.
We decided to express ΔN33 mutant in MA104 cells (MA-N33) and to test its eventual kinase activity *in vitro* on different *in vitro* synthethised ^{35}S-Met-labelled polypeptides (Δd81-130, 2+3 and 2+4T) (figure 3.23).

Since the incubation with infected cell extracts is required for NSP5 precursor *in vitro* phosphorylation (5) we supposed that the best opportunity to obtain a positive result was the direct incubation of kinase and substrates without further purifications, to mantain eventual factors present in the cell lysates. After 1 h of reaction at 37°C, the ^{35}S-Met-labelled substrates were immunoprecipitated and analysed on SDS-PAGE for gel mobility changes. None of the mutants tested were phosphorylated by ΔN33 (figure 3.23). As a control, the substrates were incubated also with untransfected cell extracts (MA104) or with extracts from vaccinia infected cells (MA-VACC).

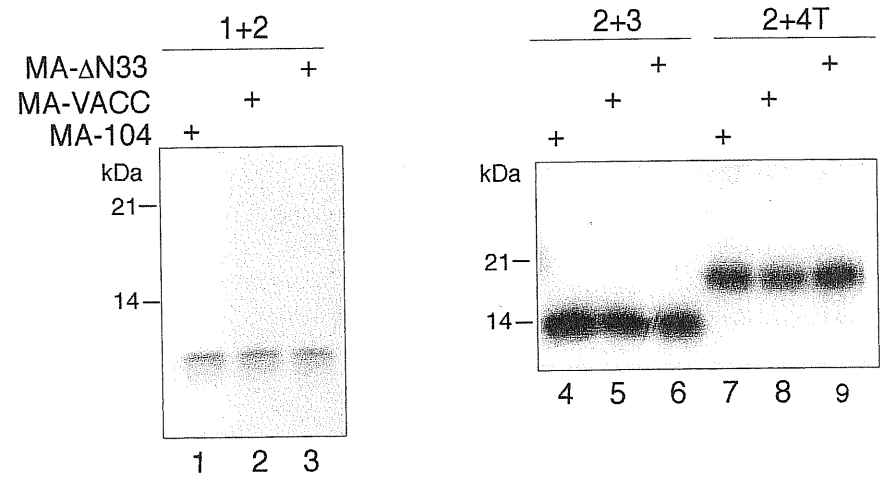

Figure 3.23. In vitro trans kinase assay.
Anti-NSP5 immunoprecipitation of different in vitro synthesised ^{35}S-Met-labelled NSP5 mutants polypeptides (1+2, 2+3 and 2+4T) previously incubated with extract of pCDNA3-ΔN33 transfected cells (MA-ΔN33). Immunoprecipitation of 1+2, 2+3 and 2+4T polypeptides incubated with untransfected (MA104) or vaccinia infected cells (MA-VACC) is also shown.

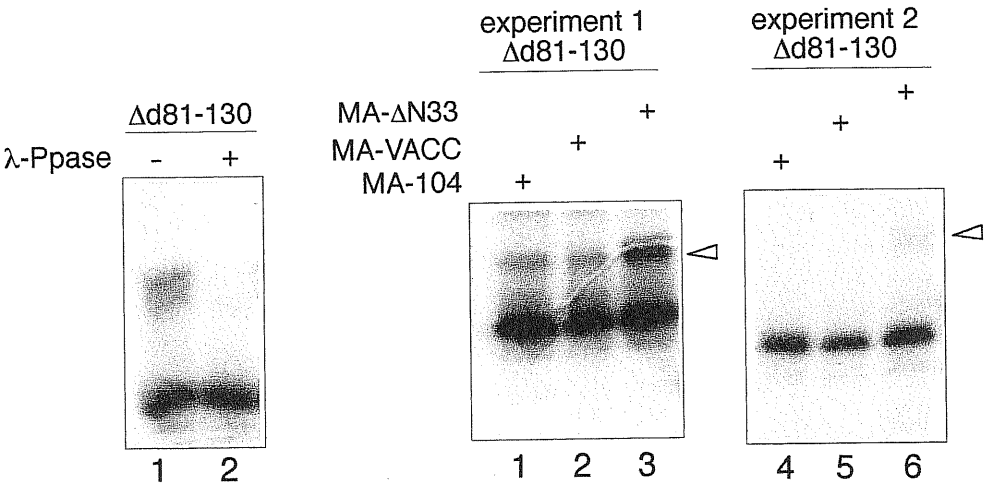

Fig. 3.24. Peculiarities of Δd81-130 deletion mutant.
A. Anti-NSP5 immunoprecipitation of *in vitro* synthesised ^{35}S-Met labelled Δd81-130 deletion mutant hyperphosphorylated during the TNT assay (lane 1). λ-Ppase treatment demonstrates the phosphate origin of the lower mobility forms (lane 2).
B and C. MA-ΔN33 extract up-regulates the phosphorylation of Δd81-130 *in vitro* syntesised mutant (lane 3), in a such extent that however was depended by the retyculocyte extracts batch (lane 6). As control, Δd81-130 was also incubated with untransfected (MA104) or vaccinia infected cells (MA-VACC).

Performing this type of assays and testing Δd81-130 mutant as a putative substrate, we discover that Δd81-130 synthetised *in vitro* sometimes underwent spontaneous hyper-phosphorylation independent from ΔN33 or any other cellular extracts (figure 3.24A, lane 1). The gel shift obtained was of 10 kDa, similar to what was observed when it was expressed *in vivo* (see figure 3.17A, lane 9). We confirmed the phosphorylated origin of these lower mobility forms by λ-Ppase treatment performed on the Δd81-130 immunoprecipitates (figure 3.24A, lane 2). This feature was not under our control and was strictly dependent on the retyculocite extract batch used. Probably some of them contain unknown cellular factors indispensable for Δd81-130 precursor maturation.

Interestingly, as shown in figure 3.24B, after incubation of in vitro translated Δd81-130 with MA-N33 extracts, an increase in the Δd81-130 phosphorylation was seen (lane 3). This feature was specifically depended on ΔN33, while untransfected or vaccinia infected cell extracts had no effect (lanes 1 and 2). This result was confirmed with two different reticulocyte batches, but nevertheless other times it was either not observed or observed in for less extent (figure 3.24C, lane 6).

This work was continued by Fulvia Vascotto and Cathrine Eichwald in the laboratory of Oscar Burrone. Using the same type of assay, they were able to discover that NSP5 have indeed a kinase enzymatic activity and that, interestingly, it was associated to the second and the fourth-tail domains only (2+4T mutant, and not ΔN33).

Investigations on NSP5 degradation

Analysis of the aminoacids sequence of NSP2 has revealed partial homology to a particular class of proteases, the metalloproteases (117). Matrix metalloproteases (MMP) are secreted zinc-containing, metallo-enzymes with specificity for degradation of components of the extra cellular matrix. Until now no experimental evidences have been reported to justify a possible involvement of rotavirus NSP2 as protease in the virus cell cycle.
However, in immunofluorescence experiments of co-transfection of NSP2 and NSP5, at the usual time of VLS detection (16 h post-transfection) we have observed that, most of NSP5 expressed was localised into VLS with almost complete absence of NSP5 protein from the background. At the same time, single NSP5 expression results in high amount of stable NSP5 homogeneously distributed in the cytoplasm of the transfected cells (see figures at page 74). Moreover, during rotavirus infection, NSP5 levels start to decrease 6 h after infection (16), suggesting that NSP5 may be modulated during infection, not only in terms of post-translational modifications, but also perhaps in terms of half-life.
In particular, from different evidences obtained in immunofluorescence experiments, I have tried to verify the hypothesis that NSP2 could affect NSP5 stability in a direct or indirect way. The hypothesis was that NSP2 could play a role in the degradation of NSP5 protein "not recruited" into VLS. Moreover, at approximately 20 h post-transfection, VLS are not any longer visible suggesting a possible NSP5 degradation and consequent VLS disagregation. However, during rotavirus infection, other specific contemporaneous viral events (such as replication and packaging) may modulate organisation of viroplasms and perhaps also NSP5 stability.

In order to study and eventually confirm the hypothesis, I performed a quantitative analysis of NSP5 expression in transient transfection

experiments in relation to the contemporaneous presence of NSP2 and VLS formation.

Different co-transfections of NSP5 and NSP2 were carried out in the presence of an equimolar ratio of plasmids encoding both proteins (ratio 1:1), that corresponds to the conditions used to visualise VLS. We decided also to test the effect of NSP2 when present in excess with respect to NSP5, co-transfecting the two plasmids in a ratio 3:1. Control experiments where performed co-transfecting pCDNA3-NSP5 with a different construct, pBCL1 (provided by Federica Benvenuti), that encodes a polypeptide of approximately 45 kDa, in the same pCDNA3 vector.

Figure 3.25A shows a time course of the transient expression of NSP2 and NSP5 in transfected cells. NSP5 or NSP5-NSP2 co-transfected extracts (ratio 1:3), were harvested at different times after transfection (12, 16, 18 and 20h) and analysed by anti-NSP5 western immunoblot. In this experiment, NSP5 expression was evident at 16 h post-transfection and, when expressed in the presence of NSP2, it becomes less stable, suggesting an NSP2-mediated degradation. However, figure 3.25B shows a combined anti-NSP5/anti-NSP2 western immunoblot of cell extracts co-transfected with NSP5 and NSP2 in a ratio 1:1 or 1:3 (respectively lanes 1 and 2) and assayed at 16 and 18 h post-transfection, showing a moderate effect of NSP2 on NSP5 levels.

These experiments are not easily reproducible, probably because the intrinsic difficulties of co-transfections and also differences in the vaccinia virus stock. In fact in same other cases, NSP5 was clearly sensitive to NSP2-induced degradation (figure 3.25C). These data thus suggest but not unequivocally support a direct NSP2 involvement in the regulation of the NSP5 stability.

A

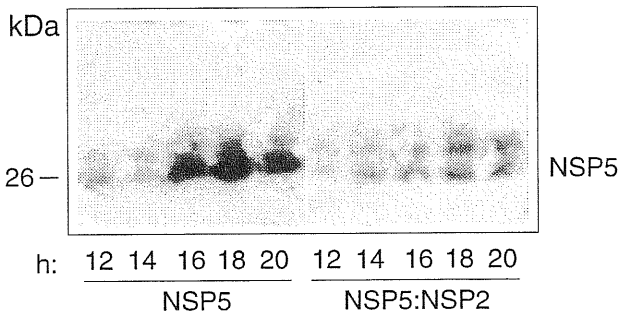

B

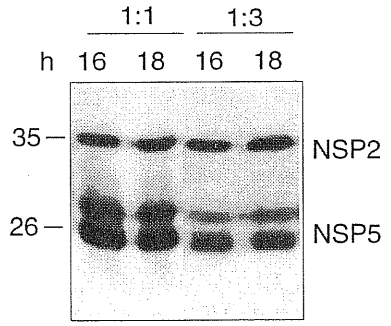

C

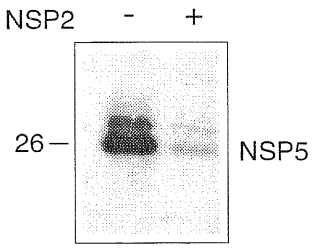

Figure 3.25.
A.Anti-NSP5 western immunoblot of the expression of NSP2 and NSP5 harvested at different times post-transfection.
B. Combined anti-NSP5/anti-NSP2 western immunoblot of NSP5/NSP2 co-transfected cell extracts 1:1 or 1:3 ratio, as indicated and analysed 16 and 18 h post-transfection.
C. Anti-NSP5 western immunoblot of the expression of NSP2 and NSP5 (ratio 1:3), harvested at 16 h post-transfectio.

In vitro degradation assay

As it was previously demonstrated, NSP5-NSP2 binding occurs also *in vitro* (see figure 3.5). To investigate if NSP2 itself could directly determine NSP5 degradation, I performed different *in vitro* assays (figure 3.26).

At first, we decided to use unpurified ^{35}S-Met-labelled *in vitro* translated material. The reaction was performed incubating *in vitro* translated NSP5 and NSP2 polypeptides together for 1 h at 37°C, followed by specific immunoprecipitation and analysis on SDS-PAGE. As shown in figure 3.26A, no degradation of NSP5 was observed when incubated either alone or with NSP2 or VP4, as negative control. We also tested *in vitro* synthesised Δd81-130 mutant because of its different degradation kinetic (see below), without any effect. Using an alternative approach, NSP5 and NSP2 where also contemporaneously synthesised in the same *in vitro* translation and analysed for NSP5 protein stability at short times of incubation (10-15-30 min) (not shown). Also in these cases a no significative difference on the in vitro expression of NSP5 was observed, suggesting that *in vitro* translated NSP2 can not affect directly the stability of *in vitro* translated NSP5.

Thus, we decided to investigate if NSP2 obtained from transfected cells could have any effect on the stability of *in vitro* translated NSP5. Once more, this assay did not give a positive result (figure 3.26B).

These series of negative results indicate that, contrary to what observed *in vivo*, *in vitro* translated NSP2 or extracts from NSP2 transfected cells do not have a sensible protease activity. However, since it is known the different post-translational modifications of NSP5 in vivo, we can not exclude that the eventual NSP2-mediated degradation be dependent of the phosphorylated/hyperphosphorylated state of NSP5.

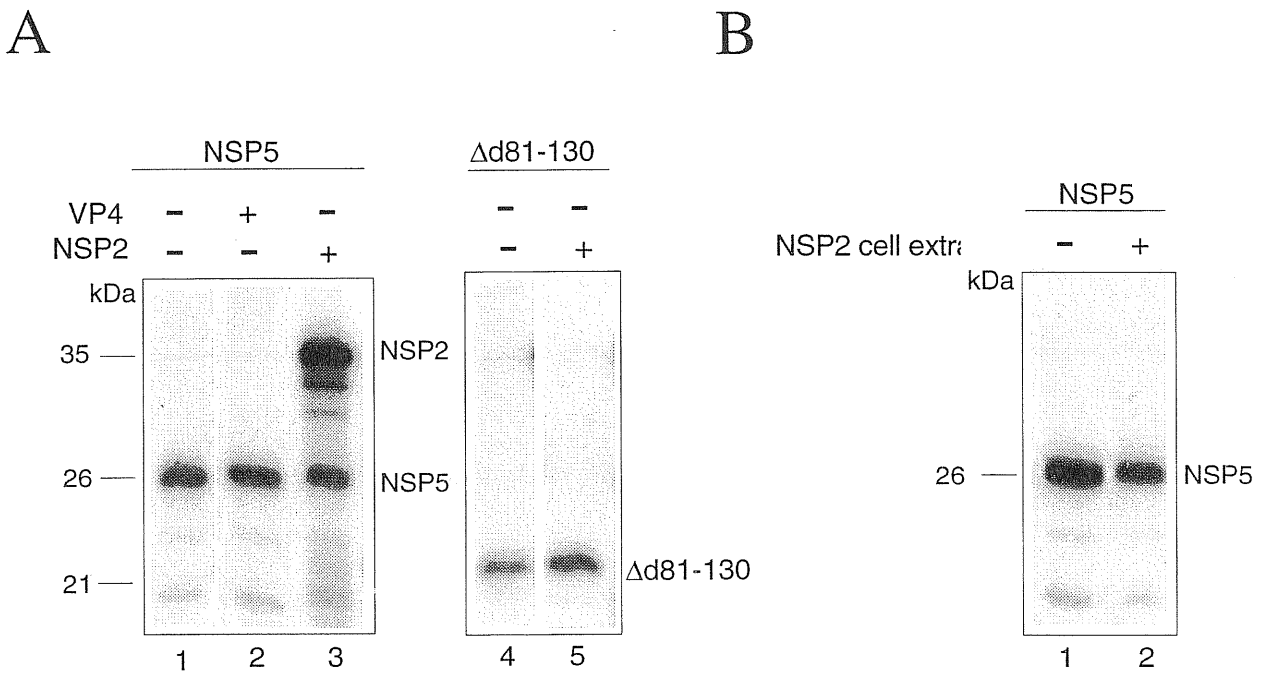

Figure 3.26. Study of the *in vitro* protease activity of NSP2.
A. ^{35}S-Met labelled wt NSP5 or Δd81-130 *in vitro* synthethised polypeptides were incubated with *in vitro* synthetised NSP2 (lanes 3 and 5) and thus immunoprecipitated using anti-NSP5 and anti-NSP2 antibodies (lane 3) or ani-NSP5 alone (lane 5). As control, ^{35}S-Met labelled wt NSP5 was also incubated with *in vitro* synthethised rotavirus VP4 and thus immunoprecipitated using anti-NSP5 antibody (lane 2).
B. NSP2 transfected cell extracts were incubated with *in vitro* synthethised ^{35}S-Met labelled NSP5 (lane 2) or with extracts of empty pCDNA3 transfected cells (lane 1).

Degradation of Δd81-130 and 2+4T mutants

Mutants Δd81-130 and 2+4T are both highly hyper-phosphorylated *in vivo* and, when expressed in the presence of NSP2, both of them form VLS. For that reason, among the other NSP5 mutants I decided to analyse them in the presence of NSP2 by western immunoblot (figure 3.27A and C). Interestingly, the results showed that both these two mutants were more sensitive to NSP2 than the wtNSP5, suggesting that NSP2 mediates in a direct or indirect way their degradation.

As it is shown in figure 3.27A, the total amount of mutant 2+4T was clearly decreased when was expressed in the presence of an excess of NSP2 (co-transfection ratio 3:1). To justify the higher amount of NSP2 used in this co-transfection, figure 3.27B shows a combined anti-NSP5/anti-NSP2 western immunoblot of extracts obtained by co-transfection of a fixed amount of pCDNA3-2+4T plasmid (1 μg), with a crescent amount of pCDNA3-NSP2 (from 0.1 to 3.5 μg). This experiment demonstrates clearly, the NSP2 dose-effect on the NSP5 mutant 2+4T.

Mutant Δd81-130 was even higher sensitive to the presence of NSP2 than mutant 2+4T, since already when co-transfected with an equivalent amount of NSP2 (ratio 1:1), Δd81-130 underwent specific protein degradation (figure 3.27C). Surprisingly, only the Δd81-130 lower mobility bands (arrow, lane 2), representing the hyperphosphorylated forms (see page 86), were NSP2-resistant, while all the Δd81-130 unphosphorylated forms were completely disappeared.

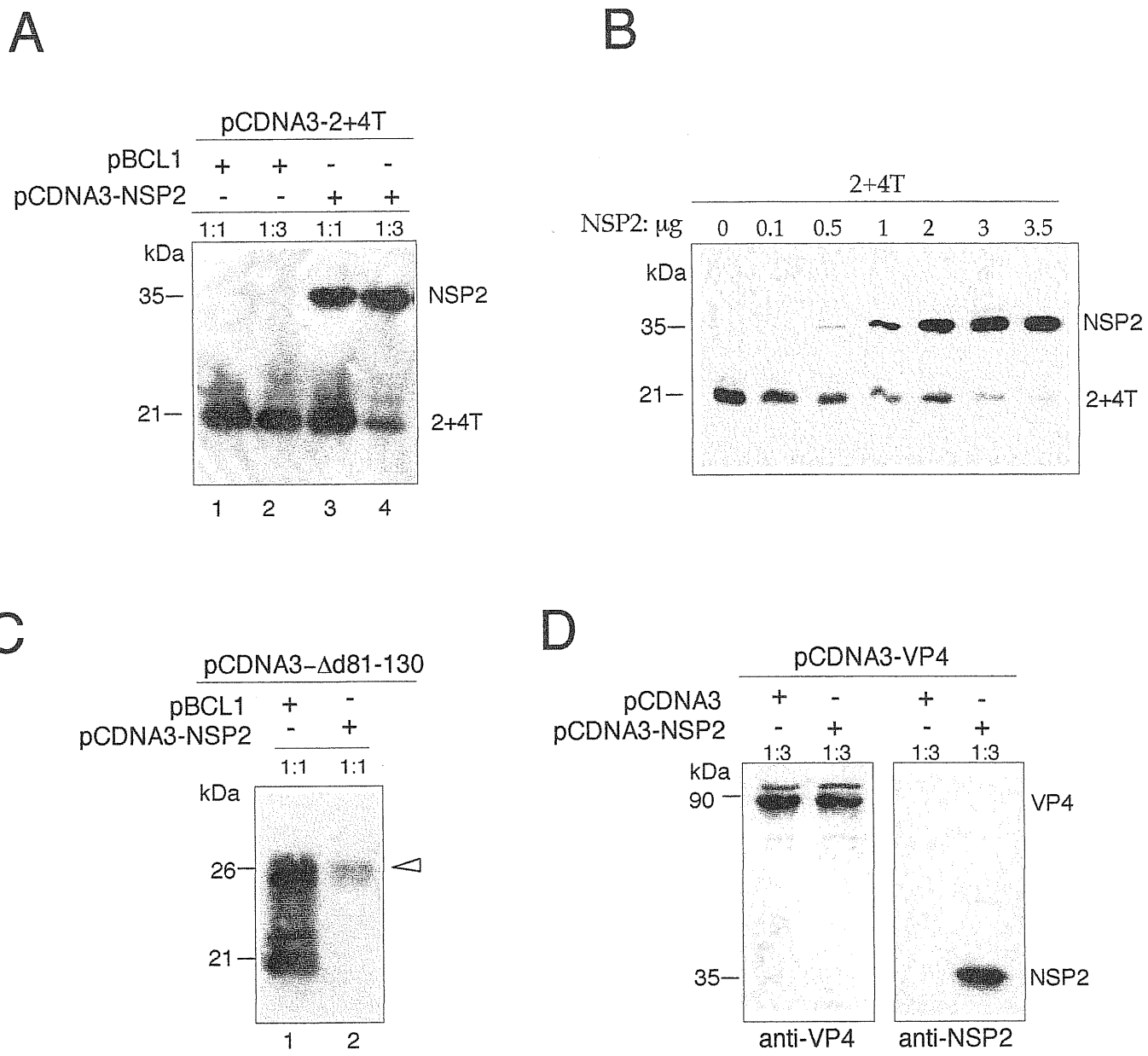

Figure 3.27. Degradation on NSP5 deletion mutants
A. Combined anti-NSP5/anti-NSP2 western immunoblot of 2+4T co-transfected with NSP2 in a ratio 1:1 or 1:3 (lanes 3 and 4).
B. Combined anti-NSP5/anti-NSP2 western immunoblot of a constant amount of pCDNA3-2+4T co-transfected with crescent amount of pCDNA3-NSP2.
C. Anti-NSP5 western immunoblot of Δd81-130 co-transfected with NSP2. Δd81-130 is sensitive to NSP2, also at low ratio (ratio 1:1) (lane 2). Resistant hyperphosphorylated species are indicated by an arrow.
D. Anti-VP4 (left) or anti-NSP2 (right) western immunoblot of VP4:NSP2 co-transfected extracts (ratio 1:3).

The effect of NSP2 on mutants Δd81-130 and 2+4T was specific, since the level of a different rotaviral protein, VP4, was completely unaffected by the presence of an excess of co-transfected NSP2 (ratio 1:3) (figure 3.27D, lane 2). These results indicate that indeed NSP2 has some effect on NSP5 stability, that can be more clearly detected on 2+4T and Δd81-130 mutants, highly phosphorylated *in vivo*, in a NSP2 independent way (see page 86 an 93). However, at present it is not yet clear whether these observations reflect a functional consequence in terms of VLS formation. The phosphorylation and degradation of the two NSP5 mutants Δd81-130 and 2+4T seem, at least in part, linked to the formation of VLS. An interesting hypothesis could be that the different NSP5 modifications could support different NSP5 roles during rotavirus replicative cycle.

Discussion

In virus infected cells, NSP5 was originally described as a polypeptide with an apparent molecular mass of 26 kDa in SDS-PAGE (45; 116). It was later shown that NSP5 is a glycoprotein with a main constituent of 28 kDa form that is further phosphorylated. In 1996, Afrikanova et al. (5) has demonstrated that this protein was able to undergo a complex phosphorylation process describing the existence of polypeptides with mobility of 32-34 kDa (hyperphosphorylated species).
The NSP5 O-glycosylation occurs in the cytoplasm of infected cells by addition of monomeric residues of N-Acetyl glucosamine (GlcNAc) (69). It was found that the highest phosphorylated isoforms are also the ones that contain less GlcNAc (5). In eukaryotic cells, O-glycosylation is known to be involved in the regulation of the degree of serine/threonine phosphorylation of many cellular and nuclear phosphoproteins, suggesting that this could also be the case of NSP5.
NSP5 phosphorylation is a very complex process with still unknown physiological significance. In this thesis we have demonstrated that in virus infected cells, NSP5 directly interacts with NSP2 with important biochemical and functional consequences.

To investigate the possible interactions between NSP5 and other proteins during rotaviral infection, we used a 12Å-long arm chemical crosslinker (DSP), cleavable by reducing agents. We have found that after crosslinking, the rotavirus non-structural protein NSP2 and the viral polymerase VP1 co-precipitated together with NSP5, using a polyclonal anti-NSP5 antibody.

NSP2 accumulates in viroplasms, sites of genome RNA replication and of the assembly of immature viral particles (146). NSP2 is an RNA binding protein

(91), and is a component of rotavirus replicase complex (7). The NSP2 RNA binding is cooperative, independent of sequence and with strong preference for single-stranded RNA over double-stranded RNA, for which it displayed little affinity (186).

The DSP crosslinker reagent was also used in the past to demonstrate that NSP2 interacts with VP1 (90). Surprisingly, after crosslinking, our anti-NSP2 antibody was not able to co-precipitate the same set of proteins, but only the free NSP2 not involved in the complex. A possible explanation is that the DSP-formed NSP5-VP1-NSP2 complex has a structure in which NSP2 is completely hidden, and therefore not available for anto-NSP2 recognition. We still don't have evidences of a functional interaction between NSP5 and VP1 and so, the presence of VP1 in anti-NSP5 immunoprecipitates from crosslinked extracts most likely corresponds to co-precipitation of the already described NSP2-VP1 interaction (90). In its purified form, recombinant NSP2 as the one derived from rotavirus infected cells, did not exist as a monomer but was present as an 8S-10S homomultimers consisting of 6±2 subunits of NSP2, also confirmed by crystallographic analysis (90; 174; 186).

NSP2, but not VP1, can be co-immunoprecipitated by anti-NSP5 antibody in mild washing conditions. This interaction was strongly stabilised after UV treatment. UV-mediated association does not involve covalent disulfide or other bonds since the two proteins are separated in SDS-PAGE under both reducing and non-reducing conditions (4). UV irradiation is usually used to detect nucleic acids-binding proteins, since it catalyses covalent binding of these molecules to aminoacid residues (21). Even though we have not detected any RNA in our immunoprecipitates, it is known that UV treatment induces crosslinking of NSP2 to RNA *in vivo* (91). Recently in our lab, it has been found that NSP5 and NSP2 expressed in co-transfected cells can also be co-immunoprecipitated after UV treatment, as it happens in infected cells (Catherine Eichwald, unpublished), thus suggesting that viral RNA has not a direct influence in the NSP5-NSP2 stabilisation. Further experiments are

needed to confirm the importance of the RNA in the stabilisation of NSP2-NSP5 interaction. It is therefore possible that following UV treatment, NSP2 may acquire a conformation that favour and stabilise a non-covalent interaction with NSP5. The interaction between NSP5 and NSP2 would be facilitated when the latter is bound to RNA. Recently, crystallographic informations of the conformation of recombinant NSP2 in solution were obtained, demonstrating that this protein may acquire two different conformations, depending upon the presence of different ligands (free nucleotides or magnesium) (174). It was proposed that NSP2 functions as a molecular motor, catalysing the packaging of viral mRNA into core-like replication intermediates through the energy derived from its recently demonstrated NTPase activity (174; 186). The fact that NSP2 can exist in different conformations, supports this hypothesis.

VP1 does not co-precipitate from UV-treated extracts, suggesting that the nature of the interactions NSP5-NSP2 and NSP5-VP1 if this latter exists, are different. An alternative possibility is that the same NSP2 has different domains involved in the NSP5-NSP2 or in NSP2-VP1 interaction, that are differently stabilised after UV treatment. Moreover, the presence of NSP2 homomultimers suggests that inside a multimer, different NSP2 molecules could be connected to different viral proteins.

NSP5-NSP2 interaction influences important biochemical and functional consequences in virus infected cells. We have demonstrated in fact that NSP2 is responsible of the up-regulation of the NSP5 phosphorylation (hyperphosphorylation) and that this appears to be essential for NSP5 localisation in viroplasms. Moreover, we found that NSP2 is also responsible to trigger destabilisation of NSP5, suggesting for NSP2 a peculiar role during the infection, as a regulator of the NSP5 half-life.

The *in vitro* phosphorylation assays performed on DSP-crosslinked immunoprecipitated extracts, showed that NSP5 was phosphorylated to an

extent very similar to that observed in infected cells. This feature was also observed *in vivo* in transient NSP5-NSP2 co-expression experiments, when the two proteins are co-expressed in an effective concentration, that facilitate their interaction. We favor the idea that the direct NSP2 and NSP5 interaction is essential for NSP5 final maturation, enhancing its hyperphosphorylation (until 32-34 kDa isoforms) *in vivo* and *in vitro*.

Recently enzymatic studies on recombinant NSP2 purified from bacteria, reveled that it is associated to a nucleoside triphosphate activity, producing a transient the covalent linkage of the γ-phosphate to NSP2 (186). In addition, *in vitro* experiments confirmed that NSP2 associated to purified immature viral particles (sub-viral particles) is significantly phosphorylated (186). Additional *in vivo* ^{32}Pi labelling experiments, however, showed that NSP2 in virus infected cells or transiently expressed in MA014 cells, is poorly or not phosphorylated (186), as also confirmed by the results obtained in our lab. The significance of NSP2 phosphorylation is not clear. A possible explanation is that *in vivo* phosphorylation of NSP2, if it exists, is extremely transient. An interesting scenario was proposed, suggesting that in virus infected cells a cascade of events initiated by the NTPase activity of NSP2 could cause the final phosphorylation of NSP5. In this view, the interaction of NSP5 with phosphorylated NSP2, would catalyse the transfer of the γ-phosphate from NSP2 to NSP5 and causes the hyperphosphorylation of NSP5 (186). However, we had never noted an NSP2 phosphorylation *in vivo* and moreover, purified NSP2 is unable to phosphorylate NSP5 *in vitro* (unpublished results of Fulvia Vascotto and Catherine Eichwald).

A characteristic feature of rotavirus infected cells is the formation of large accumulations of viral proteins and viral RNA in precise sites of the cytoplasm, called viroplasms. From previous study, NSP2 and NSP5 were shown to localise in viroplasms from the early stages of infection (146). The study of the phenotype of different rotavirus ts-mutant strains, has suggested that rotavirus viroplasms are the elective subcellular place of

replication and packaging of newly made virus particles. At the non-permissive temperature, cells infected with replication defective ts-mutants (as in mutant tsE, mapping in gene encoding NSP2), lack viroplasms (68), thus suggesting that an efficient replication requires also a correct organisation and formation of viroplasms. NSP5 function in viroplasms is still not known, since no ts-mutants NSP5 were ever found nor any other NSP5 negative mutant, strongly suggesting NSP5 importance in the replicative virus cycle.

The presence of NSP2 and NSP5 in viroplasms and the NSP5 biochemical modifications consequent to its interaction with NSP2 (hyperphosphorylation), prompted us to investigate the cytoplasmatic distribution of the two proteins in transfected cells. These experiments have shown that co-expression of NSP2 and NSP5 in the absence of any other rotaviral protein and rotavirus replication, is sufficient to organise structures significantly similar to those found in infected cells, that we have called viroplasm-like structures (VLS). Moreover, confocal microscopy has demonstrated the precise spatial co-localisation of the two proteins in viroplasm as well as in VLS, strongly confirming their interaction. However, in viroplasms found in infected cells all the replication machinery, RNA and other structural and non-structural proteins are present, thus these viroplasms are less homogeneously defined and reflect a more complex structure than VLS.

Our data permit to link NSP5 protein in the complex contest of rotavirus morphogenesis. Replication components are not yet full characterised, but the purification of an active replicase complex with anti-NSP2 antibody (7), has permitted to hypothesise that NSP2 may have a fundamental role in rotavirus replication. In particular NSP2 has higher affinity for ss- rather than for ds-RNA (186), suggesting that it may stabilise ssRNA template to present it to the polymerase VP1. The formation of VLS in the absence of the

replication context, suggests the possibility that viroplasms could be structurally organised by a primary protein-protein interaction that does not require other components. This suggests that NSP5 and NSP2 have an early "structural" function in virus replicative cycle as organisers of replicative functional viroplasm.

The results described are of particular interest if considered in the context of NSP5 post-translational modifications. We have demonstrated that NSP5 *in vitro* hyperphosphorylation is regulated by interaction with NSP2. This observation was also extended to the interaction *in vivo*, which resulted in the organisation of VLS. In order to map the NSP5 domains relevant for VLS formation and to verify the importance of NSP5 hyperphosphorylation in this process, we analysed a number of different NSP5 deletion mutants. From this analysis, we found that Δd81-130 and ΔN33 have lost the regulatory inhibition characteristic of the wt molecule and in fact, undergo spontaneous hyperphosphorylation *in vivo* generating species of decreased gel mobility, without any further dependence from NSP2. Mutant 2+4T has the same behavior as Δd81-130, differing from it only for the absence of the first domain. Interestingly, this mutants undergo spontaneous hyper-phosphorylation, and are able to organise VLS when co-express together with NSP2. All the N- and C-terminal NSP5 deletion mutants (ΔN80, ΔC18, ΔC29, ΔC48 and ΔC68) did not show a change in mobility, even though ΔN80, ΔC18, ΔC29 become phosphorylated, without any sensitivity to NSP2 presence.

From these results, we concluded that NSP5 hyperphosphorylation itself is not sufficient to organize discrete cytoplasmatic structures (VLS) (as ΔN33) and that both NSP5 and NSP2 appear to be essential for VLS formation. In fact neither wt NSP5, nor any of its mutants tested, were able to produce VLS when expressed alone. Similarly, homogeneously dispersed distribution of NSP2 is observed when expressed in absence eof NSP5. The formation of VLS, appears thus the result of a fine cooperation between NSP5

hyperphosphorylation and NSP5-NSP2 interaction. However, the exact timing and course of events that leads to VLS is not yet completely clear.

The results obtained with the NSP5 mutants analysis and in particular the inability of ΔN33 in VLS formation, suggest that the N-terminal region of NSP5 is a likely candidate domain for the protein localisation. Further experiments are needed to definitively establish if the NSP2 binding site maps in the first N-terminal 33 aminoacids of NSP5, but the data on the VLS formation favoured this hypothesis. Alternatively, the NSP5 mutants could have major structure distortions to impede interaction with NSP2, thus interfering with VLS formation.
These data indicate once more that NSP5 does not contain any region that can organise itself into VLS, without further support of NSP2. We can thus conclude that viroplasm formation is strictly related to a correct NSP5 structure that allows efficient protein-protein interaction with NSP2.

We have demonstrated the ability of the NSP5 protein N-terminal fused to EGFP to be targeted into original rotavirus-derived viroplasms, following infection of MA104 cells. This result is important because it offers the possibility of studying NSP5 mutants in the context of the infection. Indeed, the specific localisation of NSP5-EGFP in true viroplasms suggests that trans-molecular events with exogenous NSP5-EGFP protein may occur *in vivo* during infection, allowing direct study of the dynamics of protein-protein interactions in rotavirus infection. Using this same strategy, the different NSP5 mutants tagged with EGFP were also recently characterised in our laboratory in the contest of viral replication (results from Catherine Eichwald), confirming most of the results obtained without infection.

The results obtained with ΔN33 or Δ81-130 suggest a constantly "open" state of the molecule in terms of phosphorylation. The elimination of the first or the third region of NSP5 (ΔN33 or Δ81-130) appears to result in a structural change of the protein that abolishes the structural inhibitory control of the

NSP5 hyperphosphorylation, thus mimicking NSP2-dependent hyperphosphorylation of wt NSP5. We hypothesise that the N-terminal portion of NSP5 plays an inhibitory role on NSP5 hyperphosphorylation, probably through interactions that may involve the region between aminoacids 81 and 130 (region 3). An interesting possibility is that ΔN33 and Δ81-130 hyperphosphorylations are due to changes in the structural molecular constrains present in the wt, that during infection are modulated by interaction with NSP2. In this view, a complex NSP5 tertiary structure may control also the hyperphosphorylation on specific serine/threonine sites, which may be structurally accessible only after interaction with NSP2. Conformational changes can result from the interaction of NSP5 with itself or with NSP2. NSP5-NSP2 interaction was also confirmed using the yeast two-hybrid system (152). Recently the last C-terminal 10 residues of NSP5 have been reported to be involved in the formation of NSP5-NSP5 oligomers or of heterocomplexes between NSP5 and NSP6, a polypeptide encoded by the alternative ORF of gene segment 11 (73; 192). However, NSP6 is poorly studied, and NSP6 is not equally expressed in all rotavirus strains.

From the study of NSP5 mutants phosphorylation, we found that the deletion of the last C-terminal highly conserved region (residues 131-198, ΔC68) completely silences protein phosphorylation and moreover that the last C-terminal 18 residues (tail) (ΔC18) are sufficient to abolishes NSP5 hyperphosphorylation. These data were also confirmed by a different group (192). Interestingly, we recently found also that the mutant 2+4T represents the shortest NSP5 portion that is able to induce a kinase activity that phosphorylates NSP5 mutant ΔN33 (results from Catherine Eichwald and Fulvia Vascotto). Moreover, they have also found that the deletion of 4 serine residues in the B-A-B fourth domain of NSP5, inside the characteristic DSDSE repeat (residues number 153, 155, 163, 165), shut off completely NSP5 hyperphosphorylation, suggesting that they are direct regulatory key elements of the NSP5 hyperphosphorylation. We propose that the specific

phosphorylation of this 4 serine residues of the B-A-B domain represents the first step of a cascade of phosphorylation events that allows protein hyperphosphorylation and viroplasm formation. Moreover, we have shown that *in vitro* translated NSP5 polypeptide becomes phosphorylated and transformed into the 28 kDa form only when extracts from infected cells were added to the assay and hyperphosphorylation to 32-34 kDa forms occurs *in vitro* when NSP5 protein is derived from virus-infected cells (5). All these data highly supports the idea that the NSP5 hyperphosphorylation is highly regulated at different steps and suggest that an initial activation of NSP5 dependent of cellular kinases allows the further hyperphosphorylation of NSP5.

Recently, other authors have observed that the 26 kDa phosphorylated NSP5 protein purified from infected cells at earlier stages of the infection (4h post infection), is not active *in vitro* in the autophosphorylation assay, while NSP5 extracted 6h later is (16). The authors suggest that for the complete NSP5 phosphorylation are required cofactors that are not present in the early stages of the infection, that can consist of other cellular or viral proteins or also of a NSP5 modified isoform (16).

The most recent results obtained in our lab, have demonstrated that NSP5 recovered from infected cells have an associated *in vitro* kinase activity that produces highly phosphorylated species (32-34 kDa). Moreover, the NSP5 phosphorylation in the serines of the BAB domain (residues number 153, 155, 163, 165) by a specific cellular kinase activates NSP5 and allows its further hyperphosphorylation (unpublished results of Fulvia Vascotto and Catherine Eichwald).

NSP5 protein sequence contains phosphorylation recognition sites for protein kinase C (SXR/KR/KXXS and K/RXS at residues 22, 30, 75, 100 and 136) and potential substrates for casein kinase II (position 56, 154 and 165 SXXD/E) (17). Protein kinase C and casein kinase II have been shown to be active with the P phosphoprotein of vesicular stomatitis virus (11) and with paramixoviruses (121). For both these virus types, the phosphorylation of the P protein is essential for activation of the viral polymerase complex (12; 63).

A final interesting aspect of the study of the NSP5-NSP2 interaction, was the analysis of the stability of NSP5 when co-expressed together with NSP2. In the past it has been reported that analysis of NSP2 aminoacids sequence shows homology to metalloproteases (117) even if until now this hypothesis was never confirmed. We have found that in the case of NSP5 mutants 2+4T and Δd81-130, over-expression of NSP2 resulted in selective protein degradation, while wtNSP5 or other mutants co-expressed with NSP2, are less affected. However, NSP5 protein stability (as well also its hyperphosphorlation and VLS formation) seems modulated by the amount of NSP2 co-expressed in the cells and by the time of analysis, as well as by transfection efficiency. Interestingly, the NSP2-mediated degradation has much more evident and reproducible in the case of mutants 2+4T and Δd81-130, rather than NSP5 wt.
We suggest that NSP5 degradation may be conformational related. Moreover, NSP2-mediated NSP5 hyperphosphorylation or degradation may be alternative and well controlled events. Degradation of a number of proteins has been shown to be induced by phosphorylation (204) and dephosphorylation (132) and coupling between phosphorylation and ubiquitination is a characteristic way of half-life control of several proteins. Interestingly, recently ubiquitination was found involved in regulatory functions different than direct protein degradation, as in the case of the ubiquitination of NF-kB-inhibitor IκBα (31; 26).

It has been reported that short-lived proteins within eukaryotic cells, generally contain regions enriched in proline, glutammic acids, serine and threonine residues (PEST) (169). These regions were identified by statistical means as signals for protein instability. It was then demonstrated that PEST sequences indeed control the ubiquitination of regulatory short-lived proteins, such as G1 cyclins in yeast and mammalian cells (95). Phosphorylation of particular serine or threonine residues within the PEST regions of these G1 cyclins, specifies their recognition and processing by the ubiquitin-proteasome pathway (98, 202; 166). Interestingly, NSP5 contains

serine-threonine-serine stretch sequences (PxSSSxTTxSS), that resemble PEST regions localised in the NSP5 first N-terminal portion. Moreover, the N-end rule established a relationship between the N-terminal amino acid of certain proteins and their susceptibility to ubiquitination (113).
Proteasomes play an essential role in the rapid elimination of short-lived key regulatory proteins, as for example cell cycle proteins, rate-limiting enzymes or transcriptional activators. Eukaryotic cells contain multiple proteolytic systems, including the lysosomal proteases, calpains, the ATP-ubiquitin-proteasome-dependent pathway and ATP-independent non lysosomal degradation pathways. The major proteolytic activity in the cytosol is a large ATP-dependent protease (2000 kDa) known as the 26S proteasome (31). However, the importance of protein degradation has been difficult to study because the lack of selective inhibitors of the major catabolic systems of the cell. In the case of mutants 2+4T and Δd81-130, that have provided clearer results on NSP2-mediated degradation, I have also tested different aldehydes known to block proteasome-dependent and independent proteolysis (55; 168). None of these compounds was sufficient to protect 2+4T from degradation.

A first simple explanation of the NSP5 degradation demonstrated in transfected cells is that the excess of NSP5 protein that does not localise into VLS (or viroplasms), could be unstable and rapidly involved in a degradation pathway. However, the differential proteolysis of Δd81-130 deletion mutant depending upon its rate of phosphorylation, could indicate that only the NSP5 hyperphosphorylated species are organised in VLS and therefore less accessible to degradation. An interesting hypothesis, in fact, is that viroplasms are subcellular compartments that protect NSP5 from the different enzymatic activities.
More experiments are required to unequivocally verify the degradation on NSP5 studying the physiological importance of the NSP2-mediated degradation of NSP5 in virus infected cells. A possible hypothesis is that NSP2 regulates the amount of NSP5 present at different stages of infection,

and that the differentially phosphorylated forms of NSP5 are marked for different protein fate.

References

1. Aberle H, Bauer A, Stappert J, Kispert A, Kemler R. 1997. β-catenin is a target for the ubiquitin-proteasome pathway. EMBO J 1;16, 3797-804.

2. Acs G, Klett H, Schonberg M, Christman J, Levin DH, Silverstein SC. 1971. Mechanism of reovirus double-stranded ribonucleic acid synthesis in vivo and in vitro. Journal of Virology 8, 684-9.

3. Affranchino JL, Gonzalez SA. 1997. Deletion mapping of functional domains in the rotavirus capsid protein VP6. Journal of General Virology, 78, 1949-55.

4. Afrikanova I, Fabbretti E, Miozzo MC, and Burrone OR. 1998. Rotavirus NSP5 phosphorylation is up-regulated by interaction with NSP2. Journal of General Virology, 78, 2679-2686.

5. Afrikanova I, Miozzo MC, Giambiagi S and Burrone OR. 1996. Phosphorylation generates different forms of rotavirus NSP5. Journal of General Virology, 77, 2059-2065.

6. Altenburg BC, Graham DY, Estes MK. 1980. Ultrastructural study of rotavirus replication in cultured cells. Journal of General Virology, 46, 75-85.

7. Aponte C, Poncet D and Cohen J. 1996. Recovery and characterisation of a replicase complex in rotavirus-infected cells by using a monoclonal antibody against NSP2. Journal of Virology, 70, 985-991.

8. Aponte C, Mattion NM, Estes MK, Charpilienne A, Cohen J. 1993. Expression of two bovine rotavirus non-structural proteins (NSP2, NSP3) in the baculovirus system and production of monoclonal antibodies directed against the expressed proteins. Arch Virol 133, 85-95.

9. Au KS, Chan WK, Burns JW, Estes MK. 1989. Receptor activity of rotavirus nonstructural glycoprotein NS28. Journal of Virology, 63, 4553-62.

10. Ball JM, Tian P, Zeng CQ, Morris AP and Estes MK. 1996. Age-dependent diarrhea induced by a rotaviral nonstructural glycoprotein. Science, 272, 101-104.

11. Barik S, Banerjee AK. 1992a. Sequential phosphorylation of the phosphoprotein of vesicular stomatitis virus by cellular and viral protein kinases is essential for transcription activation. Journal of Virology, 66, 1109-18.

12. Barik S, Banerjee AK. 1992b. Phosphorylation by cellular casein kinase II is essential for transcriptional activity of vesicular stomatitis virus phosphoprotein P. PNAS, 15; 89, 6570-4.

13. Banchereau J and Steinman RM. 1998. Dendritic cells and the control of immunity. Nature, 392, 245.

14. Bern C, Martines J, De Jouisa I and glass Rl. 1992. The magnitude of the global problem of diarrheal disease: a ten years update. Bulletin WHO. 70, 705-714.

15. Bican P, Cohen J, Charpilienne A, Scherrer R. 1982. Purification and characterization of bovine rotavirus cores. Journal of Virology, 43, 1113-7.

16. Blackhall J, Munoz M, Fuentes A, Magnusson G. 1998. Analysis of rotavirus nonstructural protein NSP5 phosphorylation. Journal of Virology, 72, 6398-405.

17. Blackhall J, Fuentes A, Hansen K and Magnusson G. 1997. Serine protein kinase activity associated with rotavirus phosphoprotein NSP5. Journal of Virology, 71, 138-144.

18. Boyle JF and Holmes KV. 1986. RNA-binding proteins of bovine rotavirus. Journal of Virology, 58, 561-8.

19. Browne EP, Bellamy AR, Taylor JA. 2000. Membrane-destabilizing activity of rotavirus NSP4 is mediated by a membrane-proximal amphipathic domain. J Gen Virol, 81, 1955-9.

20. Brunet JP, Jourdan N, Cotte-Laffitte J, Linxe C, Geniteau-Legendre M, Servin A, Quero AM. 2000. Rotavirus infection induces cytoskeleton disorganization in human intestinal epithelial cells: implication of an increase in intracellular calcium concentration. Journal of Virology, 74, 10801-6.

21. Budowsky EI and Abdurashidova GG. 1989. Polynucleotide-protein cross-links induced by ultraviolet light and their use for structural investigation of nucleoproteins. Progress in Nucleic Acid Research and Molecular Biology, 37, 1-65.

22. Chan WK, Penaranda ME, Crawford SE, Estes MK. 1986. Two glycoproteins are produced from the rotavirus neutralization gene. Virology, 151, 243-52.

23. Chasey D and Lucas M. 1977. Detection of rotavirus in experimentally infected piglets. Res Vet Sci, 22, 124-5.

24. Chen D and Patton JT. 2000. De novo synthesis of minus strand RNA by the rotavirus RNA polymerase in a cell-free system involves a novel mechanism of initiation. RNA, 6, 1455-67.

25. Chen D, Luongo CL, Nibert ML and Patton JT. 1999. Rotavirus open cores catalyse 5′-capping and methylation of exogenous RNA: evidence that VP3 is a methyltransferase. Virology, 265, 120-130.

26. Chen Z, Hagler J, Palombella VJ, Melandri F, Scherer D, Ballard D, Maniatis T. 1995. Signal-induced site-specific phosphorylation targets I kappa B alpha to the ubiquitin-proteasome pathway. Genes Dev, 9, 1586-97.

27. Chen DY, Zeng CQY, Wentz MJ, Gorziglia M, Estes MK and Ramig RF. 1994. Template dependent in vitro replication of rotavirus RNA. Journal of Virology, 68, 7030.

28. Chen D and Ramig RF. 1993. Rescue of infectivity by sequential in vitro transcapsidation of rotavirus core particles with inner capsid and outer capsid proteins. Virology, 194, 743-751.

29. Chen D and Ramig RF. 1992. Determinants of rotavirus stability and density during CsCl purification. Virology, 186; 228-237.

30. Chen D, Gombold JL and Ramig RF. 1990. Intracellular RNA synthesis directed by temperature-sensitive mutants of simian rotavirus SA11. Virology, 178, 143-151.

31. Chen ZJ, Parent L, Maniatis T. 1996. Site-specific phosphorylation of IkappaBalpha by a novel ubiquitination-dependent protein kinase activity. Cell, 84, 853-62.

32. Chizhikov V and Patton JT. 2000. A four-nucleotide translation enhancer in the 3'-terminal consensus of the non polyadenylated mRNAs of rotavirus. RNA, 6, 814-825.

33. Chnaiderman J, Diaz J, Magnusson G, Liprandi F and Spencer E. 1998. Characterisation of a rotavirus rearranged gene 11 by gene reassortment. Arch. Virology, 143, 1711.

34. Ciarlet M, Estes MK. 1999. Human and most animal rotavirus strains do not require the presence of sialic acid on the cell surface for efficient infectivity. Journal of General Virology, 80, 943-8.

35. Ciarlet M, Crawford SE, Barone C, Bertolotti-Ciarlet A, Ramig RF, Estes MK, Conner ME. 1998. Subunit rotavirus vaccine administered parenterally to rabbits induces active protective immunity. Journal of Virology, 72, 9233-46.

36. Clark SM, Roth JR, Clark ML, Barnett BB, Spendlove RS. 1981. Trypsin enhancement of rotavirus infectivity: mechanism of enhancement. Journal of Virology, 39, 816-22.

37. Cohen J. 1977. Ribonucleic acid polymerase activity associated with purified calf Rotavirus. Journal of General Virology, 36, 395-402.

38. Conner ME, Zarley CD, Hu B, Parsons S, Drabinski D, Greiner S, Smith R, Jiang B, Corsaro B, Barniak V, Madore HP, Crawford S and Estes MK. 1996. Virus-like particles as a rotavirus vaccine. Journal of Infectious Diseases, 174, 588.

39. Coulson BS, Londrigan SL, Lee DJ. 1997. Rotavirus contains integrin ligand sequences and a disintegrin-like domain that are implicated in virus entry into cells. PNAS, 94, 5389-94 .

40. Crawford SE, Labbe' M, Cohen J, Burroughs MH, Zhou YJ and Estes MK. 1994. Characterisation of virus-like particles produced by the expression of rotavirus capsid proteins in insect cells. Journal of Virology, 68, 5945-22.

41. Davis NL and Wertz GW. 1982. Synthesis of vesicular stomatitis virus negative strand RNA in vitro: dependence on viral protein synthesis. Journal of Virology 41, 821-832.

42. Denisova E, Dowling W, LaMonica R, Shaw R, Scarlata S, Ruggeri F, Mackow ER. 1999. Rotavirus capsid protein VP5* permeabilizes membranes. Journal of Virology, 73, 3147-53.

43. Dong Y, Zeng CQ, Ball JM, Estes MK, Morris AP. 1997. The rotavirus enterotoxin NSP4 mobilizes intracellular calcium in human intestinal cells by stimulating phospholipase C-mediated inositol 1,4,5-trisphosphate production. PNAS, 94, 3960-5.

44. Dowling W, Denisova E, LaMonica R, Mackow ER. 2000. Selective membrane permeabilization by the rotavirus VP5* protein is abrogated by mutations in an internal hydrophobic domain. Journal of Virology, 74, 6368-76.

45. Ericson BL, Graham DY, Mason BB, Estes MK. 1982. Identification, synthesis, and modifications of simian rotavirus SA11 polypeptides in infected cells. Journal of Virology, 42, 825-39.

46. Espejo RT, Lopez S, Arias C. 1981. Structural polypeptides of simian rotavirus SA11 and the effect of trypsin. Journal of Virology, 37, 156-60.

47. Estes MK and Morris AP. 1999. A viral enterotoxin. A new mechanism of virus induced pathogenesis. AdvExpMedBiol, 473, 73.

48. Estes MK, Ball JM, Crawford SE, O'Neal C, Opekun AA, Graham DY, Conner ME. 1997. Virus-like particle vaccines for mucosal immunization. Adv Exp Med Biol, 412, 387-95.

49. Estes MK. 1996. Rotaviruses and their replication. In: "Fields Virology", pp. 1625-1655. Edited by: B. N. Fields et al. Philadelphia: Lippincott-Raven.

50. Estes MK and Cohen J. 1989. Rotavirus gene structure and function. Microbiol Rev, 53, 410-49.

51. Estes MK, Palmer EL, Obijeski JF. 1983. Rotaviruses: a review. Curr Top Microbiol Immunol, 105, 123-84.

52. Estes MK, Graham DY, Gerba CP and Smith EM. 1979. Simian Rotavirus SA11 replication in cell cultures. Journal of Virology, 31, 810-815.

53. Fabbretti E, Afrikanova I, Vascotto F, Burrone OR. 1999. Two non-structural rotavirus proteins, NSP2 and NSP5, form viroplasm-like structures in vivo. J Gen Virol, 80, 333-9.

54. Fang ZY, Monroe SS, Dong H, Panaranda M, Wen L, Gouvea V, Allen JR, Hung T, and Glass RI. 1992. Coding assignments of the genome of adult diarrhea rotavirus. ArchVirol, 125, 53.

55. Fenteany G, Standaert RF, Lane WS, Choi S, Corey EJ, Schreiber SL. 1995. Inhibition of proteasome activities and subunit-specific amino-terminal threonine modification by lactacystin. Science, 268, 726-31.

56. Frangioni JV and Neel BG. 1993. Solubilisation and purification of enzymnaticallyn active glutathione S-transferase (pGEX) fusion proteins. Analytycal Biochemistry 210, 179-187.

57. Fuerst RT, Earl PL, and Moss B. 1987. Use of a hybrid vaccinia virus-T7 RNA polymerase system for expression of target genes. Mol Cell Biol, 7, 2538-2544.

58. Fuerst RT, Niles GE, Studier WF, and Moss B. 1986. Eucaryotic transient-expression system based on recombinant vaccinia virus that synthesised bacteriophage T7 RNA polymerase. PNAS, 83, 8122-8126.

59. Fukuhara N, Yoshie O, Kitaoka S, Konno T. 1988. Role of VP3 in human rotavirus internalization after target cell attachment via VP7. Journal of Virology, 62, 2209-18.

60. Furuichi Y, Shatkin AJ, Stavnezer E, Bishop JM. 1975. Blocked, methylated 5'-terminal sequence in avian sarcoma virus RNA. Nature, 257, 618-20.

61. Fynan EF, Webster RG, Fuller DH, Haynes JR, Santoro JC, Robinson HL. 1993. DNA vaccines: protective immunizations by parenteral, mucosal, and gene-gun inoculations. PNAS, 90, 11478-82.

62. Gallegos CO and Patton JT. 1989. Characterization of rotavirus intermediates: a model for the assembly of single shelled particles. Virology, 172, 616-627.

63. Gao Y and Lenard J. 1995. Multimerization and transcriptional activation of the phosphoprotein (P) of vesicular stomatitis virus by casein kinase-II. EMBO J;14, 1240-7.

64. Gianbiagi S, Gonzalez Rodriguez AJ, Gomez J and Burrone O. 1994. A rearranged genomic segment 11 is common to different human rotaviruses. Archives of Virology, 136, 415-421.

65. Ginn DI, Ward RL, Hamparian VV, Hughes JH. 1992. Inhibition of rotavirus in vitro transcription by optimal concentrations of monoclonal antibodies specific for rotavirus VP6. J Gen Virol, 73, 3017-22.

66. Glass RI, Bresee JS, Parashar U, Miller M and Gentsch JR. 1997. Rotavirus vaccines at the threshold. Nature Medicine, 3, 1325.

66b. Gombold JL, Ramig RF. 1987. Assignment of simian rotavirus SA11 temperature-sensitive mutant groups A, C, F, and G to genome segments. Virology, 161, 463-73.

67. Gombold JL and Ramig RF. 1986. Analysis of reassortment of genome segments in mice mixedly infected with rotaviruses SA11 and RRV. Journal of Virology, 57, 110-6.

68. Gombold JL, Estes MK, Ramig RF. 1985. Assignment of simian rotavirus SA11 temperature-sensitive mutant groups B and E to genome segments. Virology, 143, 309-20.

69. Gonzáles SA and Burrone O. 1991. Rotavirus NS26 is modified by addition of single O-linked residues of N-acetylglucosamine. Virology, 182, 8-16.

70. Gonzalez SA, Burrone OR. 1989a. Porcine OSU rotavirus segment II sequence shows common features with the viral gene of human origin. Nucleic Acids Res 17, 6402.

71. Gonzalez SA, Mattion NM, Bellinzoni R, Burrone OR. 1989b. Structure of rearranged genome segment 11 in two different rotavirus strains generated by a similar mechanism. J Gen Virol 70, 1329-36.

72. Gonzalez RA, Espinosa R, Romero P, Lopez S, Arias CF. 2000. Relative localization of viroplasmic and endoplasmic reticulum-resident rotavirus proteins in infected cells. Arch Virol, 145, 1963-73.

73. Gonzalez RA, Torres-Vega MA, Lopez S, Arias CF. 1998. In vivo interactions among rotavirus nonstructural proteins. Arch Virol, 143, 981-96.

74. Halaihel N, Lievin V, Ball JM, Estes MK, Alvarado F, Vasseur M. 2000. Direct inhibitory effect of rotavirus NSP4(114-135) peptide on the Na(+)-D-glucose symporter of rabbit intestinal brush border membrane. Journal of Virology, 74, 9464-70.

75. Helmberger-Jones M and Patton JT. 1986. Characterisation of subviral particles in cells infected with simian rotavirus SA11. Virology, 155, 655.

76. Hewish MJ, Takada Y, Coulson BS. 2000. Integrins alpha2beta1 and alpha4beta1 can mediate SA11 rotavirus attachment and entry into cells. Journal of Virology, 74, 228-36.

77. Horie Y, Nakagomi O, Koshimura Y, Nakagomi T, Suzuki Y, Oka T, Sasaki S, Matsuda Y and Watanabe S. 1999. Diarrhea induction by rotavirus NSP4 in the homologous mouse model system. Virology, 262, 389.

78. Hsu GG, Bellamy AR and Yeager M. 1997. Projection structure of VP6, the rotavirus inner capsid protein, and comparison with bluetongue VP7. J Mol Biol, 272, 362.

79. Hua J, Chen X, Patton JT. 1994a. Deletion mapping of the rotavirus metalloprotein NS53 (NSP1): the conserved cysteine-rich region is essential for virus-specific RNA binding. Journal of Virology, 68, 3990-4000.

80. Hua J and Patton JT. 1994b. The carboxyl-half of the rotavirus non structural protein NS53 (NSP1) is not required for virus replication. Virology 198, 567-76.

81. Hua J, Mansell EA, Patton JT. 1993. Comparative analysis of the rotavirus NS53 gene: conservation of basic and cysteine-rich regions in the protein and possible stem-loop structures in the RNA. Virology, 196, 372-8.

82. Ijaz MK, Nur-E-Kamal MS, Dar FK, Uduman S, Redmond MJ, Attah-Poku SK, Dent D and Babiuk LA. 1998. Inhibition of rotavirus infection in vitro and in vivo by a synthetic peptide from VP4. Vaccine, 16, 916-20.

83. Isa P, Lopez S, Segovia L, Arias CF. 1997. Functional and structural analysis of the sialic acid-binding domain of rotaviruses. Journal of Virology, 71, 6749-56 .

84. Jacobson RM. 1999. The current status of the rotavirus vaccine. Vaccine, 26, 1690.

85. Jentsch S. 1992. The ubiquitin-conjugation system. Annu Rev Genet, 26, 179-207.

86. Ludert N, Brunet JP, Sapin C, Blais A, Cotte-Laffitte J, Forestier F, Quero AM, Trugnan G, Servin AL. 1998. Rotavirus infection reduces sucrase-isomaltase expression in human intestinal epithelial cells by perturbing protein targeting and organization of microvillar cytoskeleton. Journal of Virology, 72, 7228-36.

87. Kalica AR, Flores J, Greenberg HB. 1983. Identification of the rotaviral gene that codes for hemagglutination and protease-enhanced plaque formation. Virology, 125, 194-205.

88. Kapikian AZ; 1996a. Overview of viral gastroenteritis. ArchVirol, 12, 7.

89. Kapikian AZ, Hoshino Y, Chanock RM and Perez-Schael I. 1996b. Efficacy of a quadrivalent rhesus rotavirus-based human rotavirus vaccine aimed at preventing severe rotavirus diarrhea in infants and young children. Journal of Infectious Diseases, 174, 565.

90. Kattoura MD, Chen X and Patton JT. 1994. The rotavirus RNA-binding protein NS35 (NSP2) forms 10S multimers and interacts with the viral RNA polymerase. Virology, 202, 803-13.

91. Kattoura MD, Clapp LL and Patton JT. 1992. The rotavirus non structural protein NS35, possesses RNA-binding activity in vitro and in vivo. Virology, 192, 698-708.

92. Kohli E, Pothier P, Tosser G, Cohen J, Sandino AM, Spencer E. 1994. Inhibition of in vitro reconstitution of rotavirus transcriptionally active particles by anti-VP6 monoclonal antibodies. Arch Virol, 135, 193-200.

93. Kojima K, Taniguchi K, Urasawa T, Urasawa S. 1996. Sequence analysis of normal and rearranged NSP5 genes from human rotavirus strains isolated in nature: implications for the occurrence of the rearrangement at the step of plus strand synthesis. Virology, 224, 446-52.

94. Kong SK and Chock PB. 1992. Protein ubiquitination is regulated by phosphorylation. An in vitro study. J Biol Chem, 267, 14189-92.

95. Kornitzer D, Raboy B, Kulka RG, Fink GR. 1994. Regulated degradation of the transcription factor Gcn4. EMBO J, 13, 6021-30.

96. Kornitzer, D., B. Raboy, R. G. Kulka, and G. R. Fink. 1994. Regulated degradation of the transcription factor Gcn4. EMBO J, 13, 6021-6030.

97. Labbe' M, Charpilienne A, Crawford SE, Estes MK and Cohen J. 1991. Expression of rotavirus VP2 produces empty core-like particles. Journal of Virology, 65, 2946-52.

98. Lanker S, Valdivieso MH, Wittenberg C. 1996. Rapid degradation of the G1 cyclin Cln2 induced by CDK-dependent phosphorylation. Science, 271, 1597-6001.

99. Lawton JA, Estes MK and Prasad BV. 1999. Comparative structural analysis of transcriptionally competent and incompetent rotavirus antibody complexes. PNAS, 96, 5428.

100. Lawton JA, Estes MK and Prasad BVV. 1997a. Three-dimensional visualisation of mRNA release from actively transcribing rotavirus particles. Nature Structural Biology, 4, 118.

101. Lawton JA, Zeng CQ, Mukherjee SK, Cohen J, Estes MK and Prasad BV. 1997b. Three-dimensional structural analysis of recombinant rotavirus like particles with intact and aminoterminal deleted VP2: implications for the architecture of the VP2 capsid layer. Journal of Virology, 71, 7353.

102. Lee J, Babiuk LA, Yoo D. 1998. A neutralizing monoclonal antibody to bovine rotavirus VP8 neutralizes rotavirus infection without inhibiting virus attachment to MA-104 cells. Can J Vet Res Jan, 62, 63-7.

103. Li E, Pedraza A, Bestagno M, Mancardi S, Sanchez R, Burrone O. 1997. Mammalian cell expression of dimeric small immune proteins (SIP). Protein Eng Jun, 10, 731-6.

104. Liu M, Mattion NM, Estes MK. 1992. Rotavirus VP3 expressed in insect cells possesses guanylyltransferase activity. Virology, 188, 77-84.

105. Londrigan SL, Hewish MJ, Thomson MJ, Sanders GM, Mustafa H, Coulson BS. 2000. Growth of rotaviruses in continuous human and monkey cell lines that vary in their expression of integrins. J Gen Virol, 81, 2203-13.

106. Lopez S and Arias CF. 1993. Protein NS26 is highly conserved among porcine rotavirus strains. Nucleic Acids Res, 21, 1042.

107. Ludert JE, Mason BB, Angel J, Tang B, Hoshino Y, Feng N, Vo PT, Mackow EM, Ruggeri FM, Greenberg HB. 1998. Identification of mutations in the rotavirus protein VP4 that alter sialic-acid-dependent infection. J Gen Virol, 79, 725-9.

108. Ludert JE, Feng N, Yu JH, Broome RL, Hoshino Y, Greenberg HB. 1996a. Genetic mapping indicates that VP4 is the rotavirus cell attachment protein in vitro and in vivo. Journal of Virology, 70, 487-93.

109. Ludert JE, Krishnaney AA, Burns JW, Vo PT, Greenberg HB. 1996b. Cleavage of rotavirus VP4 in vivo. J Gen Virol, 77, 391-5.

110. Ludert JE, Michelangeli F, Gil F, Liprandi F, Esparza J. 1987. Penetration and uncoating of rotaviruses in cultured cells. Intervirology, 27, 95-101.

111. Lundgren O, Peregrin AT, Persson K, Kordasti S, Uhnoo I and Svensson L. 2000. Role of the enteric nervous system in the fluid and electrolyte secretion of rotavirus diarrhea. Science, 287, 491-495.

112. Madore HP, Estes MK, Zarley CD, Hu B, Parsons S, Digravio D, Greiner S, Smith R, Jiang B, Corsaro B, Barniak V, Crawford S, Conner ME. 1999. Biochemical and immunologic comparison of virus-like particles for a rotavirus subunit vaccine. Vaccine, 17, 2461-71.

113. Madura K, Varshavsky A. 1994. Degradation of G alpha by the N-end rule pathway. Science, 265, 1454-8.

114. Mansell EA, Ramig RF and Patton JT. 1994. Temperature-sensitive lesions in the capsid proteins of the rotavirus mutants ts-F and ts-G that affect virion assembly. Virology, 204, 69-81.

115. Mason BB, Graham DY, Estes MK. 1983. Biochemical mapping of the simian rotavirus SA11 genome. Journal of Virology, 46, 413-23.

116. Mason BB, Graham DY, Estes MK. 1980. In vitro transcription and translation of simian rotavirus SA11 gene products. Journal of Virology, 33, 1111-21.

117. Mattion N, Cohen J and Estes MK. 1994. The Rotavirus Proteins p.169-249. In: "Viral Infections of the Gastrointestinal Tract", A. Kapikian ed, Marcel Dekker, New York.

118. Mattion NM, Cohen J, Aponte C, Estes MK. 1992. Characterization of an oligomerization domain and RNA-binding properties on rotavirus nonstructural protein NS34. Virology, 190, 68-83.

119. Mattion NM, Mitchell DB, Both GW and Estes MK. 1991. Expression of rotavirus proteins encoded by alternative open reading frames of genome fragment 11. Virology, 181, 295-304.

120. Mattion N, Gonzalez SA, Burrone O, Bellinzoni R, La Torre JL and Scodeller EA. 1988. Rearrangement of genomic segment 11 in two swine rotavirus strains. Journal of General Virology, 69, 695-698.

121. Mazumder B and Barik S. 1994. Requirement of casein kinase II-mediated phosphorylation for the transcriptional activity of human respiratory syncytial viral phosphoprotein P: transdominant negative phenotype of phosphorylation-defective P mutants. Virology, 205, 104-11.

122. McCrae MA and McCorquodale JG. 1983. Molecular biology of rotaviruses. V. Terminal structure of viral RNA species. Virology, 126, 204-12.

123. McIntyre M, Rosenbaum V, Rappold W, Desselberger M, Wood D, Desselberger U. 1987. Biophysical characterization of rotavirus particles containing rearranged genomes. J Gen Virol, 68, 2961-6.

124. Meggio F, Donella Deana A, Ruzzene M, Brunati AM, Cesaro L, Guerra B, Meyer T, Mett H, Fabbro D, Furet P, et al. 1995. Different susceptibility of protein kinases to staurosporine inhibition. Kinetic studies and molecular bases for the resistance of protein kinase CK2. Eur J Biochem, 234, 317-22.

125. Mendez E, Lopez S, Cuadras MA, Romero P, Arias CF. 1999. Entry of rotaviruses is a multistep process. Virology, 263, 450-9.

126. Mendez E, Arias CF, Lopez S. 1993. Binding to sialic acids is not an essential step for the entry of animal rotaviruses to epithelial cells in culture. Journal of Virology, 67, 5253-9.

127. Mirazimi A and Svensson L. 2000. ATP is required for correct folding and disulfide bond formation of rotavirus VP7. Journal of Virology, 74, 8048-52.

128. Mirazimi A, Nilsson M, Svensson L. 1998. The molecular chaperone calnexin interacts with the NSP4 enterotoxin of rotavirus in vivo and in vitro. Journal of Virology, 72, 8705-9.

129. Musalem C, Espejo RT. 1985. Release of progeny virus from cells infected with simian rotavirus SA11. J Gen Virol, 66, 2715-24.

130. Nejmeddine M, Trugnan G, Sapin C, Kohli E, Svensson L, Lopez S, Cohen J. 2000. Rotavirus spike protein VP4 is present at the plasma membrane and is associated with microtubules in infected cells. Journal of Virology, 74, 3313-20.

131. Nilsson M, Sigstam G, Svensson L. 2000. Antibody prevalence and specificity to group C rotavirus in Swedish sera. J Med Virol, 60, 210-5.

132. Nishizawa M, Furuno N, Okazaki K, Tanaka H, Ogawa Y, Sagata N. 1993. Degradation of Mos by the N-terminal proline (Pro2)-dependent ubiquitin pathway on fertilization of Xenopus eggs: possible significance of natural selection for Pro2 in Mos. EMBO J, 12, 4021-7.

133. O'Brien JA, Taylor JA, Bellamy AR. 2000. Probing the structure of rotavirus NSP4: a short sequence at the extreme C terminus mediates binding to the inner capsid particle. Journal of Virology, 74, 5388-94.

134. Okada J, Kobayashi N, Taniguchi K, Shiomi H. 1999. Functional analysis of the heterologous NSP1 genes in the genetic background of simian rotavirus SA11. Arch Virol, 144, 1439-49.

135. O'Neal CM, Crawford SE, Estes MK, Conner ME. 1997. Rotavirus virus-like particles administered mucosally induce protective immunity. Journal of Virology, 71, 8707-17.

136. Osborne MP, Haddon SJ, Worton KJ, Spencer AJ, Starkey WG, Thornber D and Stephen J. 1991. Rotavirus-induced changes in the microcirculation of intestinal villi of neonatal mice in relation to the induction and persistence of diarrhea. J Pediatr Gastroenterol Nutr, 12, 111-120.

137. Patton JT, Chen D. 1999. RNA-binding and capping activities of proteins in rotavirus open cores. Journal of Virology, 73, 1382-91.

138. Patton JT, Jones MT, Kalbach AN, He YW and Xiaobo J. 1997. Rotavirus RNA polymerase requires the core shell protein to synthesise the double-stranded RNA genome. Journal of Virology, 71, 9618-9626.

139. Patton JT, Wentz M, Xiaobo J and Ramig RF. 1996. cis acting signals that promote genome replication in rotavirus mRNAs. Journal of Virology, 70, 3961-3971.

140. Patton JT, Hua J and Mansell EA. 1993a. Location of intrachain disulfide bonds in the VP5* and VP8* trypsin cleavage fragments of the rhesus rotavirus spike protein VP4. Journal of Virology, 67, 4848-4855.

141. Patton JT, Salter-Cid L, Kalbach A, Mansell EA and Kattoura M. 1993b. Nucleotide and aminoacid sequence analysis of the rotavirus non structural RNA-binding protein NS35(NSP2). Virology, 192, 438-446.

142. Patton JT and Gallegos CO. 1990. Rotavirus RNA replication: ssRNA extends from the replicase particle. Journal of General Virology, 71, 1087.

143. Patton JT and Gallegos CO. 1988. Structure and protein composition of rotavirus replicase particle. Virology, 166, 358-365.

144. Patton JT and Stacy-Phipps S. 1986a. Electrophoretic separation of the plus and minus strands of rotavirus SA11 double stranded RNAs. Journal of Virology Methods, 13, 185.

145. Patton JT. 1986b. Synthesis of simian Rotavirus SA11 double-stranded RNA in a cell free system. Virus Research, 6, 217-233.

146. Petrie BL, Greenberg HB, Graham DY and Estes MK. 1984. Ultrastructural localisation of rotavirus antigens using colloidal gold. Virus Research, 1, 133-152.

147. Petrie BL, Estes MK, Graham DY. 1983. Effects of tunicamycin on rotavirus morphogenesis and infectivity. Journal of Virology, 46, 270-4.

148. Piron M, Delaunay T, Grosclaude J, Poncet D. 1999. Identification of the RNA-binding, dimerization, and eIF4GI-binding domains of rotavirus nonstructural protein NSP3. Journal of Virology, 73, 5411-21.

149. Piron M, Vende P, Cohen J, Poncet D. 1998. Rotavirus RNA-binding protein NSP3 interacts with eIF4GI and evicts the poly(A) binding protein from eIF4F. EMBO J, 17, 5811-21.

150. Pizarro JL Sandino AM, Pizarro JM, Fernandez J and Spencer E. 1991. Characterization of rotavirus guanyltransferase activity associated with polypeptide VP3. Journal of General Virology, 72, 325.

151. Poch O, Sauvaget I, Delarue M, Tordo N. 1989. Identification of four conserved motifs among the RNA-dependent polymerase encoding elements. EMBO J, 8, 3867-74.

152. Poncet D, Lindenbaum P, L'Haridon R and Cohen J. 1997. In vivo an in vitro phosphorylation of Rotavirus NSP5 correlates with its localization in viroplasms. Journal of Virology, 71, 34-41.

153. Poncet D, Aponte C, Cohen J. 1996. Structure and function of rotavirus nonstructural protein NSP3. Arch Virol Suppl, 12, 29-35.

154. Poncet D, Laurent S, Cohen J. 1994. Four nucleotides are the minimal requirement for RNA recognition by rotavirus non-structural protein NSP3. EMBO J, 13, 4165-73 .

155. Poncet D, Aponte C, Cohen J. 1993. Rotavirus protein NSP3 (NS34) is bound to the 3' end consensus sequence of viral mRNAs in infected cells. Journal of Virology, 67, 3159-65.

156. Prasad BVV and MK Estes. 1997. Molecular basis of rotavirus replication, Structure – function correlation, In: "Structural biology of viruses", p.239; ed. Chiu, Burnett, Garcea, Oxford University press.

157. Prasad BV, Rothnagel R, Zeng CQ, Jakana J, Lawton JA, Chiu W, Estes MK. 1996. Visualization of ordered genomic RNA and localization of transcriptional complexes in rotavirus. Nature, 382, 471-3.

158. Prasad BV, Burns JW, Marietta E, Estes MK, Chiu W. 1990. Localization of VP4 neutralization sites in rotavirus by three-dimensional cryo-electron microscopy. Nature, 343, 476-9.

159. Prasad BVV, Wang G, Clerx JP and Chin W. 1988. 3D structure of rotavirus. J Mol Biol, 199, 269.

160. Ramig RF and Gombold JL. 1991. Rotavirus temperature-sensitive mutants are genetically stable and participate in reassortment during mixed infection of mice. Virology, 182, 468-74.

161. Ramig RF and Petrie BL. 1984. Characterization of temperature-sensitive mutants of simian rotavirus SA11: protein synthesis and morphogenesis. Journal of Virology, 49, 665-73.

162. Ramig RF. 1982. Isolation and genetic characterization of temperature-sensitive mutants of simian rotavirus SA11. Virology, 120, 93-105.

163. Rao CD, Das M, Ilango P, Lalwani R, Rao BS, Gowda K. 1995. Comparative nucleotide and amino acid sequence analysis of the sequence-specific RNA-binding rotavirus nonstructural protein NSP3. Virology, 207, 327-33.

164. Raz E, Carson DA, Parker SE, Parr TB, Abai AM, Aichinger G, Gromkowski SH, Singh M, Lew D, Yankauckas MA, et al. 1994. Intradermal gene immunization: the possible role of DNA uptake in the induction of cellular immunity to viruses. PNAS, 91, 9519-9523.

165. Ready KFM and Sabara M. 1987. In vitro assembly of bovine rotavirus nucleocapsid protein. Virology, 157, 189.

166. Rechsteiner M, Rogers SW. 1996. PEST sequences and regulation by proteolysis. Trends Biochem Sci, 21, 267-71.

167. Redmond MJ, Ijaz MK, Parker MD, Sabara MI, Dent D, Gibbons and Babiuk LA. 1993. Assembly of recombinant rotavirus proteins into virus-like particles and assessment of vaccine potential. Vaccine, 11, 278.

168. Rock KL, Gramm C, Rothstein L, Clark K, Stein R, Dick L, Hwang D, Goldberg AL. 1994. Inhibitors of the proteasome block the degradation of most cell proteins and the generation of peptides presented on MHC class I molecules. Cell, 78, 761-71.

169. Rogers, S., R. Wells, and M. Rechsteiner. 1986. Amino acid sequences common to rapidly degraded proteins: the PEST hypothesis. Science, 234, 364-368.

170. Ruiz MC, Cohen J, Michelangeli F. 2000. Role of Ca(2+)in the replication and pathogenesis of rotavirus and other viral infections. Cell Calcium, 28, 137-149.

171. Sandino AM, Fernandez J, Pizarro J, Vasquez M, Spencer E. 1994. Structure of rotavirus particle: interaction of the inner capsid protein VP6 with the core polypeptide VP3. Biol Res, 27, 39-48.

172. Shaw RD, Hempson SJ, Mackow ER. 1995. Rotavirus diarrhea is caused by nonreplicating viral particles. Journal of Virology, 69, 5946-50.

173. Shaw AL, Rothnagel R, Chen D, Ramig RF, Chin W and Prasad BVV. 1993. 3D visualisation of the rotavirus hemagglutinin structure. Cell, 74, 693.

174. Schuck P, Taraporewala Z, McPhie P and Patton JT. 2000. Rotavirus nonstructural protein NSP2 self-assembles into octamers that undergo ligand-induced conformational changes. Journal biological Chemistry, 276, 9679-87.

175. Stacy-Phipps S. and Patton JT. 1987. Synthesis of plus and minus strand RNA in rotavirus infected cells. Journal of Virology, 61, 3479.

176. Starkey WG, Candy DC, Thornber D, Collins J, Spencer AJ, Osborne MP, Stephen J. 1990. An in vitro model to study aspects of the pathophysiology of murine rotavirus-induced diarrhoea. J Pediatr Gastroenterol Nutr, 10, 361-70.

177. Stetler-Stevenson WG, Liotta LA, Kleiner DE Jr. 1993. Extracellular matrix 6: role of matrix metalloproteinases in tumor invasion and metastasis. FASEB J, 7, 1434-41.

178. Stirzaker SC, Whitfeld PL, Christie DL, Bellamy AR, Both GW. 1987. Processing of rotavirus glycoprotein VP7: implications for the retention of the protein in the endoplasmic reticulum. J Cell Biol, 105, 2897-903.

179. Suzuki H, Konno T and Numazaki Y. 1993. Electron microscopic evidence for budding process-independent assembly of double-shelled rotavirus particles during passage through endoplasmatic reticulum membranes. Journal of General Virology, 74, 2015.

180. Suzuki H. 1996. A hypothesis about the mechanism of assembly of double-shelled rotavirus particles. Arch Virol Suppl, 12, 79-85.

181. Suzuki H, Kitaoka S, Konno T, Sato T, Ishida N. 1985. Two modes of human rotavirus entry into MA 104 cells. Arch Virol, 85, 25-34.

182. Suzuki H, Konno T, Kitaoka S, Sato T, Ebina T, Ishida N. 1984. Further observations on the morphogenesis of human rotavirus in MA 104 cells. Arch Virol, 79, 147-59.

183. Tamaoki T, Nomoto H, Takahashi I, Kato Y, Morimoto M, Tomita F. 1986. Staurosporine, a potent inhibitor of phospholipid/Ca++dependent protein kinase. Biochem Biophys Res Commun, 135, 397-402.

184. Taniguchi K, Kojima K, Kobayashi N, Urasawa T, Urasawa S. 1996a. Structure and function of rotavirus NSP1. Arch Virol Suppl, 12, 53-8.

185. Taniguchi K, Kojima K, Urasawa S. 1996b. Non defective rotavirus mutants with an NSP1 gene which has a deletion of 500 nucleotides, including a cysteine-rich zinc finger motif-encoding region (nucleotides 156 to 248), or which has a nonsense codon at nucleotides 153-155. J Virol Jun;70(6):4125-30.

186. Taraporewala Z, Chen D and Patton JT. 1999. Multimers formed by the rotavirus non structural protein NSP2 bind RNA and have nucleoside triphosphatase activity. Journal of Virology, 73, 9934.

187. Taylor JA, O'Brien JA, Yeager M. 1996. The cytoplasmic tail of NSP4, the endoplasmic reticulum-localized non-structural glycoprotein of rotavirus, contains distinct virus binding and coiled coil domains. EMBO J Sep 2;15(17):4469-76.

188. Tian P, Ball JM, Zeng CQ, Estes MK. 1996. The rotavirus nonstructural glycoprotein NSP4 possesses membrane destabilization activity. J Virol Oct;70(10):6973-81.

189. Tian P, Estes MK, Hu Y, Ball JM, Zeng CQ, Schilling WP. 1995. The rotavirus nonstructural glycoprotein NSP4 mobilizes Ca2+ from the endoplasmic reticulum. J Virol Sep;69(9):5763-72.

190. Tian P, Hu Y, Schilling WP, Lindsay DA, Eiden J, Estes MK. 1994. The nonstructural glycoprotein of rotavirus affects intracellular calcium levels. J Virol Jan;68(1):251-7.

191. Timar Peregrin A., Ahlman H, Jodal M, Lundgren O. 1997. Effects of calcium channel blockade on intestinal fluid secretion: sites of action. Acta Physiol Scand. 160(4): 379-86.

192. Torres-Vega MA, Gonzales RA, Duarte M, Poncet D, Lopez S and Arias CF. 2000. The C-terminal domain of rotavirus NSP5 is essential for its multimerization hyperphosphorylation and interaction with NSP6. Journal of General Virology, 81, 821-830.

193. Valenzuela S, Pizarro J, Sandino AM, Vasquez M, Fernandez J, Hernandez O, Patton J, Spencer E. 1991. Photoaffinity labeling of rotavirus VP1 with 8-azido-ATP: identification of the viral RNA polymerase. J Virol Jul;65(7):3964-7.

194. Vasquez M, Sandino AM, Pizarro JM, Fernandez J, Valenzuela S, Spencer E. 1993. Function of rotavirus VP3 polypeptide in viral morphogenesis. J Gen Virol. 74 937-41.

195. Vende P, Piron M, Castagne N and Poncet D. 2000. Efficient translation of rotavirus mRNA requires simultaneous interaction of NSP3 with the eukaryotic translation initiation factor eIF4G and the mRNA 3' end. Journal of Virology, 74, 7064-7071.

196. Weclewicz K, Kristensson K, Svensson L. 1994. Rotavirus causes selective vimentin reorganization in monkey kidney CV-1 cells. J Gen Virol Nov;75 (Pt 11):3267-71.

197. Welch SK, Crawford SE and Estes MK. 1989. Rotavirus SA11 genome segment 11 protein is a non-structural phosphoprotein. Journal of Virology, 63, 3974-3982.

198. Wentz M, Patton JT and Ramig RF. 1996a. The 3′ terminal consensus sequence of rotavirus mRNA is the minimal promoter of the negative strand RNA synthesis. Journal of Virology, 70, 7833-7841.

199. Wentz M, Zeng CQY, Patton JT, Estes MK and Ramig RF. 1996b. Identification of the minimal replicase, and the minimal promoter of - strand synthesis, functional in rotavirus RNA replication in vitro. ArchVirol, 12, 59-67.

200. Whitfeld PL, Tyndall C, Stirzaker SC, Bellamy AR, Both GW. 1987. Location of sequences within rotavirus SA11 glycoprotein VP7 which direct it to the endoplasmic reticulum. Mol Cell Biol 7, 2491-7.

201. Wickelgren I. 2000. How rotavirus causes diarrhea. Science, 287, 409-411.

202. Won KA and Reed SI. 1996. Activation of cyclin E/CDK2 is coupled to site-specific autophosphorylation and ubiquitin-dependent degradation of cyclin E. EMBO J Aug 15;15(16):4182-93.

203. Xu A, Bellamy AR, Taylor JA. 1998. BiP (GRP78) and endoplasmin (GRP94) are induced following rotavirus infection and bind transiently to an endoplasmic reticulum-localized virion component. J Virol Dec;72(12):9865-72.

204. Yaglom J, Linskens MH, Sadis S, Rubin DM, Futcher B, Finley D. 1995. p34Cdc28-mediated control of Cln3 cyclin degradation. Mol Cell Biol Feb;15(2):731-41.

205. Yeager M, Berriman JA, Baker TS and Bellamy AR. 1994. Three-dimensional structure of the rotavirus haemagglutinin VP4 by cryo-electron microscopy and difference map analysis. EMBO J., 13, 1011-1018

206. Zarate S, Espinosa R, Romero P, Mendez E, Arias CF, Lopez S. 2000. The VP5 domain of VP4 can mediate attachment of rotaviruses to cells. J Virol Jan;74(2):593-9.

207. Zeng CQ, Estes MK, Charpilienne A, Cohen J. 1998. The N terminus of rotavirus VP2 is necessary for encapsidation of VP1 and VP3. J Virol Jan;72(1):201-8.

208. Zeng CQY, Wentz MJ, Cohen J, Estes MK and Ramig RF. 1996. Characterization and replicase activity of double-layered and single-layered particles expressed from baculovirus recombinants. Journal of Virology, 70, 2736-2742.